



P. Köhler, AWI, P.O.Box 12 01 61, 27515 Bremerhaven, Germany

To
U. Mikolajewicz
Handling Editor of
Climate of the Past

Dr. Peter Köhler
Alfred Wegener Institute (AWI)
Helmholtz Centre
for Polar and Marine Research
P.O.Box 12 01 61
27515 Bremerhaven
Germany
Phone: +49 471 4831 1687
Fax.: +49 471 4831 1149
peter.koehler@awi.de
<http://www.awi.de>

Bremerhaven, October 12, 2015

Resubmission of a Paper (number cp-2015-88)

Dear U. Mikolajewicz (handling editor),
we here resubmit our paper

On the state-dependency of the equilibrium climate sensitivity during the last 5 million years

coauthored by Peter Köhler, Bas de Boer, Anna S. von der Heydt, Lennert. B. Stap and Roderik S. W. van de Wal to Climate of the Past.

We addressed all comments of the reviewers and changed the paper accordingly. You find our replies attached. In a second PDF (compiled with latexdiff) the changes are highlighted and with red on the right hand side we refer to which main comment of the reviewers gave us reasons for these changes. Please note that latexdiff is not perfect when following changes in the reference list. Therefore, most of the references in the reference list are colour-coded, but only those which are underlined have been added.

Furthermore (also caused by the not perfect performance of latexdiff), in the introduction we added the new reference of Yin and Berger 2012 manually in the file, from which the change with latexdiff have been calculated.

In addition to what was requested by the reviewers we included a reference to a recent review on the limits of the linear approach in calculating climate sensitivity by R Knutti (published 5 Oct 2015) in the introduction and changed the color of one line in Figure 9 to increase clarity.

Looking forward to your final decision.

Yours Sincerely

Response to comments of reviewer #1

related to Köhler, P., de Boer, B., von der Heydt, A. S., Stap, L. B., and van de Wal, R. S. W.: On the state-dependency of the equilibrium climate sensitivity during the last 5 million years, *Clim. Past Discuss.*, 11, 3019-3069, doi:10.5194/cpd-11-3019-2015, 2015.

October 12, 2015

We will in the following respond in detail to all comments of the reviewer #1. Thus, the full text of the review is also contained in this response letter, with our reply written in blue in-between.

This response letter is based on the replies published online in CPD, but includes one correction (our reply to comment #1.8 and in red indicates where we have included changes in the revised manuscript referring to page numbers in the PDF, in which changes to the original submission are highlighted).

Climate sensitivity is a key parameter in the understanding of the climate behaviour and therefore in the prediction/projection of our future climate. Such a paper dealing with this topic is therefore very welcome. This paper is in addition dealing with the climate sensitivity as a function of the background climate state, a research that started worldwide a few years ago and must be encouraged. Climate sensitivity must definitely be differentiated between warm and cold climates. Finally this paper couples data and models to show the state-dependency of climate sensitivity over a very long period (5 million years) which includes a large number of extreme climate situations. All these made the review favourable to the publication of such a paper, but with revisions of some points discussed here under.

General remarks

1.1 What is important for the future is to know whether the increase of temperature due to a doubling of the present-day (pre-industrial) CO₂ concentration is equivalent or larger or smaller than a similar doubling during the previous interglacials (times when ice was similar as to-day). Such a climate sensitivity is different from the one used in this paper (K/(Wm-2)). For example, using a climate sensitivity restricted to the change of global temperature for a doubling of CO₂, Yin and Berger (2012, *Climate Dynamics*) have stressed: "Within the range of the interglacial variability with the CO₂eq concentration going from 234 to 300 ppmv, our climate sensitivity is shown to generally decrease with increasing temperature: MIS-9 has the lowest sensitivity and MIS-13 the highest. The sensitivity at MIS-5 is 10% lower than at Pre-Industrial time". The same results transferred in K/(Wm- 2) gives a decrease from 0.41 (MIS-13) to 0.37 (MIS-9) (if ΔT is divided by $5.35 \cdot \ln(2)$, i.e. 3.71).

Our reply: We acknowledge the findings of Yin and Berger 2012, which we have not discussed so far. This will be revised. However, we here base our analysis mainly on the data compilation and we therefore can not directly answer the question of which temperature change an CO₂ doubling would provide (on a hundred years timescale), since such a thing has not happened so far and therefore has not been recorded in the paleo record. We are here interested in the generic Earth system response to radiative forcing changes that has been recorded in the paleo record. We believe such an analysis is important for a better understanding of climate change itself. In restricting their study to interglacials Yin and Berger 2012 kept ice sheets at present values and find climate sensitivity decreases with increasing temperature. At first glance this might seem contrary to our finding with larger climate sensitivity during late Pleistocene interglacials when compared to late Pleistocene full glacial conditions. We here include changes in land ice sheet as albedo forcing ($\Delta R_{[LI]}$) in our approach. When investigating over the whole range of climate states (e.g. including full glacial conditions with variable $\Delta R_{[LI]}$) we therefore probe a complete different regime, which is not directly comparable with the results from interglacials-only. Furthermore and most important, as written several times in our paper (introduction, discussion) the comparison of (paleo) data-based calculations of climate sensitivity with output from GCM is not directly possible, since in the data-based approach the effect of all processes that have been active are contained in any reconstruction of global temperature, while in the model-based approach only those processes implemented in the model

can lead to changes in calculated temperature. See also our replies on comments #1.2 and #1.8 with more details on interglacials.

55 Moreover, if the climate sensitivity (mainly to CO₂) is indeed depending on the climate background, the results obtained from cold climates can hardly be used for improving the projection of our future climate (see page 3042 lines 17-19).

60 **Our reply:** This is certainly true. However, a lot of previous studies on paleo climate sensitivity focus on our knowledge of LGM climate, since (a) this can nowadays be reproduced reasonably well and (b) the climate anomaly is larger than the uncertainty in the data in this case, so the signal-to-noise ratio is good enough to justify any analysis, something which is not always the case if only interglacial climates are investigated, since the anomalies with respect to pre-industrial conditions are close to zero, and specific climate sensitivity S , which we focus on here, calculated as the ratio of changes in temperature over the changes in the radiative forcing produces for paleo data very often non-reliable results (the problem of calculating to ratio of two small numbers). Therefore, in former studies the interglacials were explicitly not considered (e.g. PALAEOSENS-Project Members, 2012; von der Heydt et al., 2014). We therefore believe one needs to investigate the state-dependency of S as systematic as possible by including also cold (LGM) and warm (Pliocene) climates in order to generate the best understanding possible. Also, we need to rely on (paleo)-data whenever possible in order to test our climate models against them and against the understanding which was derived from the data.

70 Previous works on climate sensitivity, Page 3022 lines 26 and mainly page 3023 line 4, conclusion page 3028 line : “during Pleistocene warm period S was about 45% larger than during the Pleistocene cold periods” and page 3041 lines 9-10 plead for Kohler et al. discussing such climate sensitivity considering only the interglacials/warm periods and only CO₂ if possible (more detailed discussions than what is done in sections 2.3 and 3.3).

75 **Our reply:** We will extend the discussion of our findings with respect to other publications, especially concerning the interglacial periods (e.g. results of Yin and Berger (2012)).

This remark leads to the following recommendations. The authors say on purpose that their analysis is going beyond what has been done before. It would therefore be interesting to see the relative importance of each individual improvement to explain the differences from previous studies.

80 **Our reply:** This recommendation asks for the relative importance of the different improvements by which we go beyond what was done so far. We have to clarify that we understand these improvements especially with respect to the two most recent papers on this issue, namely (a) our own data interpretation of the ice core data (von der Heydt et al., 2014) and (b) the new Pliocene CO₂ data and their interpretation (Martínez-Botí et al., 2015). As stated in the introduction our study is going beyond previous studies in four ways:

- 85 (1) we increase the amount of data;
(2) we calculate the radiative forcing of the land ice albedo from a detailed spatial analysis of land ice distributions obtained with 3-D ice sheet models;
(3) we consider polar amplification to be a function of temperature;
90 (4) we consider whether a linear or a non-linear function best describes the relationship between changes in temperature and changes in radiative forcing.

The relative importance of these four improvements is the following:

95 (1: more data) Apart from the most recent paper of Martínez-Botí et al. (2015) all previous approaches in that direction focused mainly on the time window of the last 800 kyr of the late Pleistocene, for which ice core data exist. A few others (e.g. PALAEOSENS-Project Members, 2012) made some estimates on previous times, but we here compiled all available longer CO₂ time series of the last 5 Myr which are of good quality. In doing so we are able to extrapolate the state-dependency in climate sensitivity found in the ice core data of the last 800 kyr to the last 2.1 Myr.

100 (2: land ice albedo) While the state-dependency in $S_{[CO_2]}$ depends on the chosen CO₂ data set, the state-dependency in $S_{[CO_2,LI]}$ was mainly manifested by the analysis of the 3-D ice sheet output on land ice albedo changes. The difference in the strength of the state-dependency in $S_{[CO_2,LI]}$ can be

seen when comparing our results here with that of our previous study published in von der Heydt et al. (2014) for the ice core data of the last 800 kyr. In the other study the land ice albedo changes was calculated based on simpler approaches. There, we already detected a state-dependency in $S_{[\text{CO}_2, \text{LI}]}$, but remarkably weaker than here (only different slopes in piece-wise linear regressions, but no non-linear relationship between ΔT_g and $\Delta R_{[\text{CO}_2, \text{LI}]}$).

(3: polar amplification) In our presented results we have no scenario, in which polar amplification was constant as assumed previously (e.g. van de Wal et al., 2011). We can however use our most simple approach, in which polar amplification varies as step function between a low value for times without large northern hemispheric land ice (before 2.82 Myr BP) and a high value thereafter. For times with land ice (after 2.82 Myr BP) the analysis of the ice core and Hönisch data sets lead for different assumptions on polar amplification to qualitatively similar results, e.g. a state-dependency in S (Table 1). We interpret this, that an improvement in polar amplification is important to be consistent with our state-of-the-art understanding of climate change, but not for the detection of a state-dependency in climate sensitivity. (4: linear vs non-linear) Only by using statistics and checking if a non-linearity between ΔT and ΔR exists, we were able to quantify the state-dependency of $S_{[\text{CO}_2, \text{LI}]}$ as done here. So, this is the most important step that goes beyond the most recent paper of Martínez-Botí et al. (2015) on the same topic.

The importance of most of these different aspects have been discussed already in the previous version of the MS. However, in the revision we clearly highlight their importance as summarised here.

Done: For the whole of the initial comment 1.1 additional text on pages 2,3 (intro), 18 (discussion), 20 (discussion) was included.

1.2 By introducing new data and calculations (see page 3023 bottom and page 3024 top), the authors introduce unintentionally also new hypotheses and sources of uncertainties. They discuss these uncertainties in section 2.5 and some other places in the paper, but what are the impact on the calculation of the climate sensitivity itself? Some conclusions are drawn in section 3.3 but it would be interesting to know, for example, which of the change of time series or resampling of CO2 data (page 3038 lines14-15) has the largest impact on S . This is very important for recommending in which direction studies must continue to be done to improve our knowledge.

Our reply: Following this comment we performed additional analyses of the data set based on ice core CO₂, in which one (or all) of the 3 times series $\Delta R_{[\text{LI}]}$, $\Delta R_{[\text{CO}_2]}$, and ΔT_g was (were) identical to the previous analysis of von der Heydt et al. (2014). However, since in von der Heydt et al. (2014) all data are resampled to 100 yr, but here to 2 kyr (the temporal resolution of the 3-D ice sheet models), we have to pre-process these data sets taken from the previous study as done here (resampling to 2 kyr). Furthermore, in von der Heydt et al. (2014) data are binned before any regression analysis, whose impact is finally also tested. In this additional analysis (Table 1 below) we find that even when all three data sets would be substituted with those used in von der Heydt et al. (2014) and resampled to 2 kyr we would find a non-linearity in the ΔT_g - $\Delta R_{[\text{CO}_2, \text{LI}]}$ -scatter plot and therefore a state-dependency in $S_{[\text{CO}_2, \text{LI}]}$, but this time a 2nd order polynomial would be best to fit the data (not 3rd order polynomial as found here). However, if data are binned before analysis we find a state-dependency of $S_{[\text{CO}_2, \text{LI}]}$ only for the data sets used here, or when CO₂ is substituted by the previous time series, but not when the previous versions of $\Delta R_{[\text{LI}]}$, or ΔT_g are used. In these binned data (binned into bins of either $\Delta T_g = 0.2$ K or $\Delta R_{[\text{CO}_2, \text{LI}]} = 0.2$ W m⁻²) both our new ΔT_g and $\Delta R_{[\text{LI}]}$ are important to generate this state-dependency in $S_{[\text{CO}_2, \text{LI}]}$. From the p -values of the F-tests to decide if 1st or 2nd-order polynomial's best fit the data we find that ΔT_g seems actually to be even more important than $\Delta R_{[\text{CO}_2, \text{LI}]}$ to generate the non-linearity in the binned ΔT_g - $\Delta R_{[\text{CO}_2, \text{LI}]}$ -scattered data. Please note, that for these tests we used our standard setup for polar amplification (f_{pa}) leading to a global temperature change $\Delta T_g = \Delta T_{g1}$. Also note, that here we tested if a non-linear polynomial might fit the data, while in von der Heydt et al. (2014) piece-wise linear regressions were performed for data sets, for which statistics indicated a break in the (linear) slope of the time series. So both methods are not directly comparable and our finding here, that the binned data which were based in all three variables on the old (previously used) data sets

did not show any non-linearity is not per se in conflict with the previous paper. These findings will be included in the revised manuscript.

Table 1: Sensitivity analysis 1: Investigating the importance of the three variables ΔT_g , CO_2 , ΔR_{LI} with respect to the previous analysis of the ice-core based CO_2 data of von der Heydt et al. (2014) (cited here as vdH2014). Here, all data are resampled to 2kyr while in vdH2014 data are resampled to 100 yrs and binned ΔT_g before any regression analysis. Fitting a linear or a non-linear function to the data. 5000 Monte-Carlo-generated realisations of the scattered $\Delta T_g - \Delta R_{[\text{CO}_2, \text{LI}]}$ were analysed. The data are randomly picked from the entire Gaussian distribution described by the 1σ of the given uncertainties in both ΔT_g and $\Delta R_{[\text{CO}_2, \text{LI}]}$. The parameter values of fitted polynomials are given as mean $\pm 1\sigma$ uncertainty from the different Monte-Carlo realisations. In all scenarios summarised here ΔT_g vs. $\Delta R_{[\text{CO}_2, \text{LI}]}$ with $\Delta T_g = \Delta T_{g1}$ was investigated.

Data set	n	χ^2		F	p	L	r^2 %	a	b	c	d
		1st	2nd								
Investigating the importance of ΔT_g , CO_2 , ΔR_{LI} with respect to the vdH2014:											
ice cores ^a	394	1219	1176	14.3	< 0.001	**	72	-0.43 ± 0.07	2.16 ± 0.10	0.36 ± 0.04	0.02 ± 0.00
ice cores, binned in $\Delta R_{[\text{CO}_2, \text{LI}]}$	31	56	37	14.4	< 0.001	**	81	-0.66 ± 0.37	1.61 ± 0.26	0.14 ± 0.04	0
ice cores, binned in ΔT_g	32	203	148	10.8	0.003	*	87	-0.20 ± 0.18	1.70 ± 0.20	0.14 ± 0.04	0
ice cores, CO_2 as in vdH2014 ^a	390	1283	1235	15.0	< 0.001	**	70	-0.42 ± 0.06	2.17 ± 0.10	0.37 ± 0.04	0.02 ± 0.00
ice cores, CO_2 as in vdH2014, binned in $\Delta R_{[\text{CO}_2, \text{LI}]}$ ^a	31	60	42	12.0	0.002	*	80	-0.68 ± 0.36	1.56 ± 0.25	0.14 ± 0.04	0
ice cores, CO_2 as in vdH2014, binned in ΔT_g ^a	32	213	160	9.6	0.004	*	85	-0.20 ± 0.19	1.67 ± 0.21	0.13 ± 0.04	0
ice cores, ΔR_{LI} as in vdH2014	390	1684	1373	87.7	< 0.001	**	67	-0.49 ± 0.08	1.70 ± 0.06	0.16 ± 0.01	0
ice cores, ΔR_{LI} as in vdH2014, binned in $\Delta R_{[\text{CO}_2, \text{LI}]}$	27	43	32	8.3	0.008	*	79	-0.41 ± 0.43	1.75 ± 0.34	0.16 ± 0.06	0
ice cores, ΔR_{LI} as in vdH2014, binned in ΔT_g	32	193	164	5.1	0.031	/	82	-0.39 ± 0.16	1.08 ± 0.08	0	0
ice cores, ΔT_g as in vdH2014	390	742	658	49.4	< 0.001	**	66	0.13 ± 0.12	1.13 ± 0.08	0.08 ± 0.01	0
ice cores, ΔT_g as in vdH2014, binned in $\Delta R_{[\text{CO}_2, \text{LI}]}$	31	42	35	5.6	0.025	/	73	-0.34 ± 0.23	0.63 ± 0.08	0	0
ice cores, ΔT_g as in vdH2014, binned in ΔT_g	24	40	34	3.7	0.068	/	77	-0.05 ± 0.25	0.70 ± 0.09	0	0
ice cores, ΔT_g , CO_2 , ΔR_{LI} as in vdH2014	390	788	744	22.9	< 0.001	**	62	0.25 ± 0.14	1.12 ± 0.10	0.07 ± 0.01	0
ice cores, ΔT_g , CO_2 , ΔR_{LI} as in vdH2014, binned in $\Delta R_{[\text{CO}_2, \text{LI}]}$	28	35	32	2.3	0.138	/	74	-0.07 ± 0.26	0.72 ± 0.09	0	0
ice cores, ΔT_g , CO_2 , ΔR_{LI} as in vdH2014, binned in ΔT_g	24	42	39	1.6	0.218	/	76	0.23 ± 0.30	0.80 ± 0.11	0	0

n: number of data points in data set.

χ^2 : weighted sum of squares following either a linear fit (1st order) or a non-linear fit (2nd order polynomial), for some data sets (labelled: ^a) also of 2nd or 3rd order polynomials.

F: F ratio for F test to determine, if the higher order fit describes the data better than the lower order fit (1st vs. 2nd order polynomial or 2nd vs. 3rd order polynomial).

p: p value of the F test.

L: significance level of F test (/: not significant ($p > 0.01$); *: significant at 1% level ($0.001 < p \leq 0.01$); **: significant at 0.1% level ($p \leq 0.001$)).

r^2 : correlation coefficient of the fit.

a, b, c, d: derived coefficients of fitted polynomial $y(x) = a + bx + cx^2 + dx^3$.

Done: Lower part of Table 2, extra text on page 14 (section 3.2 in results), 20 (discussion)

Along the same lines:

1.3 What is the impact of the uncertainties of the reconstruction of paleoclimate data of the last 5 million years (in particular of ΔT_g)?

Our reply: Our analysis to find any non-linearity in S or of which order of a polynomial fits the data best is based on a Monte-Carlo approach, in which the uncertainties of all data points in both x (ΔR) and y (ΔT_g) direction are considered. The uncertainties in the data, therefore have a direction impact on the calculated regressions. However, when we estimate the impact of the uncertainties by artificially reducing the uncertainties in ΔT_g ($\sigma_{\Delta T_g}$) and $\Delta R_{[\text{CO}_2, \text{LI}]}$ ($\sigma_{\Delta R}$) by a factor of 2 or 10 we find statistically the same non-linearity in the $\Delta T_g - \Delta R_{[\text{CO}_2, \text{LI}]}$ -scattered data than with the original uncertainties in all four CO_2 data sets, so ice core and Hönisch stay non-linear, Foster and Pagani stay linear (Table 2 below). So we can conclude, that our proposed state-dependency of $S_{[\text{CO}_2, \text{LI}]}$ is robust and independent of the uncertainties. However, any calculated value of S depends in detail on σ in the underlying data. This finding will be included in the manuscript.

Table 2: Sensitivity analysis 2: Investigating the importance of the uncertainties on the regression results by artificially reducing both $\sigma_{\Delta T_g}$ and $\sigma_{\Delta R}$ by a factor of 2 or 10. Fitting a linear or a non-linear function to the data. 5000 Monte-Carlo-generated realisations of the scattered $\Delta T_g - \Delta R_{[\text{CO}_2, \text{LI}]}$ were analysed. The data are randomly picked from the entire Gaussian distribution described by the 1σ of the given uncertainties in both ΔT_g and $\Delta R_{[\text{CO}_2, \text{LI}]}$. The parameter values of fitted polynomials are given as mean $\pm 1\sigma$ uncertainty from the different Monte-Carlo realisations. In all scenarios summarised here ΔT_g vs. $\Delta R_{[\text{CO}_2, \text{LI}]}$ with $\Delta T_g = \Delta T_{g1}$ was investigated.

Data set	n	χ^2		F	p	L	r^2 %	a	b	c	d
		1st	2nd								
Investigating the importance of the uncertainties:											
ice cores ^a , original uncertainties	394	1219	1176	14.3	< 0.001	**	72	-0.43 ± 0.07	2.16 ± 0.10	0.36 ± 0.04	0.02 ± 0.00
ice cores ^a , uncertainties $\times 1/2$	394	3268	3105	210.6	< 0.001	**	80	-0.36 ± 0.04	2.23 ± 0.06	0.41 ± 0.03	0.03 ± 0.00
ice cores ^a , uncertainties $\times 1/10$	394	83489	77553	30.0	< 0.001	**	83	-0.31 ± 0.01	2.34 ± 0.01	0.47 ± 0.01	0.04 ± 0.00
Hönisch, original uncertainties	52	327	256	13.6	< 0.001	**	79	-1.15 ± 0.14	1.27 ± 0.12	0.10 ± 0.02	0
Hönisch, uncertainties $\times 1/2$	52	850	598	20.7	< 0.001	**	87	-1.01 ± 0.08	1.37 ± 0.07	0.10 ± 0.01	0
Hönisch, uncertainties $\times 1/10$	52	16235	10712	25.3	< 0.001	**	89	-0.97 ± 0.02	1.40 ± 0.01	0.11 ± 0.00	0
Foster, original uncertainties	105	2589	2569	0.8	0.38	/	61	-1.53 ± 0.05	0.63 ± 0.03	0	0
Foster, uncertainties $\times 1/2$	105	8972	8954	0.2	0.65	/	61	-1.53 ± 0.03	0.67 ± 0.02	0	0
Foster, uncertainties $\times 1/10$	105	306105	306079	0.1	0.93	/	61	-1.53 ± 0.00	0.69 ± 0.00	0	0
Pagani, original uncertainties	153	5125	5040	2.5	0.11	/	45	-2.19 ± 0.07	0.82 ± 0.04	0	0
Pagani, uncertainties $\times 1/2$	153	15283	14795	5.0	0.03	/	56	-2.23 ± 0.04	1.00 ± 0.03	0	0
Pagani, uncertainties $\times 1/10$	153	343134	329292	6.3	0.01	/	60	-2.24 ± 0.01	1.07 ± 0.01	0	0

n : number of data points in data set.

χ^2 : weighted sum of squares following either a linear fit (1st order) or a non-linear fit (2nd order polynomial), for some data sets (labelled: ^a) also of 2nd or 3rd order polynomials.

F : F ratio for F test to determine, if the higher order fit describes the data better than the lower order fit (1st vs. 2nd order polynomial or 2nd vs. 3rd order polynomial).

p : p value of the F test.

L : significance level of F test: (/: not significant ($p > 0.01$); *: significant at 1% level ($0.001 < p \leq 0.01$); **: significant at 0.1% level ($p \leq 0.001$)).

r^2 : correlation coefficient of the fit.

a, b, c, d : derived coefficients of fitted polynomial $y(x) = a + bx + cx^2 + dx^3$.

Done: Upper part of Table 2, extra text on page 13-14 (section 3.2 in results).

190 1.4 What is the impact on the calculated radiative forcing of the land ice albedo from a 3-D ice sheet model uncoupled (?) to the rest of the climate system? Can the authors be a little bit more explicit on how they calculate $\Delta R_{[LI]}$? What else more than surface albedo, TOA and changes in ice-sheet area is needed to “estimate” $\Delta R_{[LI]}$? What is the relative impact of this “technique” on climate sensitivity?

195 **Our reply:** The 3-D ice sheet models from which we obtain our land ice albedo estimates are included in a modelling framework, that in a simplified form also considers changes in the climate system (see for more details de Boer et al., 2014). However, in the applied 3-D ice sheet modelling framework there is no direct effect of any calculated radiative forcing to the climate system. Further details on the importance and role of coupling these 3-D ice sheet models to more sophisticated climate models was investigated in detail by others (e.g. citations above or Ganopolski et al., 2010; Ganopolski and Calov, 2011) and is not the main focus of our paper here. We will nevertheless briefly extend the methods section on specific details here.

200 How is $\Delta R_{[LI]}$ calculated in detail? This was described in detail in Köhler et al. (2010), but will be briefly repeated here: The main input is a change in ice sheet area (ΔA_{LI}) (in m^2) from the 3-D ice sheet simulation output of de Boer et al. (2014). We then calculate the insolation at the surface I_S (in $W m^{-2}$) as a function of insolation at top of the atmosphere I_{TOA} (in $W m^{-2}$, taken from (Laskar et al., 2004)), albedo of the atmosphere α_A (unitless), and absorption ratio a within the atmosphere (unitless) for every 5° latitudinal band i :

$$I_S(i) = I_{TOA}(i) \times (1 - (\alpha_A + a))$$

Changes in land ice sheet-based radiative forcing $\Delta R_{[LI]}$ per latitudinal band are then given by

$$\Delta R_{[LI]}(i) = -I_S(i) \times \Delta A_{LI}(i) \times (\Delta \alpha) / A_{Earth}$$

210 with $\Delta \alpha = \alpha_{LI} - \alpha_{land}$ being the difference in albedo between land ice (α_{LI}) and ice-free land (α_{land}). $\Delta R_{[LI]}(i)$, if integrated over all latitudinal bands i leads to the total global number $\Delta R_{[LI]}$.

The following parameter values derived for present day and shown in Köhler et al. (2010) are used here: $\alpha_A = 0.212$, $a = 0.20$, $\alpha_{LI} = 0.75$; $\alpha_{land} = 0.2$, $A_{Earth} = 510 \times 10^{12} m^2$.

Done: Methods (section 2.1) on page 5 improved.

215 1.5 What is the impact of fixing the value of a polar amplification factor as a function of the climate state itself (page 3026 line 6; to which extend is it not a circular reasoning by claiming finally that the

climate sensitivity — which depends on polar amplification — is climate state-dependent). What is the importance of such polar amplification factor on the climate sensitivity? There are finally few figures showing the influence of different parameters on S (only Figures 8 b and e). The importance/meaning of the linearity or non-linearity of the relationship between ΔT_g and ΔR must be better explained.

Our reply: So far, the importance of polar amplification f_{pa} being a function of climate state itself has been tested by calculating results for 3 different assumptions on f_{pa} . The results on these choices are only visualised in Table 1 of the manuscript. We came to the conclusion, that the detailed choice of f_{pa} is not important for our claim on state-dependent climate sensitivity. For example, ΔT_{g2} , in which f_{pa} follows a step function and is constant for the last 2.82 Myr (and therefore constant for all times, for which the ice core and Hönisch CO_2 data exist) still leads to qualitatively the same non-linearity (state-dependencies) than other choices for polar amplification. See also our reply to comment #1.1 on the polar amplification. For the quantification of the impact of the climate-dependency of f_{pa} on climate sensitivity we replot and analyse Figure 9 (PDF of $S_{[CO_2,LI]}$) based on the other two global temperature change records ΔT_{g2} and ΔT_{g3} , see Figure 1 below. We find that changes both alternative temperature change records ΔT_{g2} and ΔT_{g3} lead to maxima in the PDF for slightly smaller values $S_{[CO_2,LI]}$. However, we like to clarify that our standard choice of $\Delta T_g = \Delta T_{g1}$ is in best agreement with our understanding of climate change. The results based on ΔT_{g2} (dotted lines) are comparable to our earlier study in which polar amplification was kept constant (van de Wal et al., 2011).

Done: Results (section 3.3) on page 16 improved.

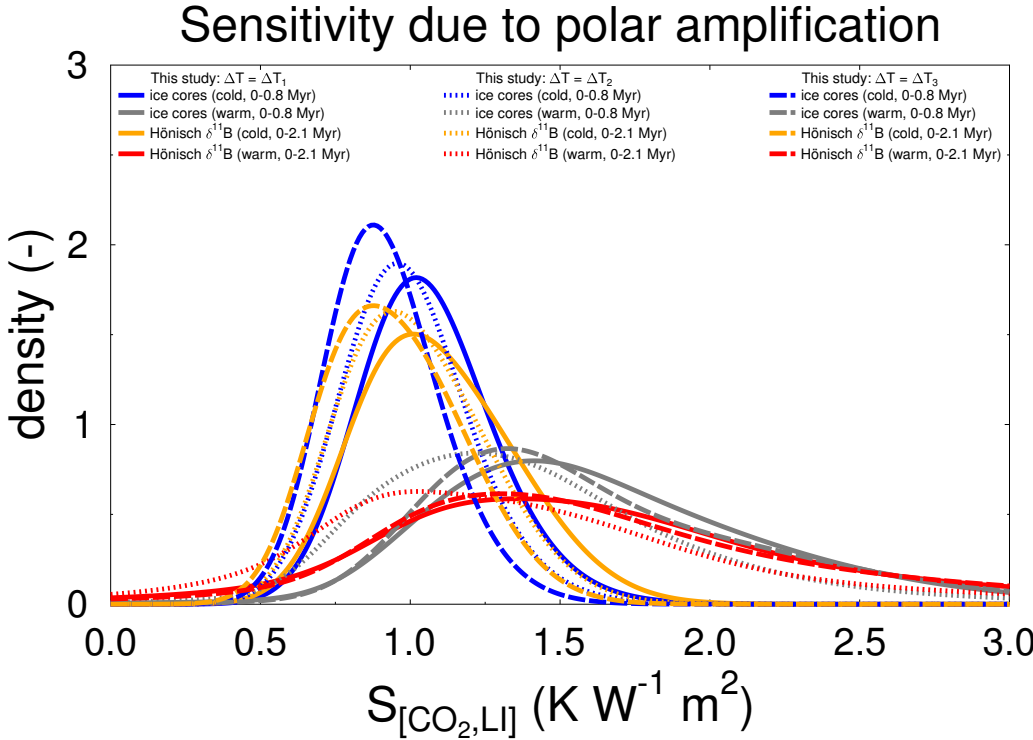


Figure 1: Replotting the probability density functions (PDF) of $S_{[CO_2,LI]}$ based on our results for ice cores or Hönisch CO_2 as a function of different polar amplifications leading to different global temperature changes (similar to previous Figure 9).

1.6 Does the fact that “if the fit follows a linear function, its value might be determined from the slope of the regression line...” (page 3031 line 8) imply that a state-dependency is absolutely requesting a non-linear

relationship between ΔT and ΔR as the authors seem to let it assume page 3024 line 7 , page 3031 lines 1 and 2 and page 3035 line 5.

245 **Our reply:** Yes, this is indeed the case: According to our understanding a state-dependency in $S_{[X]}$ is absolutely requesting a non-linear relationship between ΔT_g and $\Delta R_{[X]}$. We emphasise on that in the text to make this absolutely clear.

Done: Beginning of methods (section 2) on page 4-5 improved.

1.7 I think that what is missing the most in the paper is a figure with $S_{[CO_2]}$, $S_{[LI]}$ and $S_{[CO_2,LI]}$ as a function of ΔT_g showing clearly (?) the state-dependency of S which is the purpose of the paper.

250 **Our reply:** In our approach we investigate the response of the climate system to the radiative forcing ΔR , which drives all changes, so it also it seems straightforward to put ΔR on the x-axis. Furthermore, we believe the state-dependency can also be investigated from the figures, in which S is shown as function of ΔR (Figures 8b,e). When preparing the figures and final analysis of the paper we made the strategic decision to show in Figures 8,b,e S as a function of ΔR , not ΔT_g , because of the non-linearity in the relationship of both variables. As can be seen from Fig 7b,d the flatness of the relationship between both variables for cold conditions lead to the fact, that a range in ΔR is corresponding to a much smaller range in ΔT_g . This implies that the splitting of the data in “cold “ and “warm” periods as done here (in order to be able to compare results with the previous study of von der Heydt et al. (2014)) is not so easily done when data are plotted as S being a function of ΔT_g . Furthermore, in von der Heydt et al. (2014) binned data are split in cold and warm while here much more diverse data are contained. This leads to less defined relationships of S as a function of ΔT_g . Clearly, this is a shortcoming which urgently needs improvements. We furthermore like to emphasise that before a clear formulation of S as a function of temperature change can be given (in more detail than the PDF of S for two sub-groups of the data representing “cold” or “warm” conditions) still more theoretical work seems necessary. This might be achieved during future work, e.g. we are preparing some discussion in that directions for a workshop on that issue.

255

260

265

Done: Text at end results on page 17.

More specific remarks:

270 1.8 1. P 3021 line 23: What the authors mean by “These details” when speaking about the astronomical forcing? Is that statement not opposed to what they say page 3025 line 20. There the authors claim that they use the long term variations of the solar radiation input. It is true that these variations can hardly be visible on figure 1a. Is it due to a lack of resolution or are these variations negligible? The second possibility is probably true as the authors use annual mean insolation which variations are indeed very small (their figure 4c, black curve). This raises a real problem because the insolation forcing is not totally negligible for calculating the temperature changes, but provided the seasonal variations are used in the response of the climate system. (see the relative contribution of insolation and CO2 in Yin and Berger, 2012)

275

280 **Our reply:** What is meant by “These details” is the latitudinal and seasonal change in orbital-induced incoming solar radiation. On page 3025, line 20 the uncertainty in total solar energy output (in the solar constant) is mentioned, which refers to global incoming radiation input. Changes in annual mean insolation as a function of latitude (Fig 1a) are small and not really visible in the figure due to resolution. For example, the annual mean insolation in the band 40-80°N has a peak-to-peak amplitude on the order of a few $W m^{-2}$ on obliquity time scales (41 kyr), on which the effects of longer (eccentricity-based) variations are superimposed. The approach of calculating climate sensitivity from data always refers to global and annual values of ΔT_g and ΔR . This is based on the intrinsic definition of climate sensitivity. Truly, seasonal variations in insolation play a role for climate, but their impact can yet not be analysed with this approach. We have to acknowledge, that the approach here comes to its limits. See also the review on paleo-climate sensitivity for more details on this issue (PALAEOSSENS-Project Members, 2012). We checked the content of Yin and Berger (2012) for this issue. They found that for most of

285

290 the interglacials of the last 800 kyr the effect of the greenhouse gases on global temperature change is
larger than the effect of insolation. We therefore think following only CO₂ changes here and neglecting
these details of insolation is for first order effects a valid assumption. Also note, that in this data-based
analysis S which is the ratio of the two numbers ΔT_g , ΔR , is for interglacial climates not computable
295 for single-points since both ΔT_g and ΔR are close to zero (discussed already in PALAEOSENS-Project
Members (2012)). For interglacials S can only be determined from the overall analysis of the scatter-
plots of ΔT_g - ΔR . In such a setting, different interglacials can not be distinguished (as done in Yin and
Berger (2012)), but only the overall mean response of climate can be calculated. But be aware that
in Yin and Berger (2012) ice sheets were kept constant and therefore $\Delta R_{[LJ]} = 0 \text{ W m}^{-2}$, which also
300 makes a direct comparison of both studies difficult. Nevertheless, we will include these limitations and
the findings of Yin and Berger (2012) in a wider discussion.

Done: We have to slightly correct this reply: "These details" which are not included yet in our approach
were only the *seasonal* variations in incoming solar radiation, not the *latitudinal* changes. Latitudinal
changes are well covered as seen in Figure 1. We revised for clarity in introduction on page 2 and discuss
the consequences in the results (page 18).

305 1.9 2. Page 3022 line 26: Is the linear combination of $\Delta R_{[LJ]}$ and $\Delta R_{[CO_2]}$ giving the same weight for the
two? At least this is what can be deduced from the numerical values given page 3034. Would it not be
better to give them a weight depending on their relative uncertainty.

Our reply: When combining both $\Delta R_{[LJ]}$ and $\Delta R_{[CO_2]}$ their average values are added and the overall
uncertainty of the sum is calculated from the individual uncertainties of both variables following standard
310 error propagation methods. We believe, this approach is sufficient to account for the uncertainties.

Done: Nothing.

1.10 3. Page 3025 line 1: what is the exact meaning of eustatic here (is it total sea level variations both mass
and steric components?)

Our reply: Eustatic here means the global mean change in sea level due to changes in ice volume alone.
315 We revise for clarity.

Done: Clarified in methods, page 5.

1.11 4. Page 3026 section 2.2: what is the impact of neglecting changes of temperature in the SH?

Our reply: The inverse approach of de Boer et al. (2014) is based in the first place on the stack of
marine benthic $\delta^{18}\text{O}$, which contains the mixed signal of global deep ocean temperature and global
320 ice volume (sea level) change. The approach of de Boer et al. (2014) tries to deconvolve the changes
in ice sheets by 3-D ice sheet models as good as possible. Since most of the modelled ice sheets are
situated in the high northern hemisphere, the model is good at predicting also surface air temperature
changes in these regions. In the history of the model development various tests of the relation of
temperature change in the ocean and in the high northern latitudes have been performed, and the
325 assumed relation used here was verified with transient model simulations with more complex climate
models. In the model, the temperature anomaly calculated out of the benthic $\delta^{18}\text{O}$ stack, ΔT of the deep
ocean, is forwarded to two model routines, the 3-D ice-sheet model and the deep-water to surface-air
temperature coupling. To calculate the deep-water temperature anomaly, we used a parameterisation that
linearly relates the deep-water temperature to the 3-kyr mean NH temperature ΔT_{NH} (Bintanja et al.,
330 2005b). According to Bintanja et al. (2005a), glacial-interglacial variations in deep-water and surface
temperatures show sufficient coherence to justify the use of this relationship. The coupling coefficient
between deep ocean and northern hemisphere temperature change was determined using a simplified
atmosphere–ocean climate model (Bintanja and Oerlemans, 1996) by correlating atmosphere to deep-
water temperatures in a series of transient climate runs. A more extensive analysis of this parameterisation
335 is presented in de Boer et al. (2010). We derive global temperature changes from these high northern
hemisphere temperature changes by some assumptions on polar amplification, which we support with
GCM output (own models, two PMIP contributions to the LGM and the Pliocene). Temperature of the

SH is thus not implicitly included in this calculation, but is contained in the global temperature change via the polar amplification factor, into which global temperature field from GCMs contribute to.

340 **Done:** Methods on how to calculated ΔT_g have been extended, page 6.

1.12 5. Page 3027 line 4: what are the two choices mentioned: are they -4.6 ± 0.8 and -5.7 ± 0.6 or $-5.7 - 0.6$ and $-5.7 + 0.6$?

Our reply: The two choices of f_{pa} mentioned here are f_{pa} being a linear function of ΔT_{NH} , or f_{pa} following a step function, as illustrated in Fig 2a. We revise for clarity.

345 **Done:** Clarified in methods, page 7.

1.13 6. All the reconstructed CO₂ values are far from being homogeneous (see pages 3029 and 3030). This discussion is very welcome but what is the final impact on the climate sensitivity?

Our reply: The final impact of the reconstructed CO₂ values on climate sensitivity is, that CO₂ data beyond 2.1 Myr are (a) too sparse, (b) still dependent on the chosen approach, and (c) have too large uncertainties to come to final conclusions on the state-dependency of S for the Pliocene. We summarise this briefly in the revision.

350

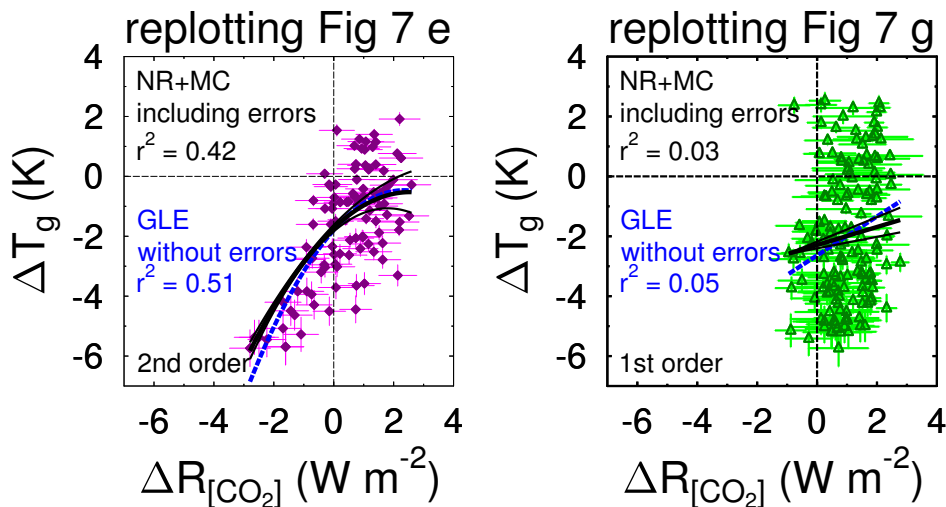
Done: Conclusions, page 20 were specified.

1.14 7. Section 3.2 is discussing the relationship between ΔT and ΔR looking for non-linearity. This is an excellent point, but I have difficulties with figure 7, namely to understand the fitting lines of figure 7e and 7g. In particular I do not see the inverse slope in the points of Fig 7e. If the black line is a fit I do not see how it can be obtained.

355

Our reply: We tested the fit in Figures 7e and 7g with a second statistical toolbox, now without considering the uncertainties in the data and without the Monte-Carlo (MC) approach. We again find the inverse slope and a similar gradient in Fig 7g, so we can exclude any fitting errors here (see Figure 2 below). Note, that the software for analysis used throughout the draft (black lines in figure) was based on numerical recipes (NR), but modified by us, while the second statistical toolbox (blue lines in figure) is the one implemented in the software Graphics Layout Engine (GLE, see <http://glx.sourceforge.net/index.html>). In details the fits differ because of (a) uncertainties and (b) Monte-Carlo, but the general picture is the same. We therefore exclude an error here.

360



365

Figure 2: Replotting Figures 7 e,g with two different softwares to calculate the (non)-linear regression functions. Black and solid lines: Numerical Recipes (NR) combined with Monte Carlo (MC) statistics,

including errors as done in the paper. Blue and broken lines: GLE only based on mean values (not considering errors).

Done: Nothing.

370 1.15 8. Page 3044 line 3: another earlier and still valid reference is Berger and Loutre (2002, Science) who were the firsts to come with such a result.

375 **Our reply:** Page 3044 line 3 is the start of the acknowledgements. We therefore believe there is a typo in the stated line (or page) number and we are not sure where this comment refers to. However, from given reference to Berger and Loutre (2002) it probably relates to the beginning of page 3043, where we discuss the disappearance of the Greenland ice sheet. We extend this discussion on the content of an additional reference of the work of Berger and Loutre, however, we believe that the more interesting paper in this context was Loutre and Berger (2000), a paper in Climatic Change, in which the Greenland ice sheet melted away for scenarios with CO₂ between 200 and 300 ppmv.

Done: Loutre and Berger 2000 included in discussion, page 19.

380 References

- Berger, A. and Loutre, M. F.: An exceptionally long interglacial ahead?, *Science*, 297, 1287–1288, 2002.
- Bintanja, R. and Oerlemans, J.: The effect of reduced ocean overturning on the climate of the last glacial maximum, *Climate Dynamics*, 12, 523–533, 1996.
- Bintanja, R., van de Wal, R., and Oerlemans, J.: Modelled atmospheric temperatures and global sea levels over the
385 past million years, *Nature*, 437, 125–128, doi: 10.1038/nature03975, 2005a.
- Bintanja, R., van de Wal, R., and Oerlemans, J.: A new method to estimate ice age temperatures, *Climate Dynamics*,
24, 197–211, doi: 10.1007/s00382-004-0486-x, 2005b.
- de Boer, B., van de Wal, R. S. W., Bintanja, R., Lourens, L. J., and Tuenter, E.: Cenozoic global ice volume and
390 temperature simulations with 1-D ice-sheet models forced by marine records, *Annals of Glaciology*, 51(55), 23–33,
doi:10.3189/172756410791392736, 2010.
- de Boer, B., Lourens, L. J., and van de Wal, R. S.: Persistent 400,000-year variability of Antarctic ice volume and the carbon
cycle is revealed throughout the Plio-Pleistocene, *Nature Communications*, 5, 2999, doi:10.1038/ncomms3999,
2014.
- Ganopolski, A. and Calov, R.: The role of orbital forcing, carbon dioxide and regolith in 100 kyr glacial cycles, *Climate
395 of the Past*, 7, 1415–1425, doi:10.5194/cp-7-1415-2011, 2011.
- Ganopolski, A., Calov, R., and Claussen, M.: Simulation of the last glacial cycle with a coupled climate ice-sheet model
of intermediate complexity, *Climate of the Past*, 6, 229–244, 2010.
- Köhler, P., Bintanja, R., Fischer, H., Joos, F., Knutti, R., Lohmann, G., and Masson-Delmotte, V.: What caused Earth's
400 temperature variations during the last 800,000 years? Data-based evidences on radiative forcing and constraints on
climate sensitivity, *Quaternary Science Reviews*, 29, 129–145, doi:10.1016/j.quascirev.2009.09.026, 2010.
- Laskar, J., Robutel, P., Joutel, F., Gastineau, M., Correia, A. C. M., and Levrard, B.: A long term numerical solution for
the insolation quantities of the Earth, *Astronomy and Astrophysics*, 428, 261–285, doi:10.1051/0004-6361:20041335,
2004.
- Loutre, M. and Berger, A.: Future Climatic Changes: Are We Entering an Exceptionally Long Interglacial?, *Climatic
405 Change*, 46, 61–90, doi:10.1023/A:1005559827189, 2000.
- Martínez-Botí, M. A., Foster, G. L., Chalk, T. B., Rohling, E. J., Sexton, P. F., Lunt, D. J., Pancost, R. D., Badger, M.
P. S., and Schmidt, D. N.: Plio-Pleistocene climate sensitivity evaluated using high-resolution CO₂ records, *Nature*,
518, 49–54, doi:10.1038/nature14145, 2015.
- PALAEOSSENS-Project Members: Making sense of palaeoclimate sensitivity, *Nature*, 491, 683–691,
410 doi:10.1038/nature11574, 2012.
- van de Wal, R. S. W., de Boer, B., Lourens, L., Köhler, P., and Bintanja, R.: Reconstruction of a continuous high-
resolution CO₂ record over the past 20 million years, *Climate of the Past*, 7, 1459–1469, doi:10.5194/cp-7-1459-2011,
2011.
- von der Heydt, A. S., Köhler, P., van de Wal, R. S., and Dijkstra, H. A.: On the state dependency of fast feedback
415 processes in (paleo) climate sensitivity, *Geophysical Research Letters*, 41, 6484–6492, doi:10.1002/2014GL061121,
2014.
- Yin, Q. and Berger, A.: Individual contribution of insolation and CO₂ to the interglacial climates of the past 800,000
years, *Climate Dynamics*, 38, 709–724, doi:10.1007/s00382-011-1013-5, 2012.

Response to comments of reviewer #2

related to Köhler, P., de Boer, B., von der Heydt, A. S., Stap, L. B., and van de Wal, R. S. W.: On the state-dependency of the equilibrium climate sensitivity during the last 5 million years, *Clim. Past Discuss.*, 11, 3019-3069, doi:10.5194/cpd-11-3019-2015, 2015.

October 12, 2015

We will in the following respond in detail to all comments of reviewer #2 (Jonah Bloch-Johnson). Thus, the text of the review is also partly contained in this response letter, with our reply written in blue in-between. However, the general comment and the first specific comments are rather long and not repeated here in full length. Please refer to the original reviewer comment for further details.

This response letter is based on the replies published online in CPD. In red we indicate where we have included changes in the revised manuscript referring to page numbers in the PDF, in which changes to the original submission are highlighted. Please also note, that we give some further clarification on the second specific comment, that has not yet been included in our online response letter.

Our reply to the first specific comment: In the first specific comment (which is rather long and therefore not repeated here) the reviewer argues for switching the independent/dependent variables in our scatter plots by plotting ΔT_g on the x-axis and ΔR on the y-axis. A lengthy chain of argument is given for motivation (including some notations on how and why radiative forcing might change), which turns out to be (partly) taken from a recent article of the reviewer (Bloch-Johnson et al., 2015). There and elsewhere a fit is calculated through ΔT_g - ΔR -data, which then represent the climate feedback parameter λ , which is defined as the negative of the inverse of the climate sensitivity $S = -1/\lambda$, while S is the variable we like to investigate in our study here.

We are aware of the literature in which the climate feedback parameter is calculated as a fit through ΔR (y)- ΔT_g (x) scatter plots (e.g. Gregory et al., 2004). Of course, also the relationship between the climate sensitivity and climate feedback parameter is well known to us (see methods in Köhler et al., 2010). However, the case here is slightly different than in the example given in the comment and in the literature cited. Here, our ΔR contains the radiative forcing (without feedbacks), whose impact on climate we like to investigate, in detail the radiative forcing of CO₂ and land ice albedo. All responses of the climate system are (fast or slow) feedbacks, that should be covered by the climate sensitivity S we calculate here. These feedbacks influence ΔR in the notation given by reviewer response, but do not influence the radiative forcing ΔR in our setup here. Therefore, in our approach the independent variable is ΔR and should be plotted on the x-axis.

Furthermore, there exist an important difference in our approach (paleo data-based) and the model-based analysis of present day results. The data we analyse are corresponding to equilibrium climate change, while in the analysis of Gregory et al. (2004) or others (e.g. Bloch-Johnson et al., 2015) all simulation results of all time step in the process of reaching equilibrium are used for analysis. This certainly leads to different results which need to be discussed and interpreted differently.

Based on the reasoning above it is in our approach much more natural to understand ΔT_g as dependent variable (y-axis), and ΔR as independent (x-axis). Furthermore, in the applied method used in data-based approaches it is typically to calculate climate sensitivity $S = \Delta T_g / \Delta R$ as the slope of any fitting function to the data with ΔT_g being on the y-axis and ΔR on the x-axis. It therefore is only naturally to continue in this direction (based on the same setting) even if non-linearity is now contained in the underlying relationship of both variables.

All said above is in our view already a valid argument to continue in our analysis based on the setting as so far given (with ΔR being on the x-axis). However, since the reviewer argues, that by changing x and y in the scatter plot we would improve the fit of the (non)-linear functions to the data we nevertheless briefly tested this prediction. When changing x and y (for our standard case with $\Delta T_g = \Delta T_{g1}$ for the scatter plots through $\Delta R_{[CO_2, LI]} - \Delta T_g$) we can hardly improve the fits to the data. The r^2 for the fits through the ice core-based CO₂ values is even reduced by 10% , for the Hönisch data r^2 is reduced by 5%, for the Foster data r^2 is

increased by 6%, for the Pagani data r^2 is increased by 4% ($\Delta R_{[\text{CO}_2, \text{LI}]}$). We also checked for the ice core data that binning of data prior to Monte-Carlo statistics does not influence these results. For the fits through $\Delta R_{[\text{CO}_2, \text{LI}]} - \Delta T_g$ the r^2 for the ice core data become smaller by 7% if x and y are changed, for the three other data sets there are hardly any changes, especially no major improvements.

Much more important, however, is the fact that the non-linearities are completely different now. We now find only a linear relationship between ΔT_g and ΔR for ice core and Hönisch data, but a non-linearity for Foster and Pagani in the $\Delta T_g - \Delta R_{[\text{CO}_2, \text{LI}]}$ scatter plot, where we previously found only a linear relationship. However, when plotting the data with changed x and y it becomes apparent that a polynomial of higher order is probably not the best choice for a function to be fit to the data, maybe some other non-linear function might help (e.g. log-function). Therefore, the statistical results we obtain here whether a linear or non linear fit better describes the data once x and y have been switched should be treated with care and they are probably of limited relevance. For all those reasons given above we refrain from any further investigations in the direction of switching x and y .

Done: Clarification in intro (page 3) End of section 3.2 (page 14) and end of 3.3 (page 17) extended.

The second specific comment concerns the non-linear relationship of sea level rise and land ice radiative forcing. Given the central importance of this non-linearity to the paper, it would be useful to have a more direct explanation of the workings of the ANICE model rather than only relying on a citation to previous work. The de Boer et al. 2014 paper can still be referenced, but some of its most relevant points could be brought over, and specifically which elements of the three-dimensional picture are most important for creating the non-linearity. This would help readers judge the robustness of this result. It would also be good to have a brief explanation of what ICE-5G is.

Our reply: We will improve the description of the ice sheet model ANICE and also of ICE-5G in order to clarify the text for the reader.

Done and further explanation: Methods extended, pages 5-6. However, note that the most important contribution to the non-linearity is no specific feature of the 3-D ice sheet models, but simply a results that simpler approaches can due to their restrictions not consider the latitudinal dependency of land ice area and therefore miss one complexity of the estimated ice-albedo radiative forcing by their design.

The third specific comment concerns arguments about the difference in sensitivity between the Pliocene and Pleistocene using the sensitivities gleaned from the Hönisch and Foster datasets. Figures 9 and 10 strike me as suggesting that both the present paper and Martinez-Boti et al. are right that the cold Pleistocene and the Pliocene have similar sensitivities, while the sensitivity in the warm Pleistocene was significantly higher than either (compare the peaks of the Hönisch ^{11}B cold Pleistocene, warm Pleistocene, and the Martinez-Boti ^{11}B Pliocene sensitivity distributions in Figure 9; the first and third are close together, while the second is much higher.) Note that this sort of “third-order” sensitivity (two changes in strength) is not uncommon seen in models (“Climate feedbacks under a very broad range of forcing”, Colman and McAvaney, 2009; “Fast atmosphere-ocean model runs with large changes in CO₂”, Russell et al., 2013), though typically the other way around (the present is relatively insensitive, e.g., Russell et al., 2013, surrounded on either side by a growing ice albedo feedback and a growing water vapour feedback). Some discussion on this point might be warranted.

Our reply: The important point on the compilation of S from our and other studies is, that Martinez-Boti never searched for any non-linearity in their data set. Also, they lumped all data of the last 800 kyr (the ice core data) together, so mixing cold climate states with climate state comparable to present day. However, we agree that extending the discussion of this issue might improve our draft and bring more clarity to our conclusions.

Done: Discussion extended, page 17.

A few other smaller comments:

105 – Part of the above discussion of the ice sheet model should also note how deep ocean temperatures are used to estimate ΔT_{NH} , and if this relationship contributes to the non-linearity derived in this paper in any way.

110 – **Our reply:** A similar comment was brought up by reviewer #1 and in answering it (#1.2) we made additional analysis in which we tested which data-set improvement is most important for the found non-linearity. It turned out that in the revised global temperature change and the revised land ice albedo change are similarly important for finding a non-linearity in the ΔT - ΔR scattered data.

Done: Nothing.

115 – As someone relatively unfamiliar with the proxy literature, I found Section 2.3 particularly useful in understanding the various CO₂ proxies available.

Our reply: Thank you. We also believe that this discussion of the CO₂ data is especially valuable for people not very familiar with the field.

Done: Nothing.

120 – I was a bit confused as to the units of the colorbar in Figure 1c. Are the colors representative of the globally-normalized forcing of the entire global ice sheet (in which case color would be independent of the y-axis) or are they supposed to represent the impact of the 5° latitudinal bins, in which case the units should be something like “W/m² per 5°”?

125 **Our reply:** The plotted change in Fig 1c are the globally-normalised forcing of the ice sheets in the respective 5° latitudinal bins. Since we have been asked in #1.4 from reviewer 1 to be more specific how ΔR from land ice sheets is calculated we bring more details on how the data to Fig 1c have been calculated.

Done: Nothing is changed. The data in all subpanels of Figure 1 are for latitudinal bands of 5°. We can not see, why units in sub-figure 1c should have different units than that of sub-figure 1a showing I_{TOA} .

130 3 Technical Corrections

This paper has some grammar mistakes:

Our reply: Thanks for spotting and reporting all these mistakes which we will all correct accordingly.

135 **Done:** All have been corrected, most as have been suggested.

References

- Bloch-Johnson, J., Pierrehumbert, R. T., and Abbot, D. S.: Feedback temperature dependence determines the risk of high warming, *Geophysical Research Letters*, 42, 4973–4980, doi:10.1002/2015GL064240, 2015.
- 140 Gregory, J. M., Ingram, W. J., Palmer, M. A., Jones, G. S., Stott, P. A., Thorpe, R. B., Lowe, J. A., Johns, T. C., and Williams, K. D.: A new method for diagnosing radiative forcing and climate sensitivity, *Geophysical Research Letters*, 31, L03 205, doi:10.1029/2003GL018747, 2004.
- Köhler, P., Bintanja, R., Fischer, H., Joos, F., Knutti, R., Lohmann, G., and Masson-Delmotte, V.: What caused Earth's temperature variations during the last 800,000 years? Data-based evidences on radiative forcing and constraints on
145 climate sensitivity, *Quaternary Science Reviews*, 29, 129–145, doi:10.1016/j.quascirev.2009.09.026, 2010.

On the state-dependency of the equilibrium climate sensitivity during the last 5 million years

P. Köhler¹, B. de Boer^{2,3,4}, A. S. von der Heydt³, L. B. Stap³, and
R. S. W. van de Wal³

¹Alfred-Wegener-Institut Helmholtz-Zentrum für Polar-und Meeresforschung (AWI), P.O. Box 12
01 61, 27515 Bremerhaven, Germany

²Department of Earth Sciences, Faculty of Geosciences, Utrecht University, Budapestlaan 4, 3584
CD Utrecht, the Netherlands

³Institute for Marine and Atmospheric Research Utrecht (IMAU), Utrecht University,
Princetonplein 5, 3584 CC Utrecht, the Netherlands

⁴now at: School of Earth and Environment, University of Leeds, Leeds, UK

Correspondence to: P. Köhler (peter.koehler@awi.de)

Abstract. ~~It is a~~ still open question ~~is~~ how equilibrium warming in response to increasing radiative forcing – the specific equilibrium climate sensitivity S – ~~is depending depends~~ on background climate. We here present paleo-data based evidence on the state-dependency of S , by using CO₂ proxy data together with 3-D ice-sheet model-based reconstruction of land ice albedo over
5 the last 5 million years (Myr). We find that the land-ice albedo forcing depends non-linearly on the background climate, while any non-linearity of CO₂ radiative forcing depends on the CO₂ data set used. This non-linearity was in similar approaches not accounted for due to previously more simplistic approximations of land-ice albedo radiative forcing being a linear function of sea level change. ~~Important~~ The latitudinal dependency of ice sheet area changes is important for the non-
10 linearity between land-ice albedo and sea level ~~is a latitudinal dependency in ice sheet area changes~~. In our setup, in which the radiative forcing of CO₂ and of the land-ice albedo (LI) is combined, we find a ~~state-dependency~~ state-dependence in the calculated specific equilibrium climate sensitivity $S_{[\text{CO}_2, \text{LI}]}$ for most of the Pleistocene (last 2.1 Myr). During Pleistocene intermediate glaciated climates and interglacial periods, $S_{[\text{CO}_2, \text{LI}]}$ is on average $\sim 45\%$ larger than during Pleistocene full
15 glacial conditions. In the Pliocene part of our analysis (2.6–5 Myr BP) the CO₂ data uncertainties ~~prevents prevent~~ a well-supported calculation for $S_{[\text{CO}_2, \text{LI}]}$, but our analysis suggests that during times without a large land-ice area in the Northern Hemisphere (e.g. before 2.82 Myr BP) the specific equilibrium climate sensitivity $S_{[\text{CO}_2, \text{LI}]}$ was smaller than during interglacials of the Pleistocene. We thus find support for a previously proposed state-change in the climate system with the wide ap-
20 pearance of northern hemispheric ice sheets. This study points for the first time to a so far overlooked non-linearity in the land-ice albedo radiative forcing, which is important for similar paleo data-based approaches to calculate climate sensitivity. However, the implications of this study for a suggested warming under CO₂ doubling are not yet entirely clear since the necessary corrections for other

slow feedbacks are in detail unknown and the still existing uncertainties in the ice sheet simulations
25 and global temperature reconstructions are large.

1 Introduction

One measure to describe the potential anthropogenic impact on climate is the equilibrium global annual mean surface air temperature rise caused by the radiative forcing of a doubling of atmospheric CO₂ concentration. While this quantity, called equilibrium climate sensitivity (ECS), can be
30 calculated from climate models (e.g. Vial et al., 2013), it is for model validation also important to make estimates based on paleo-data. This is especially relevant since some important feedbacks of the climate system are not incorporated in all models. For example, when coupling a climate model interactively to a model of stratospheric chemistry, including ozone, the calculated transient warming on a hundred-years time scale differs by 20 % from results without such an interactive coupling
35 (Nowack et al., 2015).

Both approaches, model-based (Stocker et al., 2013) and data-based (PALAEOSENS-Project Members, 2012; Hansen et al., 2013), still span a wide range for ECS, e.g. of 1.9–4.4 K (90 % confidence interval) in the most recent simulations compiled in the IPCC assessment report (Stocker et al., 2013), or 2.2–4.8 K (68 % probability) in a paleo data compilation covering examples from the
40 last 65 million years (PALAEOSENS-Project Members, 2012). Reducing the uncertainty in ECS is challenging, but some understanding ~~on~~of model-based differences now emerges (Vial et al., 2013; Shindell, 2014).

The ultimate cause for orbital-scale climate change are latitudinal and seasonal changes in the incoming solar radiations (Milankovitch, 1941; Laskar et al., 2004), which are then amplified by
45 various feedbacks in the climate system (Hays et al., 1976). ~~These details~~ So far, seasonality in incoming solar radiation ~~are is~~ not resolved in our approach, ~~which~~.

1.8

A major restriction of any geological data-based estimate of climate sensitivity is that there was no period in Earth's history during which the atmospheric CO₂ concentration and global temperature varied as rapidly as today. Therefore, in all these data-based approaches (including our study here)
50 ECS defined as global equilibrium temperature rise in response to a doubling of atmospheric CO₂ can only be roughly estimated. Such data-based studies are nevertheless important to find any specific pattern how global temperature changed with respect to a given variation in the radiative forcing. Our approach focuses on the contribution of various climate feedbacks to the reconstructed global temperature changes (PALAEOSENS-Project Members, 2012). When using paleo-data to
55 calculate climate sensitivity one has to correct for slow feedbacks, whose impacts on climate are incorporated in the temperature reconstructions. Slow feedbacks are of interest in a more distant future (Zeebe, 2013), but are not yet considered in climate simulations using fully coupled climate models underlying the fifth assessment report of the IPCC (Stocker et al., 2013). More generally,

1.1

60 from paleo-data the specific equilibrium climate sensitivity $S_{[X]}$ is calculated, which is, in line with
the proposed nomenclature of PALAEOSSENS-Project Members (2012), the ratio of the equilibrium
global (g) surface temperature change ΔT_g over the specific radiative forcing ΔR of the processes
 X , hence $S_{[X]} = \Delta T_g \cdot \Delta R_{[X]}^{-1}$. In this concept “slow feedbacks” are considered as forcing. The
division in “forcing” and “feedback” is based on the time scale of the process. PALAEOSSENS-
Project Members (2012) found that a century is a well justified time scale that might distinguish
65 fast feedbacks from slow forcings. All relevant processes that are not considered in the forcing term
 X will impact on climate change ~~as feedbacks.~~ nevertheless as feedbacks and are contained in the
calculated climate sensitivity. This has to be kept in mind for comparing model-based and data-based
approaches and makes their comparison difficult, since in model-based results only those processes
implemented in the model have an impact on calculated temperature change.

1.1 2.first

70 In practical terms, the paleo-data that are typically available for the calculation of S are the ra-
diative forcing of CO_2 and surface albedo changes caused by land ice (LI) sheets. Thus $S_{[\text{CO}_2, \text{LI}]}$
can be calculated containing the radiative forcing of two processes, which are most important dur-
ing glacial/interglacial timescales of the late Pleistocene (Köhler et al., 2010). The whole approach
therefore relies on the simplification that the climate response of the CO_2 radiative forcing and the
75 surface albedo radiative forcing are similar. We are aware that such a simplification might not be
possible for every radiative forcing, since Shindell (2014) showed that the per unit radiative forcing
of well-mixed greenhouse gases (e.g. CO_2 or CH_4) leads to a different climate response than that
of aerosols or ozone. However, we are not aware that a difference in the response has been shown
for radiative forcing from surface albedo changes ($\Delta R_{[\text{LI}]}$) and CO_2 ($\Delta R_{[\text{CO}_2]}$). Hence we combine
80 them linearly.

Both model-based (e.g. Crucifix, 2006; Hargreaves et al., 2007; Yoshi-
mori et al., 2011; Caballero and Huber, 2013; Goldner et al., 2013; Kutzbach
et al., 2013; Meraner et al., 2013) (Yin and Berger, 2012), and paleo-data-based
(PALAEOSSENS-Project Members, 2012) (PALAEOSSENS-Project Members, 2012; von der Heydt et al., 2014) approaches
85 have already indicated that S varies for different background climates. See also a recent review of
Knutti and Rugenstein (2015) on the limits of linear models to constrain climate sensitivity. The
majority of simulation studies shows a rise in climate sensitivity for a warmer background climate.
One of the exceptions based on analysis for mainly colder than present climates (Kutzbach et al.,
2013) finds the opposite (rise in climate sensitivity for colder climate) with various versions of the
90 CCSM model, which points to the still existing disagreements among models. However, Caballero
and Huber (2013) using the same model find rising climate sensitivity for a warmer climates as the
majority of studies.

The state-dependent character of S based on paleo-data was only recently investigated more sys-
tematically in von der Heydt et al. (2014). It was found that the strength of some of the fast feedbacks
95 depends on the background climate state. This is in agreement with other model-based approaches

which proposed a state-dependency of water vapour (Meraner et al., 2013) or clouds (Crucifix, 2006; Hargreaves et al., 2007). Distinguishing different climate regimes in paleo-data covering the last 800 000 years (0.8 Myr), the time window of the ice core records, von der Heydt et al. (2014) revealed a $\sim 36\%$ larger $S_{[\text{CO}_2, \text{LI}]}$ for “warm” background climates when compared to “cold” climates.

100 However, a limitation in this analysis was ~~that~~ average “warmer” climates were still colder than present day and interglacial periods were largely undersampled. A recent investigation (Martínez-Botí et al., 2015) found that $S_{[\text{CO}_2, \text{LI}]}$ for the late Pleistocene and the Plio–Pleistocene transition have been similar suggesting that no state-dependency in the specific equilibrium climate sensitivity is observed in their proxy data.

105 Here we consider changes in $S_{[\text{CO}_2, \text{LI}]}$ over the last 5 Myr. We go beyond previous studies in various ways. First, we increase the amount and spread of the underlying data ~~which then~~, which offers the possibility to calculate $S_{[\text{CO}_2, \text{LI}]}$ based on paleo-data ~~including most of~~ covering the Pleistocene and ~~the Pliocene, the most of the Pliocene. The~~ latter is the rather warm epoch between ~ 2.6 and 5.3 Myr BP that has been suggested as a paleo-analogue for the future (Haywood et al., 2010).

110 Second, we calculate the radiative forcing of the land ice albedo from a detailed spatial analysis of simulated land ice distribution obtained with 3-D ice-sheet models enhancing the embedded complexity of the underlying physical climate system with respect to previous studies. Third, ~~previously~~ (e.g. van de Wal et al., 2011) polar amplification was previously assumed to be constant over time (e.g. van de Wal et al., 2011). However, climate models (Haywood et al., 2013) indicate that during 115 the Pliocene, when less ice was present on the Northern Hemisphere, the temperature perturbations were more uniformly spread over all latitudes. We incorporate this changing polar amplification in our global temperature record. Fourth, we explicitly analyse for the first time whether the relationship between temperature change and radiative forcing is better described by a linear or non-linear function. If the applied statistics inform us that the ΔT_g – ΔR -relationship contains a non-linearity, then 120 the specific equilibrium climate sensitivity is state-dependent. Any knowledge on a state-dependency of S is important for the interpretation of paleo data and for the projection of long-term future climate change.

2 Methods

We calculate the radiative forcing of CO_2 and land-ice albedo, $\Delta R_{[\text{CO}_2, \text{LI}]}$, by applying the same 125 energy balance model as used before for the late Pleistocene (Köhler et al., 2010). This approach uses CO_2 data from ice cores ~~and based on different~~, as well as from proxies from three different labs published for the last 5 Myr and calculates changes in surface albedo from ~~zonal-averaged~~ zonally-averaged changes in land ice area. The latter are here based on results from 3-D ice-sheet model simulations (de Boer et al., 2014) ~~that~~ deconvolved the benthic $\delta^{18}\text{O}$ stack LR04 (Lisiecki 130 and Raymo, 2005) into its temperature and sea level (ice volume) component. The time series of

global temperature change ΔT_g over the last 5 Myr used here is also based on this deconvolution. The reconstructed records of ice volume and temperature changes are therefore mutually consistent.

A state-dependency in $S_{[CO_2,LI]}$ is then supported by the data, if a non-linear function (higher order polynomial) gives a statistically better fit to the scattered data of ΔT_g versus $\Delta R_{[CO_2,LI]}$ than a linear fit.

135

1.6

2.1 Ice-sheet models, changes in surface albedo and radiative forcing $\Delta R_{[LI]}$

Using an inverse modelling approach and the 3-D ice-sheet model ANICE (de Boer et al., 2014), the benthic $\delta^{18}O$ stack LR04 (Lisiecki and Raymo, 2005) is deconvolved in deep-ocean temperature, ~~eustatic ice volume-based~~ sea-level variations, and a representation of the four main ice sheets in

140

1.10

Antarctica, Greenland, Eurasia, and North America. The spatial resolution (grid cell size) for the Antarctic, Eurasian, and North American ice sheets is $40\text{ km} \times 40\text{ km}$, while Greenland is simulated by cells of $20\text{ km} \times 20\text{ km}$. In the vertical dimension velocities and temperature are calculated at 15 layers. In ANICE shallow ice and shallow shelf approximations are used. With respect to the full Stokes 3-D description that completely describes the temporal and spatial evolution of an ice body some higher-order stress terms are therefore neglected in ANICE in order to allow for long transient runs. A detailed description of the model is found in de Boer et al. (2013).

145

2.second

This approach combines paleo-data and mass conservation for $\delta^{18}O$ with physical knowledge on ice sheet growth and decay. It therefore includes a realistic estimate of both volume and surface area of the major ice sheets. The calculated change in deep-ocean temperature is in this ice sheet-centred approach connected with temperature anomalies over land in the Northern Hemisphere (NH) high latitude band ($40\text{--}85^\circ\text{N}$, ΔT_{NH}), in which the Greenland, Eurasian, and North American ice sheets grow. Temporal resolution of all simulation results from the 3-D ice-sheet models is 2 kyr.

150

From these results, published previously (de Boer et al., 2014) the latitudinal distribution of land-ice area in latitudinal bands i of 5° ($\Delta A_{LI}(i)$) is calculated (Fig. 1b) ~~;~~ which leads to changes in ~~surface albedo and~~ the land-ice sheet-based radiative forcing, $\Delta R_{[LI]}$, with respect to preindustrial times. ~~$\Delta R_{[LI]}$ is now~~ $\Delta R_{[LI]}(i)$ for every latitudinal band (Fig. 1c) is calculated from local surface insolation $I_S(i)$, changes in ice-sheet area $\Delta A_{LI}(i)$, and surface albedo anomalies ($\Delta\alpha$), normalized to its global impact (by division to the Earth's surface area A_{Earth} , $\Delta R_{[LI]}(i) = -I_S(i) \times \Delta A_{LI}(i) \times (\Delta\alpha)/A_{\text{Earth}}$ and integrated thereafter. For the calculation of $I_S(i)$

155

1.4

the annual mean insolation at the top of the atmosphere (TOA) ~~;~~ I_{TOA} , and changes in ice-sheet area in latitudinal bands of 5° at each latitude, $I_{\text{TOA}}(i)$, (Fig. 1)a) is reduced by absorption a and reflection α_A within the atmosphere ($I_S(i) = I_{\text{TOA}}(i) \times (1 - (\alpha_A + a))$). The values of the parameters $a = 0.2$ and ~~globally integrated thereafter~~ $\alpha_A = 0.212$ are here held constant on their present values derived in Köhler et al. (2010). This approach to calculate $\Delta R_{[LI]}$ is based on surface albedo anomalies

160

($\Delta\alpha$), implying that always ice-free latitudes contribute nothing to $\Delta R_{[LI]}$. It is assumed that ice sheets cover land when growing, thus local surface albedo α rises as applied previously (Köh-

165

ler et al., 2010) from 0.2 to 0.75. For calculating $f_{\text{TOA}} - I_{\text{TOA}}(i)$ (Fig. 1a), which varies due to orbital configurations (Laskar et al., 2004), we use a solar constant of 1360.8 W m^{-2} , the mean of more than 10 years of daily data satellite since early 2003 as published by the SORCE project
170 (<http://lasp.colorado.edu/home/sorce>) (Kopp and Lean, 2011). Changes in solar energy output are not considered, but are based on present knowledge (Roth and Joos, 2013) smaller than 1 W m^{-2} during the last 10 kyr, and, following our earlier approach (Köhler et al., 2010), presumably smaller than 0.2 %.

For validation of the ANICE ice sheet model we compare the spatial and temporal variable results
175 in $\Delta R_{\text{[L]}}$ obtained for Termination I (the last 20 kyr) with those based on the land ice sheet distribution of Peltier (2004). This paper describes an approach called ICE-5G (Peltier, 2004) in which data on sea level change which include the contribution from glacial isostatic adjustment are used to obtain a physically consistent picture, that also considers viscoelastic modelling of the mantle of Earth, how the land ice sheet distribution during the last deglaciation might have looked like. For
180 this comparison the ICE-5G data are treated similarly as those from ANICE, e.g. only data every 2 kyr are considered and averaged on latitudinal bands of 5° . The spatial distribution of land ice in the most recent version of ICE-6G (Peltier et al., 2015) are similar to ICE-5G and therefore no significant difference to ICE-6G are expected and the comparison to that version is omitted.

2.second

2.2 Global temperature change ΔT_g

185 In the ANICE model (de Boer et al., 2014) the temperature anomaly of the deep ocean (deconvolved from the benthic $\delta^{18}\text{O}$ stack) is coupled to the NH temperature change ΔT_{NH} by a fixed ratio that has been derived in a series of transient climate runs. A more extensive analysis of this parameterisation is presented in de Boer et al. (2010).

1.11

We calculate global surface temperature change ΔT_g from these ANICE-based NH temperature
190 anomalies, ΔT_{NH} , using a polar amplification (pa) factor f_{pa} which itself depends on climate (Fig. 2).

Based on results from two modelling inter-comparison projects f_{pa} was determined to be 2.7 ± 0.3 for the Last Glacial Maximum (LGM, about 20 kyr BP) (PMIP3/CMIP5 (Braconnot et al., 2012)) and 1.6 ± 0.1 for the mid Pliocene Warm Period (mPWP, about 3.2 Myr BP) (PlioMIP (Haywood et al., 2013)). In our standard setup (calculating ΔT_{g1}) we linearly inter- and extrapolate f_{pa} as
195 function of ΔT_{NH} based on these two anchor values for all background climates found during the last 5 Myr (insert in Fig. 2a). Climate models already suggest that polar amplification is not constant, but how it is changing over time is not entirely clear (Masson-Delmotte et al., 2006; Abe-Ouchi et al., 2007; Hargreaves et al., 2007; Yoshimori et al., 2009; Singarayer and Valdes, 2010). We therefore calculate an alternative global temperature change ΔT_{g2} in which we assume polar amplification
200 f_{pa} to be a step function, with $f_{\text{pa}} = 1.6$ (the mPWP value) taken for times with large northern hemispheric land ice (according to our results before 2.82 Myr BP), and with $f_{\text{pa}} = 2.7$ (the LGM value) thereafter. This choice is motivated by investigations with a coupled ice sheet-climate model,

from which northern hemispheric land ice was identified to be the main controlling factor for the polar amplification (Stap et al., 2014).

205 At the LGM ΔT_g was, based on the eight PMIP3 models contributing to this estimate in f_{pa} ,
–4.6 ± 0.8 K, so slightly colder, but well overlapping the most recent LGM estimate (Annan and
Hargreaves, 2013) of $\Delta T_g = -4.0 \pm 0.8$ K. If we take into consideration that the MARGO sea
surface temperature (SST) data underlying this LGM temperature estimate (Annan and Hargreaves,
2013) are potentially biased towards too warm tropical SSTs (Schmidt et al., 2014), the PMIP3
210 results are a good representation of LGM climate. The ΔT_g For both choices of f_{pa} (varying linear
as function of ΔT_{NH} or as step function over time) the global temperature change at LGM obtained
in our reconstruction is ~~for both choices of f_{pa} –5.7 ± 0.6 K~~ $\Delta T_g = -5.7 \pm 0.6$ K, so slightly colder
than other approaches, but within the uncertainties overlapping with the PMIP3-based results. **1.12**

The global temperature changes obtained with both approaches on f_{pa} are very similar and mainly
215 differ for some glacial periods in the late Pliocene and some interglacial periods in the Pleistocene
(Fig. 2c). Results from the eight models (CCSM4, CNRM-CM5, FGOALS-g2, GISS-E2-R, IPSL-
CM5A-LR, MIROC-ESM, MPI-ESM-P, MRI-CGCM3) which contributed the relevant results to
the PMIP3/CMIP5-database until mid of January 2014 were analysed averaging uploaded results
over the last available 30 years. Warming within the mPWP based on PlioMIP was $+2.7 \pm 1.2$ K,
220 overlapping with our calculated global surface temperature change within the uncertainties (Fig. 2c).
The models contributing to PlioMIP, experiment 2 (coupled atmosphere–ocean models) are CCSM4,
COSMOS, GISS-E2-R, HadCM3, IPSL-CM5A, MIROC4m, MRI-CGCM2.3 and NorESM-L.

As third alternative (ΔT_{g3}) we constrain the global temperature changes by the values from PMIP3
for the LGM (–4.6 K) and from PlioMIP for the mPWP (+2.7 K) and vary f_{pa} freely. If done
225 so, f_{pa} rises to ~ 3.3 during glacial maxima of the Pleistocene and to ~ 1.0 during the Pliocene.
Our approach based on the ΔT_{NH} reconstruction is not able to meet all four constraints given by
PMIP3/PlioMIP (ΔT_g , f_{pa} for both the LGM and the mPWP) at the same time. This mainly illus-
trates that the approach used in de Boer et al. (2014), although coherently solving for temperature and
ice volume, underestimates polar temperature change prior to the onset of the NH glacial inception,
230 since it only calculates ice-volume and deep-water temperature change from benthic $\delta^{18}O$.

Throughout the following our analysis is based on the temperature time series ΔT_{g1} . However,
we repeat our analysis with the alternative temperature time series to investigate the robustness of
our approach to the selected time series. As can be seen in the results our main conclusions and
functional dependencies are independent from the choice of ΔT_g and are also supported if based on
235 either ΔT_{g2} or ΔT_{g3} (see Table 1).

The modelled surface–air temperature change ΔT_{NH} was already compared (de Boer et al., 2014)
with three independent proxy-based records of sea surface temperature (SST) change in the North
Atlantic (Lawrence et al., 2009), equatorial Pacific (Herbert et al., 2010) and Southern Ocean
(Martínez-García et al., 2010) which cover at least the last 3.5 Myr. The main features of the sim-

240 ulated temperature change and the data-based SST reconstruction agree: the overall cooling trend
from about 3.5 to 1 Myr ago is found in the simulation results and in all SST records, [and](#) so is the
strong glacial–interglacial (100 kyr) variability thereafter.

2.3 Radiative forcing of CO₂, $\Delta R_{[\text{CO}_2]}$

Several labs developed different proxy-based approaches to reconstruct atmospheric CO₂ before the
245 ice-core time window of the last 0.8 Myr. Since we are interested how CO₂ might have changed
over the last 5 Myr and on its relationship to global climate we only consider longer time series for
our analysis. Thus, some approaches, e.g. based on stomata, with only a few data points during the
last 5 Myr are not considered (see Beerling and Royer, 2011). The considered CO₂ data are in detail
(Fig. 3):

- 250 a. ice core CO₂ data were compiled by Bereiter et al. (2015) into a stacked ice core CO₂
record covering the last 0.8 Myr including a revision of the CO₂ data from the lowest part
of the EPICA Dome C ice core. Originally, the stack as published (Bereiter et al., 2015) con-
tains 1723 data points before year 1750 CE, the beginning of the industrialisation, but was
here resampled to the 2 kyr time step of the ice-sheet simulation results by averaging avail-
255 able data points, and reducing the sample size to $n = 394$. The stack contains data from the
ice cores at Law Dome (Rubino et al., 2013; MacFarling-Meure et al., 2006) (0–2 kyr BP),
EPICA Dome C (Monnin et al., 2001, 2004; Schneider et al., 2013; Siegenthaler et al., 2005;
Bereiter et al., 2015) (2–11 kyr BP, 104–155 kyr BP, 393–806 kyr BP), West Antarctic Ice
Sheet Divide (Marcott et al., 2014) (11–22 kyr BP), Siple Dome (Ahn and Brook, 2014) (22–
260 40 kyr BP), Talos Dome (Bereiter et al., 2012) (40–60 kyr BP), EPICA Donning Maud Land
(Bereiter et al., 2012) (60–104 kyr BP) and Vostok (Petit et al., 1999) (155–393 kyr BP).
- b. CO₂ based on $\delta^{11}\text{B}$ isotopes measured on planktonic shells of *G. sacculifer* from the Hönisch-
lab (Hönisch et al., 2009) ($n = 52$) is obtained from ODP668B located in the eastern equatorial
Atlantic. The data go back until 2.1 Myr BP and agree favourably with the ice core CO₂
265 during the last 0.8 Myr.
- c. CO₂ data from the Foster-lab (Foster, 2008; Martínez-Botí et al., 2015) are available for the
last 3.3 Myr ($n = 105$) obtained via $\delta^{11}\text{B}$ from ODP site 999 in the Caribbean Sea. CO₂ purely
based on *G. ruber* $\delta^{11}\text{B}$ was reconstructed for the last glacial cycle (Foster, 2008) and for about
0.8 Myr during the Plio–Pleistocene transition (Martínez-Botí et al., 2015). We take both these
270 data sets using identical calibration as plotted previously (Martínez-Botí et al., 2015). The
overlap of the data with the ice core CO₂ is reasonable with the tendency for overestimating
the maximum anomalies in CO₂ (by more than +50 ppmv during warm previous interglacials
and by –25 ppmv during the LGM, Fig. 3b).

d. CO₂ reconstructions based on alkenone from the Pagani-lab (Pagani et al., 2010; Zhang et al., 2013) ($n = 153$) cover the whole 5 Myr and are derived from different marine sediment cores. Site 925 is contained in both publications, although with different uncertainties. From site 925 we use the extended and most recent CO₂ data of Zhang et al. (2013) containing 50 data points over the last 5 Myr, 18 points more than initially published. Data from the sites 806, 925 and 1012 are offset from the ice core CO₂ reference during the last 0.8 Myr by +50 to +100 ppmv, while data from site 882 have no overlapping data points with the ice cores. It is not straightforward how these CO₂ data from the Pagani-lab that are offset from the ice core CO₂ might be corrected. Therefore, we refrain from applying any corrections but keep these offsets in mind for our interpretation.

Other CO₂ data based on B/Ca (Tripathi et al., 2009) are not considered here, since critical issues concerning its calibration have been raised (Allen et al., 2012). A second $\delta^{11}\text{B}$ -based record of the Hönisch-lab (Bartoli et al., 2011) from *G. sacculifer* obtained from ODP site 999 is not used for further analysis, because $\delta^{11}\text{B}$ was measured on other samples than proxies that are necessary to determine the related climate state (e.g. $\delta^{18}\text{O}$). Thus, a clear identification if glacial or interglacial conditions were prevailing for individual data points was difficult. Furthermore, these calculated CO₂ values (Bartoli et al., 2011) have very high uncertainties, 1σ is $3\times$ larger than in the original Hönisch-lab data set (Hönisch et al., 2009). These CO₂ data of Bartoli et al. (2011) disagrees with the most recent data from the Foster-lab (Martínez-Botí et al., 2015), especially before the onset of northern hemispheric glaciation around 2.8 Myr ago. Another CO₂ time series from the Foster-lab (Seki et al., 2010) based on a mixture of both alkenones or $\delta^{11}\text{B}$ approaches covering the last 5 Myr is not considered here, since the applied size-correction for the alkenone producers has subsequently been shown to be incorrect (Badger et al., 2013).

Radiative forcing based on CO₂ is calculated using $\Delta R_{[\text{CO}_2]} = 5.35 \text{ W m}^{-2} \cdot \ln(\text{CO}_2/\text{CO}_{2,0})$ with $\text{CO}_{2,0} = 278 \text{ ppmv}$ being the preindustrial reference value (Myhre et al., 1998).

2.4 How to calculate the specific equilibrium climate sensitivity $S_{[\text{CO}_2, \text{LI}]}$

The specific equilibrium climate sensitivity for a forcing X is defined as $S_{[X]} = \Delta T_g \cdot \Delta R_{[X]}^{-1}$. In an analysis of $S_{[X]}$ when calculated for every point in time for the last 0.8 Myr based on ice core data PALAEOSENS-Project Members (2012) revealed the range of possible values, which fluctuated widely not following a simple functionality, even when analysed as moving averages. This study also clarified that $S_{[X]}$ based on small disturbances in ΔT_g or $\Delta R_{[X]}$ are due to dating uncertainties prone to unrealistic high/low values. Only when data are analysed in a scatter-plot a non-linear functionality between ΔT_g and $\Delta R_{[X]}$, and therefore a state-dependency of $S_{[X]}$, emerges as signal out of the noisy data (von der Heydt et al., 2014).

Here, ΔT_g is approximated as a function of $\Delta R_{[X]}$ by fitting a non-linear function (a polynomial up to the third order, $y(x) = a + bx + cx^2 + dx^3$) to the scattered data of ΔT_g vs. $\Delta R_{[X]}$. The

310 individual contribution of land ice albedo and CO₂ to a state-dependency of $S_{[\text{CO}_2, \text{LI}]}$ can be investigated by analysing both $S_{[\text{CO}_2]}$ and $S_{[\text{CO}_2, \text{LI}]}$. If the best fit follows a linear function, e.g. for state-independent behaviour of $S_{[X]}$, its values might be determined from the slope of the regression line in the $\Delta T_g - \Delta R_{[X]}$ -space. However, note that here a necessary condition for the calculation of $S_{[X]}$ over the whole range of $\Delta R_{[X]}$, but not for the analysis of any state-dependency is, that any
 315 fitting function crosses the origin with $\Delta R_{[\text{CO}_2, \text{LI}]} = 0 \text{ W m}^{-2}$ and $\Delta T_g = 0 \text{ K}$, implying for the fitting parameters that $a = 0$. This is also in line with the general concept that without any change in the external forcing no change in global mean temperature should appear. Since the data sets have apparent offsets from the origin we first investigate which order of the polynomial best fits the data by allowing parameter a to vary from 0.

320 For the calculation of mean values of $S_{[\text{CO}_2, \text{LI}]}$ we then analyse in a second step the $S_{[\text{CO}_2, \text{LI}]} - \Delta R_{[\text{CO}_2, \text{LI}]}$ -space, where $S_{[\text{CO}_2, \text{LI}]} = \Delta T_g \cdot \Delta R_{[\text{CO}_2, \text{LI}]}^{-1}$ is first calculated individually for every data point and then stacked for different background conditions (described by $\Delta R_{[\text{CO}_2, \text{LI}]}$). In doing so we circumvent the problem that the regression function needs to meet the origin, that appeared in the $\Delta T_g - \Delta R_{[X]}$ -space. Some of the individual values of $S_{[\text{CO}_2, \text{LI}]}$ are still unrealistically high/low,
 325 therefore values in $S_{[\text{CO}_2, \text{LI}]}$ outside the plausible range of $0 - 3 \text{ K W}^{-1} \text{ m}^2$ are rejected from further analysis.

The scattered data of $S_{[\text{CO}_2, \text{LI}]}$ as function of $\Delta R_{[\text{CO}_2, \text{LI}]}$ are then compiled in a probability density function (PDF), in which we also consider the given uncertainties of the individual data points. For the calculation of the PDFs we distinguish between a few different climate states, when supported by
 330 the data. For the time being the data coverage is too sparse and uncertainties are too large to calculate any state-dependent values of $S_{[\text{CO}_2, \text{LI}]}$ in greater detail.

The fitting routines (Press et al., 1992) use the method of general linear least squares. Here, a function $\chi^2 = \sum_i^n \frac{(y_i - y(x))^2}{\sigma_y^2}$ is minimised, which calculates the sum of squares of the offsets of the fit from the n data points normalised by the average variance σ_y^2 . Since established numerical methods
 335 for calculating a non-linear fit through data cannot consider uncertainties in x we base our regression analysis on a Monte-Carlo approach. Data points are randomly picked from the Gaussian distribution described by the given 1σ standard deviation of each data point in both directions x ($\Delta R_{[X]}$) and y (ΔT_g). We generated 5000 of these data sets, calculated their individual non-linear fits and further analysed results based on averages of the regression parameters. The Monte-Carlo approach
 340 converges if the number of replicates exceeds 1000, e.g. variations in the mean of the parameters are at least an order of magnitude smaller than the uncertainties connected with the averaging of the results. We used the χ^2 of the fitting routines in F tests to investigate if a higher order polynomial would describe the scattered data in the $(\Delta T_g - \Delta R_{[X]})$ -parameter space better than a lower order polynomial and use the higher order polynomial only if it significantly better describes the data at
 345 the 1% level (p value of F test: $p \leq 0.01$, Table 1).

2.5 Uncertainty estimates

As previously described in detail (Köhler et al., 2010) standard error propagation is used to calculate uncertainties in ΔT and ΔR . For $\Delta R_{[LI]}$, changes in surface albedo are assumed to have a 1σ -uncertainty of 0.1, ~~simulated~~, Simulated changes in land-ice-area have a relative uncertainty of 10% in the various simulation scenarios performed in de Boer et al. (2014) ~~a relative uncertainty of 10%~~. The different approaches to reconstruct CO_2 all have different uncertainties as plotted in Fig. 3. Ice core CO_2 has a 1σ uncertainty of 2ppmv, while those based on other proxies have individual errors connected with the data-points that are on the order of 20–50 ppmv. Radiative forcing based on CO_2 , $\Delta R_{[CO_2]} = 5.35 \text{ W m}^{-2} \cdot \ln(CO_2/CO_{2,0})$ has in addition to the uncertainty in CO_2 itself also another 10 % 1σ -uncertainty (Forster et al., 2007). The uncertainty in the incoming insolation is restricted to known variations in the solar constant to be of the order of 0.2%. Annual mean global surface temperature ΔT_g is solely based on the polar amplification factor f_{pa} and ΔT_{NH} . Uncertainty in ΔT_{NH} is estimated based on eight different model realisations of the deconvolution of benthic $\delta^{18}O$ into sea level and temperature (de Boer et al., 2014). Based on the analysis of the PMIP3 and PlioMIP results the polar amplification factor $f_{pa} = \Delta T_{NH} \cdot \Delta T_g^{-1}$ has a relative uncertainty of 10 % (see Fig. 2a).

These uncertainties used in an error propagation lead to the $\sigma_{\Delta T_g}$, $\sigma_{\Delta R_{[CO_2]}}$ and $\sigma_{\Delta R_{[CO_2,LI]}}$ of the individual data points and are used to constrain the Monte-Carlo statistics. The stated uncertainties of the parameters of the polynomials fitting the scattered ΔT – ΔR -data given in Table 1 and used to plot and calculate $S_{[CO_2,LI]}$ are derived from averaging results of the Monte-Carlo approach. Note, that higher order polynomials give more constrains on the parameters and therefore lead to smaller uncertainties.

3 Results

3.1 Individual radiative forcing contributions from land ice albedo and CO_2

We calculate a resulting radiative forcing of CO_2 , $\Delta R_{[CO_2]}$, that span a range from -2.8 to $+2.5 \text{ W m}^{-2}$ compared to preindustrial conditions (Fig. 4b). The uncertainty in $\Delta R_{[CO_2]}$ depends on the proxy. It is about 10% in ice cores, and generally less than 0.5 W m^{-2} for other proxies with the exception of some individual points from the Pagani-lab with uncertainties around 1 W m^{-2} .

In contrast to these rather uncertain and patchy results the ice-sheet simulations lead to a continuous time series of surface albedo changes and $\Delta R_{[LI]}$ ranging between -4 W m^{-2} during ice ages of the late Pleistocene and $+1 \text{ W m}^{-2}$ during interglacials of the Pliocene (Fig. 4c). During warmer than preindustrial climate $\Delta R_{[LI]}$ is thus rather small and between 4.2 and 3.0 Myr ago only slightly higher than $\Delta R_{[orbit]}$, the radiative forcing due to global annual mean insolation changes caused by variations in the orbital parameters of the solar system (Laskar et al., 2004) (Fig. 4c).

380 Reconstructed $\Delta R_{[LI]}$ for the last 20 kyr agrees reasonable-resonably well with an alternative based
on the ICE-5G ice sheet reconstruction of Peltier (2004) (Fig. 5). Changes in land ice fraction in
the northern high latitudes around 15 kyr are more abrupt around 70° N in ICE-5G than in ANICE
(Fig. 5b, e). The northward retreat of the southern edge of the NH ice sheets happens later in ICE-5G
than in ANICE. In combination, both effects lead to only small differences in the spatial and temporal
385 distribution of the radiative forcing $\Delta R_{[LI]}$ when based on either ANICE or ICE-5G (Fig. 5c and f).

The ice-albedo forcing $\Delta R_{[LI]}$ has a non-linear relationship to sea level change (Fig. 6a), which is
caused by the use of the sophisticated 3-D ice-sheet models. Hence other approaches which approxi-
mate $\Delta R_{[LI]}$ directly from sea level (Hansen et al., 2008; Martínez-Botí et al., 2015), simpler 1-D ice
sheet models or calculate $\Delta R_{[LI]}$ from global land ice area changes without considering latitudinal
390 dependency (Köhler et al., 2010; von der Heydt et al., 2014) lack an important non-linearity of the
climate system. This non-linearity in the $\Delta R_{[LI]}$ -sea level relationship is also weakly contained in
results based on ICE-5G for Termination I (Fig. 6a). However, when plotting identical time steps of
Termination I from results based on ANICE, the non-linearity is not yet persisting. This implies $\bar{\tau}$
that a larger pool of results from various different climates need to be averaged in order to obtain
395 a statistically robust functional relationship between $\Delta R_{[LI]}$ and sea level (as done in this study).

The combined forcing $\Delta R_{[CO_2,LI]}$ can only be obtained for the data points for which CO₂ data ex-
ist (Fig. 4d). The combined forcing ranges from -6 to -7 W m^{-2} during the Last Glacial Maximum
(LGM) to, in general, positive values during the Pliocene with a maximum of $+3 \text{ W m}^{-2}$. Between
5.0 and 2.7 Myr ago (most of the Pliocene) the ice sheet area and $\Delta R_{[LI]}$ are continuously smaller
400 than today, apart from two exceptions around 3.3 Myr and after 2.8 Myr ago, (Fig. 4c) suggesting
warmer temperatures throughout. Proxy data suggest that CO₂ and $\Delta R_{[CO_2]}$ were in the Pliocene
mostly higher than during preindustrial times.

3.2 Detecting any state-dependency in $S_{[CO_2,LI]}$

As explained in detail in Sect. 2.4 $S_{[CO_2,LI]}$ can be considered state-dependent if the scattered data of
405 ΔT_g against $\Delta R_{[CO_2,LI]}$ are better described by a non-linear rather than a linear fit. The plots for the
different CO₂ approaches reveal proxy-specific results (Fig. 7). Ice core data ($r^2 = 0.72$) are best
described by a third order polynomial, the Hönisch data ($r^2 = 0.79$) by a second order polynomial,
while for the Foster ($r^2 = 0.61$) and Pagani ($r^2 = 0.45$) data a second order fit is not statistically
significantly better than a linear fit (Table 1).

410 The fit through the Hönisch data agrees more with the fit through the ice core CO₂ data than
with the fit through the other CO₂-proxy-based approaches, however the Hönisch data set extends
only 2.1 Myr back in time and contains no CO₂ data in the warm Pliocene. Thus, the finding of
a state-dependency in climate sensitivity obtained from the ice core data covering predominately
colder than present periods which we find here – and for which a first indication was published in
415 von der Heydt et al. (2014) – is extended to the last 2.1 Myr, where the climate states similar to the

present climate are better sampled than in the ~~the~~ late Pleistocene record as used in von der Heydt et al. (2014). However, we can still not extrapolate this finding to the warmer than present climates of the last 5 Myr since the ice core and Hönisch data do not cover these periods and the Foster and Pagani data do not suggest a similar relationship. These findings remain qualitatively the same if our
420 analyses are based on the alternative global temperature changes ΔT_{g2} or ΔT_{g3} (Table 1).

When analysing the contribution from land ice albedo ($\Delta R_{[LI]}$) and CO₂ radiative forcing ($\Delta R_{[CO_2]}$) separately, we find a similar non-linearity in the $\Delta T_g - \Delta R_{[CO_2]}$ scatter plot only in the CO₂ data from ice cores (Fig. 7a). The relationship between temperature and radiative forcing of CO₂ are best described by a linear function in the Hönisch and Pagani data sets (Fig. 7c and g, Ta-
425 ble 1) or in data from the Foster-lab even by a second order polynomial with inverse slope leading to a decline in $S_{[CO_2]}$ for rising $\Delta R_{[CO_2]}$ (Fig. 7e). This inverse slope obtained for the Foster data between ΔT_g and $\Delta R_{[CO_2]}$ is the only case in which a detected nonlinearity partly depends on the use of the temperature change time series, e.g. the relationship is linear when based on ΔT_{g3} (Table 1). Furthermore, this inverse slope might be caused by the under-representation of data for negative ra-
430 diative forcing. However, when data in the $\Delta T_g - \Delta R_{[X]}$ -scatter plots are binned in x or y direction to overcome any uneven distribution of data no change in the significance of the non-linearities are observed. The data scatter is large and regression coefficients between $\Delta R_{[CO_2]}$ and ΔT_g for Foster ($r^2 = 0.42$) and Pagani ($r^2 = 0.03$) are small. This large scatter and weak quality of the fit in the Pagani data is probably caused by some difficulties in the alkenone-based proxy, e.g. size depen-
435 dency, and variations in the degree of passive vs. active uptake of CO₂ by the alkenone-producing coccolithophorids (Bolton and Stoll, 2013). Furthermore, van de Wal et al. (2011) already showed that the relationship of CO₂ to temperature change during the last 20 Myr is opposite in sign for alkenone-based CO₂ than for other approaches.

The ice-albedo forcing $\Delta R_{[LI]}$ ~~has~~ in our simulation results based on 3-D ice-sheet models
440 (de Boer et al., 2014) has a specific relationship to global temperature change. Here both a step function or linear change in the polar amplification factor f_{pa} lead to similar results (Fig. 6b). However, when ~~not 3-D ice-sheet models (de Boer et al., 2014) as used here, but simpler~~ overly simplified ap-
proaches to calculate $\Delta R_{[LI]}$ are applied ~~;~~ (e.g. based on 1-D ice-sheet models (de Boer et al., 2010), related to sea level (Hansen et al., 2008; Martínez-Botí et al., 2015), or based on global land ice area
445 changes without considering their latitudinal changes in detail (Köhler et al., 2010; PALAEOSENS-Project Members, 2012; von der Heydt et al., 2014)) the $\Delta T_g - \Delta R_{[LI]}$ -relationship is more linear. The range of $\Delta R_{[LI]}$ proposed for the same range of ΔT_g is then reduced by 30 % (Fig. 6b and c). $\Delta R_{[LI]}$ is effected by ice-sheet area rather than ice sheet volume. 3-D ice-sheet models include this effect better than calculations based on 1-D ice sheet models or directly from sea level variations.
450 This non-linearity between ice volume (or sea level) and ice area is supported by data and theory of the scaling of glaciers (Bahr, 1997; Bahr et al., 2015). In addition, latitudinal variation of land-ice

distribution **affect-affects** the radiative forcing $\Delta R_{[LI]}$ in a non-linear way (Fig. 1), and thereby likely contributes to a state-dependency in the equilibrium climate sensitivity $S_{[CO_2,LI]}$.

To verify the robustness of our findings with respect to the uncertainties attached to all data points we performed an additional sensitivity study by artificially reducing the uncertainties in ΔT_g ($\sigma_{\Delta T_g}$) and $\Delta R_{[CO_2,LI]}$ ($\sigma_{\Delta R}$) by a factor of 2 or 10. For both reduction factors we find statistically the same non-linearities in the ΔT_g - $\Delta R_{[CO_2,LI]}$ -scattered data than with the original uncertainties in all four CO_2 data sets (non-linearity in data sets based on CO_2 in ice cores and from Hönisch-lab, only linear if based on Foster- or Pagani-lab CO_2 data, Table 2). Our proposed state-dependency of $S_{[CO_2,LI]}$ is therefore independent of the assumed uncertainties. Any calculated value of $S_{[CO_2,LI]}$ nevertheless depends in detail on the assumed uncertainties in the underlying data. **1.3**

Since a first detection of any state-dependency in $S_{[CO_2,LI]}$ has already been performed for the ice core CO_2 data in von der Heydt et al. (2014) it is of interest to investigate which of our improvements with respect to this earlier analysis are most important. We therefore performed a further sensitivity study in which some of the three time series ΔT_g , $\Delta R_{[CO_2]}$, and $\Delta R_{[LI]}$ were identical to the approach of von der Heydt et al. (2014). However, since in this earlier study all data have been resampled to 100 yr, we have to pre-process these data sets prior to Monte-Carlo statistics to 2-kyr averages to match the temporal resolution of the 3-D ice-sheet models used here. In this additional analysis (Table 2) we find that even when all three data sets are substituted with those used in von der Heydt et al. (2014) we find a non-linearity in the ΔT_g - $\Delta R_{[CO_2,LI]}$ -scatter plot that points to a state-dependency in $S_{[CO_2,LI]}$. However, the r^2 is then 10% smaller than in our results indicating a weaker correlation between temperature change and radiative forcing and a 2nd order polynomial is sufficient to fit the data, while in our best guess these ice core based CO_2 data are best described by a 3rd order polynomial. If data are binned before analysis, similarly as in von der Heydt et al. (2014), we find a non-linearity in the scattered data only for the data sets used in this study, or when CO_2 is substituted by the previous time series, but not when the previous versions of $\Delta R_{[LI]}$, or ΔT_g are used. In these binned data both our improved time series of ΔT_g and $\Delta R_{[LI]}$ are necessary to generate this non-linearity indicating a state-dependency in $S_{[CO_2,LI]}$. The analysis of both studies are still in detail different (higher order polynomial versus piece-wise linear regressions) and therefore the absence of any non-linearity in the binned data when all three time series have been substituted by those from the previous study are not contradictory to our stated non-linearity. **1.2**

In model-based approaches the final radiative forcing ΔR including all feedbacks from an obtained temperature change leads to a different nomenclature in which temperature change is the independent variable, typically plotted on the x-axis (e.g. Bloch-Johnson et al., 2015). Our approach differs from those studies since feedbacks are not contained in ΔR (but in S) which we only understand as the forcing terms. Therefore, ΔR is in our study the independent variable that determines the background condition of the climate system. **2.first**

3.3 Calculating the specific equilibrium climate sensitivity $S_{[\text{CO}_2, \text{LI}]}$

490 The non-linear regression of the $\Delta T_g - \Delta R_{[\text{CO}_2, \text{LI}]}$ scatter plot revealed that both the ice core CO_2 and the Hönisch-lab data contain a state-dependency in $S_{[\text{CO}_2, \text{LI}]}$. As explained in Sect. 2.4 we analyse for both data sets the mean and uncertainty in $S_{[\text{CO}_2, \text{LI}]}$ from probability density functions for different background climate states represented by $\Delta R_{[\text{CO}_2, \text{LI}]}$ based on the point-wise results (Fig. 8). For both the Pagani and Foster data sets the slopes of the linear regression lines in $\Delta T_g -$
 495 $\Delta R_{[\text{CO}_2, \text{LI}]}$ might in principle be used to calculate $S_{[\text{CO}_2, \text{LI}]}$, ~~however~~. However both data sets have a rather large offset in the y direction (ΔT_g) (y interception is far away from the origin), that might bias these results. These offsets are nearly identical when calculations are based on the alternative global temperature changes ΔT_{g2} or ΔT_{g3} (Table 1). Note ~~;~~ that $S_{[\text{CO}_2, \text{LI}]}$ as calculated for each data point in Fig. 8 also contains 20 and 11 outsiders in the ice core and Hönisch data
 500 sets, respectively, that fall not in the most plausible range of $0.0 - 3.0 \text{ K W}^{-1} \text{ m}^2$. These outsiders are typically generated ~~;~~ when dividing smaller anomalies in ΔT_g and $\Delta R_{[\text{CO}_2, \text{LI}]}$ during interglacials, when already small uncertainties generate a large change in the ratio in $\Delta T_g \cdot \Delta R_{[\text{CO}_2, \text{LI}]}^{-1}$. They are neglected from further analysis.

$S_{[\text{CO}_2, \text{LI}]}$ based on the ice core and Hönisch-lab data ~~falls rarely~~ rarely falls below $0.8 \text{ K W}^{-1} \text{ m}^2$
 505 (Fig. 8). We distinguish in both data sets “cold” from “warm” conditions using the threshold of $\Delta R_{[\text{CO}_2, \text{LI}]} = -3.5 \text{ W m}^{-2}$ to make our results comparable to the piece-wise linear analysis of “warm” and “cold” periods in von der Heydt et al. (2014). For the ice core data of the last 0.8 Myr the $S_{[\text{CO}_2, \text{LI}]}$ is not normally distributed, but has a long tail towards higher values (Fig. 8c). However, this long tail is partially caused by data points with $\Delta R_{[\text{CO}_2, \text{LI}]}$ not far from 0 W m^{-2} , which
 510 are prone to high uncertainties. Only conditions during “cold” periods, representing glacial maxima, have a nearly Gaussian distribution in $S_{[\text{CO}_2, \text{LI}]}$ with a mean value of $1.05_{-0.21}^{+0.23} \text{ K W}^{-1} \text{ m}^2$. For “warm” periods the PDF is skewed with $S_{[\text{CO}_2, \text{LI}]} = 1.56_{-0.44}^{+0.60} \text{ K W}^{-1} \text{ m}^2$. Results based on the Hönisch data covering the last 2.1 Myr are nearly identical with $S_{[\text{CO}_2, \text{LI}]} = 1.07_{-0.24}^{+0.29} \text{ K W}^{-1} \text{ m}^2$ (“cold”) and $S_{[\text{CO}_2, \text{LI}]} = 1.51_{-0.55}^{+0.68} \text{ K W}^{-1} \text{ m}^2$ (“warm”). Both data sets thus consistently suggest
 515 that during Pleistocene warm periods $S_{[\text{CO}_2, \text{LI}]}$ was about $\sim 45\%$ larger than during Pleistocene cold periods.

In a piece-wise linear regression analysis of data covering the last 0.8 Myr a state-dependency in climate sensitivity was already detected (von der Heydt et al., 2014), including a rise in $S_{[\text{CO}_2, \text{LI}]}$ from $0.98 \pm 0.27 \text{ K W}^{-1} \text{ m}^2$ during “cold” periods to $1.34 \pm 0.12 \text{ K W}^{-1} \text{ m}^2$ during “warm” periods
 520 of the late Pleistocene. To allow a direct comparison with our study we here cite results shown in the Supplement of von der Heydt et al. (2014) in which the global temperature anomaly was similar to our ΔT_g . Some important details, however, of our study and the previous study (von der Heydt et al., 2014) differ because (i) the assumed changes in temperature and land ice albedo are based on different time series and (ii) we here use CO_2 as resampled to the 2 kyr temporal spacing of the 3-D
 525 ice-sheet models while all data are resampled at 100 years time steps and binned before analysis in

von der Heydt et al. (2014). Note, that we tested that data binning does not lead to large changes in our results and conclusions. Nevertheless, the calculated $S_{[\text{CO}_2, \text{LI}]}$ of the “cold” periods (von der Heydt et al., 2014) matches within the uncertainties our glacial values derived from the ice cores, but the values for the “warm” periods are smaller in the previous estimates of von der Heydt et al. (2014) than in our results (Fig. 9). This difference in the “warm” period for both studies is caused by the revised $\Delta R_{[\text{LI}]}$, which mainly leads to differences with respect to previous studies for intermediate glaciated and interglacial climates.

The calculated PDFs of $S_{[\text{CO}_2, \text{LI}]}$ (Fig. 9) based on ice cores or Hönisch-lab data are qualitatively the same if based on the alternative assumptions on polar amplification which also includes a case with a constant polar amplification during the Pleistocene. The mean values of the PDF of $S_{[\text{CO}_2, \text{LI}]}$ are then shifted by less than $0.15 \text{ K W}^{-1} \text{ m}^2$ for “cold” periods and by less than $0.25 \text{ K W}^{-1} \text{ m}^2$ for “warm” periods towards smaller values.

1.5

The 5 Myr-long data sets from the Foster- and Pagani-lab show no indication of state-dependency. One might argue that these 5 Myr-long time series should be split in times when large ice sheets in the NH were present or not, because their presence should have an influence on climate and its sensitivity. According to our simulation results (Fig. 1b) the appearance of large NH land ice first happened around 2.82 Myr BP, also the time which has be-been suggested by Sarinthein (2013) for the onset of NH land ice and when Martínez-Botí et al. (2015) found a pronounced decline in CO_2 . Note that the start of northern hemispheric glaciation in our 3-D ice-sheet simulations was first gradual and intensified around 2.7 Myr ago (Fig. 1b), in agreement with other studies (Raymo, 1994; Haug et al., 2005). We tested the Foster-lab data for any changes in the regression analysis, when the data set was split in two time windows, one with and one without NH ice sheets. We found significantly different relationships between temperature change and radiative forcing for most of the Pleistocene than for either an ice-free NH Pliocene (Foster-lab data 2.82–3.3 Myr BP) or all available Pliocene data (Foster-lab data 2.5–3.3 Myr BP) (Fig. 10). For the Pleistocene $\Delta T_g - \Delta R_{[\text{CO}_2, \text{LI}]}$ data are in themselves non-linear (thus $S_{[\text{CO}_2, \text{LI}]}$ is state dependent), and for the Pliocene the relationship seems to be linear (thus $S_{[\text{CO}_2, \text{LI}]}$ to be constant) over the time window. However, the fit through $\Delta T_g - \Delta R_{[\text{CO}_2, \text{LI}]}$ is of low quality ($r^2 = 0.04$ for 2.82–3.3 Myr BP and $r^2 = 0.23$ for 2.5–3.3 Myr BP) which prevents us from calculating any quantitative values of $S_{[\text{CO}_2, \text{LI}]}$ based on them. Remember, that in all regression analyses we consider the uncertainties in both x and y direction in all data points by the application of Monte-Carlo statistics, something which also distinguishes our approach from Martínez-Botí et al. (2015) and possibly contributes to different results.

Nevertheless, our data compilation clearly points to a regime shift in the climate system with different climate sensitivities before and after 2.82 Myr BP. From the available proxy-based data indicating CO_2 around 400 ppmv in large parts of the Pliocene, together with our simulated global temperature change of around 2 K and ice-sheet albedo forcing of about 0.5 W m^{-2} (Fig. 4) we can estimate that in the NH-ice free Pliocene $S_{[\text{CO}_2, \text{LI}]}$ was around $1 \text{ K W}^{-1} \text{ m}^2$, in agreement with

Martínez-Botí et al. (2015). This is of similar size as our results for full glacial conditions of most of the Pleistocene, but smaller than during intermediate glaciated to interglacial conditions of the late Pleistocene. A possible reason could be that in the warm Pliocene the sea ice-albedo feedback might have been weaker or even absent (von der Heydt et al., 2014), but some studies (Stevens and Bony, 2013; Fedorov et al., 2013) also suggest that processes are missing in state-of-the-art climate models. A recent study (Kirtland Turner, 2014) concluded that at the onset of the northern hemispheric glaciation a fundamental change in the interplay of the carbon cycle and the climate system occurred leading to a switch from in-phase glacial/interglacial changes in deep ocean $\delta^{18}\text{O}$ and $\delta^{13}\text{C}$ to anti-phase changes. If true such a change in the carbon cycle/climate system might also affect climate sensitivity.

A more direct calculation of the specific equilibrium climate sensitivity $S_{[\text{CO}_2,\text{LI}]}$ as a function of background climate state that goes beyond the PDFs provided so far is desirable but with the available data and within the given theoretical and methodological framework not yet possible.

1.7 2.first

4 Discussion

Martínez-Botí et al. (2015) recently analysed the ice core CO_2 and the new CO_2 data from the Foster-lab around the end of the Pliocene separately finding $S_{[\text{CO}_2,\text{LI}]}$ of 0.91 ± 0.10 and $1.01 \pm 0.19 \text{K W}^{-1} \text{m}^2$, respectively. Both results are within their uncertainties nearly indistinguishable, thus Martínez-Botí et al. (2015) concluded that $S_{[\text{CO}_2,\text{LI}]}$ is not state-dependent, since it did not change between Pliocene and Pleistocene. However, since they based the radiative forcing of land-ice albedo ($\Delta R_{[\text{LI}]}$) on a linear function of sea level they miss an important non-linearity of the climate system. We find that the large uncertainty in $\Delta R_{[\text{CO}_2]}$ might also be another reason for state-independency in $S_{[\text{CO}_2,\text{LI}]}$ in the Foster-lab data set. $S_{[\text{CO}_2,\text{LI}]}$ based on the ice core analysis of Martínez-Botí et al. (2015) is slightly smaller than our results based on the cold periods from the ice core data set (Fig. 9). This indicates that the information ~~;-which are-~~ which is relevant to suggest any state dependency in $S_{[\text{CO}_2,\text{LI}]}$ are mainly contained in data covering the so-called “warm” climates of the Pleistocene. Thus, especially the land-ice area distribution and $\Delta R_{[\text{LI}]}$ from intermediate glaciated states are important here. However, it should be emphasized that Martínez-Botí et al. (2015) never attempted to detect any state-dependency in $S_{[\text{CO}_2,\text{LI}]}$ within either the Pleistocene or the Pliocene data sets. In searching for non-linearities in the scattered data of ΔT_g versus $\Delta R_{[\text{CO}_2,\text{LI}]}$ by statistical methods we here go beyond their approach.

2.third

Comparing data-based estimates of $S_{[\text{CO}_2,\text{LI}]}$ directly with climate model results (e.g. Lunt et al., 2010) is not straightforward and in the following not performed, because in climate models only those processes considered explicitly as forcing will have an impact on calculated temperature change, while the data-based temperature reconstruction contains the effect of all processes (PALAEOSENS-Project Members, 2012). Furthermore, in Fedorov et al. (2013) climate simulation

600 results have been discussed to understand which processes and mechanisms were responsible for the spatially very heterogeneous changes observed during the last 5 Myr, e.g. the increase in the polar amplification factor over time. Since the results of Fedorov et al. (2013) were unable to explain all observations it was concluded that a combination of different dynamical feedbacks are underestimated in the climate models. We are not able to generate spatially explicit results. However, from our analysis we could conclude that equilibrium climate sensitivity represented by $S_{[\text{CO}_2, \text{LI}]}$ was a function of background climate state and probably changed dramatically between conditions with
605 and without Northern Hemisphere land ice.

The contribution of greenhouse gas radiative forcing and of seasonally and latitudinally variable incoming solar radiation to the simulated global temperature anomalies of the last eight interglacials have been analysed individually before (Yin and Berger, 2012). It was found that the greenhouse gas forcing was the main driver of the simulated temperature change with the incoming solar radiation amplifying or dampening its signal for all but one interglacials (Marine Isotope Stage (MIS) 7), with two interglacials (MIS 1 and MIS 19) having variations close to zero. Furthermore, they calculated the ECS (temperature rise for a doubling of CO_2) for the different interglacial background conditions and found ECS to decrease with increasing background temperature. A calculation of climate sensitivity for individual points in time has been performed before
615 (PALAEOSENS-Project Members, 2012) but has been rejected due to large uncertainties, mainly during interglacials since in the definition of S one then needs to calculate the ratio of two small numbers in ΔT_g , and $\Delta R_{[\text{CO}_2, \text{LI}]}$, which has typically a low signal-to-noise-ratio. At first glance this might seem contrary to our finding with larger climate sensitivity during late Pleistocene interglacials when compared to late Pleistocene full glacial conditions. However, as mentioned already in the
620 previous paragraph the comparison of (paleo) data-based calculations of S with ECS calculated from climate models is not directly possible. Furthermore, in our approach we include changes in land ice sheet (albedo forcing or $\Delta R_{[\text{LI}]}$) while Yin and Berger (2012) kept ice sheets at present state. When investigating $S_{[\text{CO}_2, \text{LI}]}$ over the whole range of climate states (from full glacial conditions to a warm Pliocene with a (nearly) ice-free northern hemisphere resulting in a variable forcing term $\Delta R_{[\text{LI}]}$) we
625 therefore probe a complete different climate regime, which is not directly comparable with results obtained from simulations of interglacials only.

1.1 1.8

There exist some intrinsic uncertainties in our approach based on the underlying data sets $\bar{\tau}$ which are not included in the Monte-Carlo statistic. For example, the global temperature anomaly in the LGM still disagrees between various approaches (Annan and Hargreaves, 2013; Schmittner et al.,
630 2011; Schmidt et al., 2014) and Pliocene sea level and ice sheet dynamics are still a matter of debate (Rohling et al., 2014; Dolan et al., 2015; Koenig et al., 2015; Rovere et al., 2014; de Boer et al., 2015). Taking these issues into account might lead to changes in our quantitative estimates, but not necessarily to a revision of our main finding of state-dependency in $S_{[\text{CO}_2, \text{LI}]}$. **A support of our findings** In the light of the existing uncertainties, our findings must be supported by other mod-

635 elling approaches ~~is in the light of the existing uncertainties nevertheless necessary~~ to come to firm
conclusions. Furthermore, our assumption that we can estimate equilibrium climate sensitivity from
paleo data implicitly assumes that these data represent predominately equilibrium climate states.
This might be a simplification, but since filtering out data points ~~in~~ in which temperature changed
abruptly ~~led~~ led to similar results (PALAEOSENS-Project Members, 2012), it should have only mi-
640 nor effect on the conclusions.

To calculate in detail the effect of climate change on temperature it would be important to also
include other forcing agents, e.g. CH₄, N₂O or aerosols. For the Pliocene strong chemistry-climate
feedbacks have been proposed (Unger and Yue, 2014) suggesting high ozone and aerosol levels and
potentially high CH₄ values. This implies that the relationship of CO₂ to other forcing agents might
645 have been different for cold climates of the late Pleistocene than for warm climates of the Pliocene.
Therefore, assumptions on the influence of other slow feedbacks based on data of the late Pleistocene
(Köhler et al., 2010) cannot be extrapolated to the Pliocene. Hence, we restrict our analysis of the
Pliocene data to $S_{[CO_2,LI]}$ and again emphasize that an estimate of climate sensitivity for “actuo” or
present day, S^a , from our paleo sensitivity (PALAEOSENS-Project Members, 2012) is ~~especially~~
650 ~~for those data not straight forward~~ not straightforward, especially for these data.

For the Pleistocene data we might roughly approximate the implications of our findings for equi-
librium temperature changes under CO₂ doubling, or ECS, by considering the so far neglected feed-
backs (CH₄, N₂O, aerosols, or vegetation). However, we are aware that this is a simplification, since
it was already shown that the per unit radiative forcing climate effect of well-mixed greenhouse
655 gases and aerosols differs (Shindell, 2014). In paleo-data of the last 0.8 Myr the equilibrium climate
sensitivity considering all feedbacks was only about two thirds of $S_{[CO_2,LI]}$ (PALAEOSENS-Project
Members, 2012). A CO₂ doubling would then lead to an equilibrium rise in global temperature
of on average 2.5 K (68 % probability range: 2.0–3.5 K) or to on average 3.7 K (68 % probability
range: 2.5–5.5 K) during Pleistocene full glacial climates (“cold”) or Pleistocene “warm” climates
660 (intermediate glaciated to interglacial conditions), respectively. Both average values of ECS are well
within the range proposed by paleo data and models so far (PALAEOSENS-Project Members, 2012;
Stocker et al., 2013), but we especially emphasise the potential existence of a long tail of $S_{[CO_2,LI]}$
towards higher values. Such estimates of ECS are due to the different effect of various forcings very
uncertain and for Pliocene climate states not yet possible (see above). These long-term temperature
665 change estimates for a doubling of CO₂ are mainly of interest for model validation. To be appli-
cable to the not so distant future these equilibrium estimates need to be corrected for oceanic heat
uptake to calculate any transient temperature response (Zeebe, 2013). Whether climate in the future
is more comparable to climate states of interglacials of the late Pleistocene or to the warm Pliocene
is difficult to say, although this has, according to our results, major implications for the expected
670 equilibrium temperature rise. ~~For projected future greenhouse gas emissions the~~ The Greenland ice
sheet might completely dissappear (Levermann et al., 2013) on the long-term for the projected future

greenhouse gas emissions, but it ~~is projected to~~ might reduce its ice volume in the next two thousand years by less than 50%. ~~This suggests that for~~ Another study (Loutre and Berger, 2000) suggests that the Greenland ice sheet might also disappear on the long run for atmospheric CO₂ concentrations between 200 and 300 pmmv. These studies suggest that for the coming millennia the Earth ~~still~~ contains ~~might still~~ contain a significant amount of northern hemispheric land ice and thus climate and the proposed climate sensitivity $S_{[\text{CO}_2, \text{LI}]}$ are probably more comparable to interglacials of the late Pleistocene, before the system ~~switches~~ might switch in the more distant future towards an ice-free Northern Hemisphere more comparable to the warm Pliocene.

1.15

When compared to the two most recent contributions to this topic (von der Heydt et al., 2014; Martínez-Botí et al., 2015) our study goes beyond them by four improvements that have been layed out in detail in the introduction. The most important of these improvements is the systematical detection of state-dependency in $S_{[\text{CO}_2, \text{LI}]}$ using Monte-Carlo statistics. However, only by analysing more data we have been able to extend the finding of state-dependency in $S_{[\text{CO}_2, \text{LI}]}$ from the ice core data of the last 800kyr to the last 2.1Myr. Furthermore, the improvements in the underlying time series of $\Delta R_{[\text{LI}]}$ have been important to obtain a data set in which the state-dependency $S_{[\text{CO}_2, \text{LI}]}$ can be detected. The role of the ΔT_g time series seems at first glance to be of similar importance than that of $\Delta R_{[\text{LI}]}$. However, state-dependency in $S_{[\text{CO}_2, \text{LI}]}$ was also obtained for the alternative temperature time series ΔT_{g2} or ΔT_{g3} and therefore a detailed knowledge of ΔT_g is of minor importance for our overall conclusions.

1.1 1.2

5 Conclusions

In conclusion, we find that the specific equilibrium climate sensitivity based on radiative forcing of CO₂ and land ice albedo, $S_{[\text{CO}_2, \text{LI}]}$, is state-dependent, if CO₂ data from ice cores or from the Hönisch-lab, based on $\delta^{11}\text{B}$, are analysed. The state-dependency arises from the non-linear relationship between changes in radiative forcing of land ice albedo, $\Delta R_{[\text{LI}]}$, and changes in global temperature. Previous studies were not able to detect such a state-dependency because land ice albedo forcing was not based on results from 3-D ice-sheet models which contain much of this non-linearity. So far, the state-dependency of $S_{[\text{CO}_2, \text{LI}]}$ based on ice core CO₂, which was derived from predominantly glacial conditions of the late Pleistocene, can be extrapolated to the last 2.1Myr. During intermediate glaciated and interglacial periods of most of the Pleistocene $S_{[\text{CO}_2, \text{LI}]}$ was on average by about $\sim 45\%$ higher (mean: $1.54 \text{ K W}^{-1} \text{ m}^2$; 68% probability range: $1.0\text{--}2.2 \text{ K W}^{-1} \text{ m}^2$) than during full glacial conditions of the Pleistocene (mean $1.06 \text{ K W}^{-1} \text{ m}^2$; 68% probability range: $0.8\text{--}1.4 \text{ K W}^{-1} \text{ m}^2$). ~~Data uncertainties for the Pliocene do not allow~~ Before 2.1 Myr BP the published CO₂ data are too sparse, depend on the applied methodology, and have too large uncertainties to come to a statistically well-supported conclusion on the value of $S_{[\text{CO}_2, \text{LI}]}$. The data available so far

1.13

suggest that the appearance of northern hemispheric land-ice sheets changed the climate system and accordingly influenced climate sensitivity. In the Pliocene, $S_{[\text{CO}_2, \text{LI}]}$ was therefore probably smaller than during interglacials of the Pleistocene.

710 *Acknowledgements.* PMIP3 model output was derived from the LGM scenarios of CMIP5, PlioMIP model
out from uploaded results published of its large scale features (Haywood et al., 2013). We acknowledge the
World Climate Research Programme’s Working Group on Coupled Modelling, which is responsible for CMIP.
For CMIP the US Department of Energy’s Program for Climate Model Diagnosis and Intercomparison provides
coordinating support and led development of software infrastructure in partnership with the Global Organization
715 for Earth System Science Portals. We thank the climate modeling groups from which we took results from
both PMIP3 and PlioMIP as available mid January 2014 and as listed in the Methods Section of this paper
for producing and making available their model output. We also thank G. Foster for providing CO₂ data and
comments on our manuscript, B. Hönlisch for insights to the measurements of the Bartoli data set and G. Knorr
and J. Bijma for helpful comments. Financial support for B. de Boer was partially provided through the NWO-
720 VICI grant of L. J. Lourens. L. Stap was funded by NWO-ALW. This paper contributes to the program of
the Netherlands Earth System Science Centre (NESSC), financially supported by the Ministry of Education,
Culture and Science (OCW). Data sets of ΔT_g and $\Delta R_{[\text{LI}]}$ will be available from www.pangaea.de.

References

- Abe-Ouchi, A., Segawa, T., and Saito, F.: Climatic Conditions for modelling the Northern Hemisphere ice sheets throughout the ice age cycle, *Clim. Past*, 3, 423–438, doi:10.5194/cp-3-423-2007, 2007.
- 725 Ahn, J. and Brook, E. J.: Siple Dome ice reveals two modes of millennial CO₂ change during the last ice age, *Nature Communications*, 5, 3723, doi:10.1038/ncomms4723, 2014.
- Allen, K. A., Hönisch, B., Eggins, S. M., and Rosenthal, Y.: Environmental controls on B/Ca in calcite tests of the tropical planktic foraminifer species *Globigerinoides ruber* and *Globigerinoides sacculifer*, *Earth Planet. Sc. Lett.*, 351–352, 270–280, doi:10.1016/j.epsl.2012.07.004, 2012.
- 730 Annan, J. D. and Hargreaves, J. C.: A new global reconstruction of temperature changes at the Last Glacial Maximum, *Clim. Past*, 9, 367–376, doi:10.5194/cp-9-367-2013, 2013.
- Badger, M. P. S., Schmidt, D. N., Mackensen, A., and Pancost, R. D.: High-resolution alkenone palaeobarometry indicates relatively stable *p*CO₂ during the Pliocene (3.3–2.8 Ma), *Philos. T. R. Soc. A*, 371, doi:10.1098/rsta.2013.0094, 2013.
- 735 Bahr, D. B.: Global distributions of glacier properties: a stochastic scaling paradigm, *Water Resour. Res.*, 33, 1669–1679, doi:10.1029/97WR00824, 1997.
- Bahr, D. B., Pfeffer, W. T., and Kaser, G.: A review of volume-area scaling of glaciers, *Rev. Geophys.*, 53, 95–140, doi:10.1002/2014RG000470, 2015.
- 740 Bartoli, G., Hönisch, B., and Zeebe, R. E.: Atmospheric CO₂ decline during the Pliocene intensification of Northern Hemisphere glaciations, *Paleoceanography*, 26, PA4213, doi:10.1029/2010PA002055, 2011.
- Berling, D. J. and Royer, D. L.: Convergent Cenozoic CO₂ history, *Nat. Geosci.*, 4, 418–420, doi:10.1038/ngeo1186, 2011.
- Bereiter, B., Lüthi, D., Siegrist, M., Schüpbach, S., Stocker, T. F., and Fischer, H.: Mode change of millennial CO₂ variability during the last glacial cycle associated with a bipolar marine carbon seesaw, *P. Natl. Acad. Sci. USA*, 109, 9755–9760, doi:10.1073/pnas.1204069109, 2012.
- 745 Bereiter, B., Eggleston, S., Schmitt, J., Nehrbass-Ahles, C., Stocker, T. F., Fischer, H., Kipfstuhl, S., and Chappellaz, J.: Revision of the EPICA Dome C CO₂ record from 800 to 600 kyr before present, *Geophys. Res. Lett.*, 42, 542–549, doi:10.1002/2014GL061957, 2015.
- [Borch-Johnson, J., Pierrehumbert, R. T., and Abbot, D. S.: Feedback temperature dependence determines the risk of high warming, *Geophysical Research Letters*, 42, 4973–4980, doi:10.1002/2015GL064240, 2015.](#)
- Bolton, C. T. and Stoll, H. M.: Late Miocene threshold response of marine algae to carbon dioxide limitation, *Nature*, 500, 558–562, doi:10.1038/nature12448, 2013.
- Braconnot, P., Harrison, S. P., Kageyama, M., Bartlein, P. J., Masson-Delmotte, V., Abe-Ouchi, A., Otto-Bliesner, B., and Zhao, Y.: Evaluation of climate models using palaeoclimatic data, *Nature Climate Change*, 2, 417–424, doi:10.1038/nclimate1456, 2012.
- 755 Caballero, R. and Huber, M.: State-dependent climate sensitivity in past warm climates and its implications for future climate projections, *P. Natl. Acad. Sci. USA*, 110, 14162–14167, doi:10.1073/pnas.1303365110, 2013.
- 760 Crucifix, M.: Does the Last Glacial Maximum constrain climate sensitivity?, *Geophys. Res. Lett.*, 33, L18701, doi:10.1029/2006GL027137, 2006.

- de Boer, B., van de Wal, R. S. W., Bintanja, R., Lourens, L. J., and Tunter, E.: Cenozoic global ice volume and temperature simulations with 1-D ice-sheet models forced by $\delta^{18}\text{O}$ records, *Ann. Glaciol.*, 51, 23–33, doi:10.3189/172756410791392736, 2010.
- 765 de Boer, B., van de Wal, R., Lourens, L., Bintanja, R., and Reerink, T.: A continuous simulation of global ice volume over the past 1 million years with 3-D ice-sheet models, *Climate Dynamics*, 41, 1365–1384, doi:10.1007/s00382-012-1562-2, 2013.
- de Boer, B., Lourens, L. J., and van de Wal, R. S.: Persistent 400,000-year variability of Antarctic ice volume and the carbon cycle is revealed throughout the Plio–Pleistocene, *Nature Communications*, 5, 2999, doi:10.1038/ncomms3999, 2014.
- 770 de Boer, B., Dolan, A. M., Bernales, J., Gasson, E., Goelzer, H., Golledge, N. R., Sutter, J., Huybrechts, P., Lohmann, G., Rogozhina, I., Abe-Ouchi, A., Saito, F., and van de Wal, R. S. W.: Simulating the Antarctic ice sheet in the late-Pliocene warm period: PLISMIP-ANT, an ice-sheet model intercomparison project, *The Cryosphere*, 9, 881–903, doi:10.5194/tc-9-881-2015, 2015.
- 775 Dolan, A. M., Hunter, S. J., Hill, D. J., Haywood, A. M., Koenig, S. J., Otto-Bliesner, B. L., Abe-Ouchi, A., Bragg, F., Chan, W.-L., Chandler, M. A., Contoux, C., Jost, A., Kamae, Y., Lohmann, G., Lunt, D. J., Ramstein, G., Rosenbloom, N. A., Sohl, L., Stepanek, C., Ueda, H., Yan, Q., and Zhang, Z.: Using results from the PlioMIP ensemble to investigate the Greenland Ice Sheet during the mid-Pliocene Warm Period, *Clim. Past*, 11, 403–424, doi:10.5194/cp-11-403-2015, 2015.
- 780 Fedorov, A. V., Brierley, C. M., Lawrence, K. T., Liu, Z., Dekens, P. S., and Ravelo, A. C.: Patterns and mechanisms of early Pliocene warmth, *Nature*, 496, 43–49, doi:10.1038/nature12003, 2013.
- Forster, P., Ramaswamy, V., Artaxo, P., Bernsten, T., Betts, R., Fahey, D., Haywood, J., Lean, J., Lowe, D., Myhre, G., Nganga, J., Prinn, R., Raga, G., Schulz, M., and Dorland, R. V.: Changes in atmospheric constituents and in radiative forcing, in: *Climate Change 2007: The Physical Science Basis. Contribution of Working Group I to the Fourth Assessment Report of the Intergovernmental Panel on Climate Change*, edited by: Solomon, S., Qin, D., Manning, M., Chen, Z., Marquis, M., Averyt, K. B., Tignor, M., and Miller, H. L., Cambridge University Press, Cambridge, UK and New York, NY, USA, 129–234, 2007.
- 785 Foster, G. L.: Seawater pH, $p\text{CO}_2$ and $[\text{CO}_3^{2-}]$ variations in the Caribbean Sea over the last 130 kyr: a boron isotope and B/Ca study of planktic foraminifera, *Earth Planet. Sc. Lett.*, 271, 254–266, 2008.
- 790 Goldner, A., Huber, M., and Caballero, R.: Does Antarctic glaciation cool the world?, *Clim. Past*, 9, 173–189, doi:10.5194/cp-9-173-2013, 2013.
- Hansen, J., Sato, M., Kharecha, P., Beerling, D., Berner, R., Masson-Delmotte, V., Pagani, M., Raymo, M., Royer, D. L., and Zachos, J. C.: Target atmospheric CO_2 : where should humanity aim?, *The Open Atmospheric Science Journal*, 2, 217–231, doi:10.2174/1874282300802010217, 2008.
- 795 Hansen, J., Sato, M., Russell, G., and Kharecha, P.: Climate sensitivity, sea level and atmospheric carbon dioxide, *Philos. T. R. Soc. A*, 371, doi:10.1098/rsta.2012.0294, 2013.
- Hargreaves, J. C., Abe-Ouchi, A., and Annan, J. D.: Linking glacial and future climates through an ensemble of GCM simulations, *Clim. Past*, 3, 77–87, doi:10.5194/cp-3-77-2007, 2007.
- Haug, G. H., Ganopolski, A., Sigman, D. M., Rosell-Mele, A., Swann, G. E. A., Tiedemann, R., Jaccard, S. L., 800 Bollamnn, J., maslin, M. A., Leng, M. J., and Eglinton, G.: North Pacific seasonality and the glaciation of North America 2.7 million years ago, *Nature*, 433, 821–825, 2005.

- Hays, J. D., Imbrie, J., and Shackelton, N. J.: Variations in the Earth's orbit: pacemaker of the ice ages, *Science*, 194, 1121–1132, 1976.
- Haywood, A. M., Dowsett, H. J., Otto-Bliesner, B., Chandler, M. A., Dolan, A. M., Hill, D. J., Lunt, D. J.,
805 Robinson, M. M., Rosenbloom, N., Salzmann, U., and Sohl, L. E.: Pliocene Model Intercomparison Project (PlioMIP): experimental design and boundary conditions (Experiment 1), *Geosci. Model Dev.*, 3, 227–242, doi:10.5194/gmd-3-227-2010, 2010.
- Haywood, A. M., Hill, D. J., Dolan, A. M., Otto-Bliesner, B. L., Bragg, F., Chan, W.-L., Chandler, M. A.,
Contoux, C., Dowsett, H. J., Jost, A., Kamae, Y., Lohmann, G., Lunt, D. J., Abe-Ouchi, A., Pickering, S. J.,
810 Ramstein, G., Rosenbloom, N. A., Salzmann, U., Sohl, L., Stepanek, C., Ueda, H., Yan, Q., and Zhang, Z.: Large-scale features of Pliocene climate: results from the Pliocene Model Intercomparison Project, *Clim. Past*, 9, 191–209, doi:10.5194/cp-9-191-2013, 2013.
- Herbert, T. D., Peterson, L. C., Lawrence, K. T., and Liu, Z.: Tropical Ocean temperatures over the past 3.5 million years, *Science*, 328, 1530–1534, doi:10.1126/science.1185435, 2010.
- 815 Hönisch, B., Hemming, N. G., Archer, D., Siddall, M., and McManus, J. F.: Atmospheric carbon dioxide concentration across the Mid-Pleistocene Transition, *Science*, 324, 1551–1554, doi:10.1126/science.1171477, 2009.
- Kirtland Turner, S.: Pliocene switch in orbital-scale carbon cycle/climate dynamics, *Paleoceanography*, 29, 1256–1266, doi:10.1002/2014PA002651, 2014.
- [Knutti, R. and Rugenstein, M. A. A.: Feedbacks, climate sensitivity and the limits of linear models, Philosophical Transactions of the Royal Society of London A: Mathematical, Physical and Engineering Sciences, 373, 20150146, doi:10.1098/rsta.2015.0146, 2015.](#)
- Koenig, S. J., Dolan, A. M., de Boer, B., Stone, E. J., Hill, D. J., DeConto, R. M., Abe-Ouchi, A., Lunt, D. J.,
Pollard, D., Quiquet, A., Saito, F., Savage, J., and van de Wal, R.: Ice sheet model dependency of the simulated
825 Greenland Ice Sheet in the mid-Pliocene, *Clim. Past*, 11, 369–381, doi:10.5194/cp-11-369-2015, 2015.
- Köhler, P., Bintanja, R., Fischer, H., Joos, F., Knutti, R., Lohmann, G., and Masson-Delmotte, V.: What caused Earth's temperature variations during the last 800,000 years? Data-based evidences on radiative forcing and constraints on climate sensitivity, *Quaternary Sci. Rev.*, 29, 129–145, doi:10.1016/j.quascirev.2009.09.026, 2010.
- 830 Kopp, G. and Lean, J. L.: A new, lower value of total solar irradiance: evidence and climate significance, *Geophys. Res. Lett.*, 38, L01706, doi:10.1029/2010GL045777, 2011.
- Kutzbach, J. E., He, F., Vavrus, S. J., and Ruddiman, W. F.: The dependence of equilibrium climate sensitivity on climate state: applications to studies of climates colder than present, *Geophys. Res. Lett.*, 40, 3721–3726, doi:10.1002/grl.50724, 2013.
- 835 Laskar, J., Robutel, P., Joutel, F., Gastineau, M., Correia, A. C. M., and Levrard, B.: A long term numerical solution for the insolation quantities of the Earth, *Astron. Astrophys.*, 428, 261–285, doi:10.1051/0004-6361:20041335, 2004.
- Lawrence, K. T., Herbert, T. D., Brown, C. M., Raymo, M. E., and Haywood, A. M.: High-amplitude variations in North Atlantic sea surface temperature during the early Pliocene warm period, *Paleoceanography*, 24,
840 PA2218, doi:10.1029/2008PA001669, 2009.

- Levermann, A., Clark, P. U., Marzeion, B., Milne, G. A., Pollard, D., Radic, V., and Robinson, A.: The multimillennial sea-level commitment of global warming, *P. Natl. Acad. Sci. USA*, 110, 13745–13750, doi:10.1073/pnas.1219414110, 2013.
- 845 Lisiecki, L. E. and Raymo, M. E.: A Pliocene–Pleistocene stack of 57 globally distributed benthic $\delta^{18}\text{O}$ records, *Paleoceanography*, 20, PA1003, doi:10.1029/2004PA001071, 2005.
- Loutre, M. and Berger, A.: Future Climatic Changes: Are We Entering an Exceptionally Long Interglacial? Climatic Change, 46, 61–90, doi:10.1023/A:1005559827189, 2000.
- Lunt, D. J., Haywood, A. M., Schmidt, G. A., Salzmann, U., Valdes, P. J., and Dowsett, H. J.: Earth system sensitivity inferred from Pliocene modelling and data, *Nat. Geosci.*, 3, 60–64, doi:10.1038/ngeo706, 2010.
- 850 MacFarling-Meure, C., Etheridge, D., Trudinger, C., Langenfelds, R., van Ommen, T., Smith, A., and Elkins, J.: Law Dome CO_2 , CH_4 and N_2O ice core records extended to 2000 years BP, *Geophys. Res. Lett.*, 33, L14810, doi:10.1029/2006GL026152, 2006.
- Marcott, S. A., Bauska, T. K., Buizert, C., Steig, E. J., Rosen, J. L., Cuffey, K. M., Fudge, T. J., Severinghaus, J. P., Ahn, J., Kalk, M. L., McConnell, J. R., Sowers, T., Taylor, K. C., White, J. W., and Brook, E. J.: 855 Centennial scale changes in the global carbon cycle during the last deglaciation, *Nature*, 514, 616–619, doi:10.1038/nature13799, 2014.
- Martínez-Botí, M. A., Foster, G. L., Chalk, T. B., Rohling, E. J., Sexton, P. F., Lunt, D. J., Pancost, R. D., Badger, M. P. S., and Schmidt, D. N.: Plio–Pleistocene climate sensitivity evaluated using high-resolution CO_2 records, *Nature*, 518, 49–54, doi:10.1038/nature14145, 2015.
- 860 Martínez-García, A., Rosell-Melé, A., McClymont, E. L., Gersonde, R., and Haug, G. H.: Subpolar link to the emergence of the modern equatorial Pacific cold tongue, *Science*, 328, 1550–1553, doi:10.1126/science.1184480, 2010.
- Masson-Delmotte, V., Kageyama, M., Braconnot, P., Charbit, S., Krinner, G., Ritz, C., Guilyardi, E., Jouzel, J., Abe-Ouchi, A., Cruci, M., Gladstone, R. M., Hewitt, C. D., Kitoh, A., LeGrande, A. N., Marti, O., Merkel, U., 865 Ohgaito, T. M. R., Otto-Bliesner, B., Peltier, W. R., Ross, I., Valdes, P. J., Vettoretti, G., Weber, S. L., Wolk, F., and YU, Y.: Past and future polar amplification of climate change: climate model intercomparisons and ice-core constraints, *Clim. Dynam.*, 26, 513–529, 2006.
- Meraner, K., Mauritsen, T., and Voigt, A.: Robust increase in equilibrium climate sensitivity under global warming, *Geophys. Res. Lett.*, 40, 5944–5948, doi:10.1002/2013GL058118, 2013.
- 870 Milankovitch, M.: *Kanon der Erdbestrahlung und seine Anwendung auf das Eiszeitenproblem*, Special Publications Vol. 132, vol. 33 of Section Mathematics and Natural Sciences, Royal Serbian Acadademy, Belgrad, 1941.
- Monnin, E., Indermühle, A., Dällenbach, A., Flückiger, J., Stauffer, B., Stocker, T. F., Raynaud, D., and Barnola, J.-M.: Atmospheric CO_2 concentrations over the last glacial termination, *Science*, 291, 112–114, 875 doi:10.1126/science.291.5501.112, 2001.
- Monnin, E., Steig, E. J., Siegenthaler, U., Kawamura, K., Schwander, J., Stauffer, B., Stocker, T. F., Morse, D. L., Barnola, J.-M., Bellier, B., Raynaud, D., and Fischer, H.: Evidence for substantial accumulation rate variability in Antarctica during the Holocene, through synchronization of CO_2 in the Taylor Dome, Dome C and DML ice cores, *Earth Planet. Sc. Lett.*, 224, 45–54, 2004.

- 880 Myhre, G., Highwood, E. J., Shine, K. P., and Stordal, F.: New estimates of radiative forcing due to well mixed greenhouse gases, *Geophys. Res. Lett.*, 25, 2715–2718, 1998.
- Nowack, P. J., Luke Abraham, N., Maycock, A. C., Braesicke, P., Gregory, J. M., Joshi, M. M., Osprey, A., and Pyle, J. A.: A large ozone-circulation feedback and its implications for global warming assessments, *Nature Climate Change*, 5, 41–45, doi:10.1038/nclimate2451, 2015.
- 885 Pagani, M., Liu, Z., LaRiviere, J., and Ravelo, A. C.: High Earth-system climate sensitivity determined from Pliocene carbon dioxide concentrations, *Nat. Geosci.*, 3, 27–30, doi:10.1038/ngeo724, 2010.
- PALAEOSSENS-Project Members: Making sense of palaeoclimate sensitivity, *Nature*, 491, 683–691, doi:10.1038/nature11574, 2012.
- Peltier, W. R.: Global glacial isostasy and the surface of the ice-age Earth: the ICE-5G (VM2) model and
890 GRACE, *Annu. Rev. Earth Pl. Sc.*, 32, 111–149, doi:10.1146/annurev.earth.32.082503.144359, 2004.
- Peltier, W. R., Argus, D. F., and Drummond, R.: Space geodesy constrains ice age terminal deglaciation: the global ICE-6G_C (VM5a) model, *J. Geophys. Res.-Sol. Ea.*, 120, 450–487, doi:10.1002/2014JB011176, 2015.
- Petit, J. R., Jouzel, J., Raynaud, D., Barkov, N. I., Barnola, J.-M., Basile, I., Bender, M., Chappellaz, J.,
895 Davis, M., Delaygue, G., Delmotte, M., Kotlyakov, V. M., Legrand, M., Lipenkov, V. Y., Lorius, C., Pépin, L., Ritz, C., Saltzman, E., and Stievenard, M.: Climate and atmospheric history of the past 420,000 years from the Vostok ice core, Antarctica, *Nature*, 399, 429–436, 1999.
- Press, W. H., Teukolsky, S. A., Vetterling, W. T., and Flannery, B. P.: *Numerical Recipes in Fortran*, second edition, Cambridge University Press, Cambridge, 1992.
- 900 Raymo, M. E.: The initiation of Northern Hemisphere glaciation, *Annu. Rev. Earth Pl. Sc.*, 22, 353–383, 1994.
- Rohling, E. J., Foster, G. L., Grant, K. M., Marino, G., Roberts, A. P., Tamisiea, M. E., and Williams, F.: Sea-level and deep-sea-temperature variability over the past 5.3 million years, *Nature*, 508, 477–482, doi:10.1038/nature13230, 2014.
- Roth, R. and Joos, F.: A reconstruction of radiocarbon production and total solar irradiance from the
905 Holocene ¹⁴C and CO₂ records: implications of data and model uncertainties, *Clim. Past*, 9, 1879–1909, doi:10.5194/cp-9-1879-2013, 2013.
- Rovere, A., Raymo, M., Mitrovica, J., Hearty, P., O’Leary, M., and Inglis, J.: The Mid-Pliocene sea-level conundrum: Glacial isostasy, eustasy and dynamic topography, *Earth Planet. Sc. Lett.*, 387, 27–33, doi:10.1016/j.epsl.2013.10.030, 2014.
- 910 Rubino, M., Etheridge, D. M., Trudinger, C. M., Allison, C. E., Battle, M. O., Langenfelds, R. L., Steele, L. P., Curran, M., Bender, M., White, J. W. C., Jenk, T. M., Blunier, T., and Francey, R. J.: A revised 1000-year atmospheric $\delta^{13}\text{C}$ -CO₂ record from Law Dome and South Pole, Antarctica, *J. Geophys. Res.-Atmos.*, 118, 8482–8499, doi:10.1002/jgrd.50668, 2013.
- Sarnthein, M.: Transition from late Neogene to early Quaternary environments, in: *The Encyclopedia of Quaternary Science*, vol. 2, edited by: Elias, S., Elsevier, Amsterdam, 151–166, 2013.
- 915 Schmidt, G. A., Annan, J. D., Bartlein, P. J., Cook, B. I., Guilyardi, E., Hargreaves, J. C., Harrison, S. P., Kageyama, M., LeGrande, A. N., Konecky, B., Lovejoy, S., Mann, M. E., Masson-Delmotte, V., Risi, C., Thompson, D., Timmermann, A., Tremblay, L.-B., and Yiou, P.: Using palaeo-climate comparisons to constrain future projections in CMIP5, *Clim. Past*, 10, 221–250, doi:10.5194/cp-10-221-2014, 2014.

- 920 Schmittner, A., Urban, N. M., Shakun, J. D., Mahowald, N. M., Clark, P. U., Bartlein, P. J., Mix, A. C., and
Rosell-Melé, A.: Climate sensitivity estimated from temperature reconstructions of the Last Glacial Maxi-
mum, *Science*, 334, 1385–1388, doi:10.1126/science.1203513, 2011.
- Schneider, R., Schmitt, J., Köhler, P., Joos, F., and Fischer, H.: A reconstruction of atmospheric carbon dioxide
and its stable carbon isotopic composition from the penultimate glacial maximum to the last glacial inception,
925 *Clim. Past*, 9, 2507–2523, doi:10.5194/cp-9-2507-2013, 2013.
- Seki, O., Foster, G. L., Schmidt, D. N., Mackensen, A., Kawamura, K., and Pancost, R. D.: Alkenone and
boron-based Pliocene $p\text{CO}_2$ records, *Earth Planet. Sc. Lett.*, 292, 201–211, doi:10.1016/j.epsl.2010.01.037,
2010.
- Shindell, D. T.: Inhomogeneous forcing and transient climate sensitivity, *Nature Climate Change*, 4, 274–277,
930 doi:10.1038/nclimate2136, 2014.
- Siegenthaler, U., Stocker, T. F., Monnin, E., Lüthi, D., Schwander, J., Stauffer, B., Raynaud, D., Barnola, J.-M.,
Fischer, H., Masson-Delmotte, V., and Jouzel, J.: Stable carbon cycle–climate relationship during the late
Pleistocene, *Science*, 310, 1313–1317, doi:10.1126/science.1120130, 2005.
- Singarayer, J. S. and Valdes, P. J.: High-latitude climate sensitivity to ice-sheet forcing over the last 120 kyr,
935 *Quaternary Sci. Rev.*, 29, 43–55, doi:10.1016/j.quascirev.2009.10.011, 2010.
- Stap, L. B., van de Wal, R. S. W., de Boer, B., Bintanja, R., and Lourens, L. J.: Interaction of ice sheets and
climate during the past 800 000 years, *Clim. Past*, 10, 2135–2152, doi:10.5194/cp-10-2135-2014, 2014.
- Stevens, B. and Bony, S.: What are climate models missing?, *Science*, 340, 1053–1054,
doi:10.1126/science.1237554, 2013.
- 940 Stocker, T. F., Qin, D., Tignor, G.-K. P. M., Allen, S., Boschung, J., Nauels, A., Xia, Y., Bex, V., and Midgley, P.
(Eds.): IPCC, 2013: Climate Change 2013: The Physical Science Basis. Contribution of Working Group I
to the Fifth Assessment Report of the Intergovernmental Panel on Climate Change, Cambridge University
Press, Cambridge, UK and New York, NY, USA, 2013.
- Tripati, A. K., Roberts, C. D., and Eagle, R. A.: Coupling of CO_2 and ice sheet stability over major climate
945 transitions of the last 20 million years, *Science*, 326, 1394–1397, doi:10.1126/science.1178296, 2009.
- Unger, N. and Yue, X.: Strong chemistry–climate feedbacks in the Pliocene, *Geophys. Res. Lett.*, 41, 527–533,
doi:10.1002/2013GL058773, 2014.
- van de Wal, R. S. W., de Boer, B., Lourens, L. J., Köhler, P., and Bintanja, R.: Reconstruction of a continuous
high-resolution CO_2 record over the past 20 million years, *Clim. Past*, 7, 1459–1469, doi:10.5194/cp-7-1459-
950 2011, 2011.
- Vial, J., Dufresne, J.-L., and Bony, S.: On the interpretation of inter-model spread in CMIP5 climate sensitivity
estimates, *Clim. Dynam.*, 41, 3339–3362, doi:10.1007/s00382-013-1725-9, 2013.
- von der Heydt, A. S., Köhler, P., van de Wal, R. S., and Dijkstra, H. A.: On the state dependency of fast feedback
processes in (paleo) climate sensitivity, *Geophys. Res. Lett.*, 41, 6484–6492, doi:10.1002/2014GL061121,
955 2014.
- Yin, Q. and Berger, A.: Individual contribution of insolation and CO_2 to the interglacial climates of the past
800,000 years, *Climate Dynamics*, 38, 709–724, doi:10.1007/s00382-011-1013-5, 2012.
- Yoshimori, M., Yokohata, T., and Abe-Ouchi, A.: A comparison of climate feedback strength between CO_2
doubling and LGM experiments, *J. Climate*, 22, 3374–3395, doi:10.1175/2009JCLI2801.1, 2009.

- 960 Yoshimori, M., Hargreaves, J. C., Annan, J. D., Yokohata, T., and Abe-Ouchi, A.: Dependency of
feedbacks on forcing and climate state in physics parameter ensembles, *J. Climate*, 24, 6440–6455,
doi:10.1175/2011JCLI3954.1, 2011.
- Zeebe, R. E.: Time-dependent climate sensitivity and the legacy of anthropogenic greenhouse gas emissions,
P. Natl. Acad. Sci. USA, 110, 13739–13744, doi:10.1073/pnas.1222843110, 2013.
- 965 Zhang, Y. G., Pagani, M., Liu, Z., Bohaty, S. M., and DeConto, R.: A 40-million-year history of atmospheric
CO₂, *Philos. T. R. Soc. A*, 371, 20130096, doi:10.1098/rsta.2013.0096, 2013.

Table 1. Fitting a linear or a non-linear function to the data. 5000 Monte-Carlo-generated realisations of the scattered $\Delta T_g - \Delta R_{[\text{CO}_2]}$ or $\Delta T_g - \Delta R_{[\text{CO}_2, \text{L}]}$ were analysed. The data are randomly picked from the entire Gaussian distribution described by the 1σ of the given uncertainties in both ΔT_g and $\Delta R_{[X]}$. The parameter values of fitted polynomials are given as mean $\pm 1\sigma$ uncertainty from the different Monte-Carlo realisations. Data sets differ in the underlying ΔT_g and CO_2 data. ΔT_g : either ΔT_g or polar amplification f_{pa} are fixed at LGM and mPWP at values from PMIP3 and PlioMIP with different functionality for f_{pa} (see methods for details). CO_2 data from ice cores and Hönisch-, Foster- and Pagani-labs.

Data set	n	χ^2		F	p	L	r^2	a	b	c	d
		1st	2nd								
ΔT_{g1} : fixed polar amplification factor f_{pa} at LGM and mPWP, else a linear function of ΔT_{NH}											
analysing ΔT_g vs. $\Delta R_{[\text{CO}_2]}$											
ice cores	394	2123	1839	60.4	< 0.001	**	56	-1.28 ± 0.09	3.67 ± 0.18	0.89 ± 0.08	0
Hönisch	52	580	545	3.2	0.08	/	53	-2.15 ± 0.13	1.36 ± 0.12	0	0
Foster	105	4199	3845	9.4	< 0.01	*	42	-1.73 ± 0.11	0.95 ± 0.09	-0.19 ± 0.05	0
Pagani	153	9152	9109	0.7	0.40	/	3	-2.29 ± 0.11	0.30 ± 0.11	0	0
analysing ΔT_g vs. $\Delta R_{[\text{CO}_2, \text{L}]}$											
ice cores ^a	394	1219	1176	14.3	< 0.001	**	72	-0.43 ± 0.07	2.16 ± 0.10	0.36 ± 0.04	0.02 ± 0.00
Hönisch	52	327	256	13.6	< 0.001	**	79	-1.15 ± 0.14	1.27 ± 0.12	0.10 ± 0.02	0
Foster	105	2589	2569	0.8	0.38	/	61	-1.53 ± 0.05	0.63 ± 0.03	0	0
Pagani	153	5125	5040	2.5	0.11	/	45	-2.19 ± 0.07	0.82 ± 0.04	0	0
ΔT_{g2} : fixed polar amplification factor f_{pa} at LGM and mPWP, else a step function											
analysing ΔT_g vs. $\Delta R_{[\text{CO}_2]}$											
ice cores	394	2668	2415	41.0	< 0.001	**	56	-0.92 ± 0.08	3.41 ± 0.17	0.74 ± 0.07	0
Hönisch	52	725	697	2.0	0.17	/	55	-1.78 ± 0.12	1.36 ± 0.11	0	0
Foster	105	4911	4369	12.7	< 0.001	**	39	-1.47 ± 0.11	0.09 ± 0.09	-0.21 ± 0.05	0
Pagani	153	9729	9683	0.7	0.40	/	02	-2.08 ± 0.11	0.27 ± 0.10	0	0
analysing ΔT_g vs. $\Delta R_{[\text{CO}_2, \text{L}]}$											
ice cores	394	1874	1568	76.3	< 0.001	**	72	-0.46 ± 0.06	1.41 ± 0.05	0.11 ± 0.01	0
Hönisch	52	370	317	8.2	< 0.01	*	80	-0.85 ± 0.13	1.13 ± 0.11	0.07 ± 0.02	0
Foster	105	3243	3146	3.1	0.08	/	55	-1.37 ± 0.08	0.58 ± 0.05	0	0
Pagani	153	5778	5704	2.0	0.17	/	43	-2.00 ± 0.06	0.76 ± 0.04	0	0
ΔT_{g3} : fixed ΔT_g at LGM and mPWP, polar amplification factor f_{pa} is a linear function of ΔT_{NH}											
analysing ΔT_g vs. $\Delta R_{[\text{CO}_2]}$											
ice cores	394	1788	1482	81.2	< 0.001	**	53	-1.39 ± 0.08	3.15 ± 0.16	0.84 ± 0.07	0
Hönisch	52	471	431	4.6	0.04	/	50	-2.10 ± 0.11	1.09 ± 0.10	0	0
Foster	105	3967	3793	4.7	0.03	/	30	-1.90 ± 0.06	0.76 ± 0.06	0	0
Pagani	153	9660	9620	0.62	0.43	/	2	-1.99 ± 0.11	0.30 ± 0.11	0	0
analysing ΔT_g vs. $\Delta R_{[\text{CO}_2, \text{L}]}$											
ice cores ^a	394	1038	944	39.0	< 0.001	**	70	-0.50 ± 0.07	2.17 ± 0.10	0.44 ± 0.04	0.03 ± 0.00
Hönisch	52	305	222	18.3	< 0.001	**	76	-1.26 ± 0.13	1.13 ± 0.11	0.10 ± 0.02	0
Foster	105	2778	2752	1.0	0.33	/	51	-1.44 ± 0.04	0.56 ± 0.03	0	0
Pagani	153	6063	5883	4.6	0.03	/	39	-1.89 ± 0.07	0.81 ± 0.05	0	0

n : number of data points in data set.

χ^2 : weighted sum of squares following either a linear fit (1st order) or a non-linear fit (2nd order polynomial), for some data sets (labelled: ^a) also of 2nd or 3rd order polynomials.

F : F ratio for F test to determine, if the higher order fit describes the data better than the lower order fit (1st vs. 2nd order polynomial or 2nd vs. 3rd order polynomial).

p : p value of the F test.

L : significance level of F test (/: not significant ($p > 0.01$), *: significant at 1% level ($0.001 < p \leq 0.01$), **: significant at 0.1% level ($p \leq 0.001$)).

r^2 : correlation coefficient of the fit.

a, b, c, d : derived coefficients of fitted polynomial $y(x) = a + bx + cx^2 + dx^3$.

Table 2. Continued Sensitivity analyses: (1): Investigating the importance of the uncertainties on the regression results by artificially reducing both $\sigma_{\Delta T_g}$ and $\sigma_{\Delta R}$ by a factor of 2 or 10. (2): Investigating the importance of the three variables ΔT_g , CO_2 , $\Delta R_{[\text{L}]}]$ with respect to the previous analysis of the ice-core based CO_2 data of von der Heydt et al. (2014) (cited here as vdH2014). Here, all data are resampled to 2kyr while in vdH2014 data are resampled to 100 yrs and binned ΔT_g before any regression analysis. Fitting a linear or a non-linear function to the data. 5000 Monte-Carlo-generated realisations of the scattered $\Delta T_g - \Delta R_{[\text{CO}_2, \text{L}]}$ were analysed. The data are randomly picked from the entire Gaussian distribution described by the 1σ of the given uncertainties in both ΔT_g and $\Delta R_{[\text{CO}_2, \text{L}]}$. The parameter values of fitted polynomials are given as mean $\pm 1\sigma$ uncertainty from the different Monte-Carlo realisations. In all scenarios summarised here ΔT_g vs. $\Delta R_{[\text{CO}_2, \text{L}]}$ with $\Delta T_g = \Delta T_{\text{gl}}$ was investigated.

Data set	n	χ^2		F	p	L	r^2	a	b	c	d
		1st	2nd								
Sensitivity analysis 1: Investigating the importance of the uncertainties											
ice cores ^a , original uncertainties	394	1219	1176	14.3	< 0.001	**	72	-0.43 ± 0.07	2.16 ± 0.10	0.36 ± 0.04	0.02 ± 0.00
ice cores ^a , uncertainties $\times 1/2$	394	3268	3105	210.6	< 0.001	**	80	-0.36 ± 0.04	2.23 ± 0.06	0.41 ± 0.03	0.03 ± 0.00
ice cores ^a , uncertainties $\times 1/10$	394	83489	77553	30.0	< 0.001	**	83	-0.31 ± 0.01	2.34 ± 0.01	0.47 ± 0.01	0.04 ± 0.00
Hönisch, original uncertainties	52	327	256	13.6	< 0.001	**	79	-1.15 ± 0.14	1.27 ± 0.12	0.10 ± 0.02	0
Hönisch, uncertainties $\times 1/2$	52	850	598	20.7	< 0.001	**	87	-1.01 ± 0.08	1.37 ± 0.07	0.10 ± 0.01	0
Hönisch, uncertainties $\times 1/10$	52	16235	10712	25.3	< 0.001	**	89	-0.97 ± 0.02	1.40 ± 0.01	0.11 ± 0.00	0
Foster, original uncertainties	105	2589	2569	0.8	0.38	/	61	-1.53 ± 0.05	0.63 ± 0.03	0	0
Foster, uncertainties $\times 1/2$	105	8972	8954	0.2	0.65	/	61	-1.53 ± 0.03	0.67 ± 0.02	0	0
Foster, uncertainties $\times 1/10$	105	306105	306079	0.1	0.93	/	61	-1.53 ± 0.00	0.69 ± 0.00	0	0
Pagani, original uncertainties	153	5125	5040	2.5	0.11	/	45	-2.19 ± 0.07	0.82 ± 0.04	0	0
Pagani, uncertainties $\times 1/2$	153	15283	14795	5.0	0.03	/	56	-2.23 ± 0.04	1.00 ± 0.03	0	0
Pagani, uncertainties $\times 1/10$	153	343134	329292	6.3	0.01	/	60	-2.24 ± 0.01	1.07 ± 0.01	0	0
Sensitivity analysis 2: Investigating the importance of ΔT_g , CO_2 , $\Delta R_{[\text{L}]}$ in the data set from ice cores with respect to the vdH2014 data at 2 kyr intervals (if available)											
this study ^a	394	1219	1176	14.3	< 0.001	**	72	-0.43 ± 0.07	2.16 ± 0.10	0.36 ± 0.04	0.02 ± 0.00
CO_2 as in vdH2014 ^a	390	1283	1235	15.0	< 0.001	**	70	-0.42 ± 0.06	2.17 ± 0.10	0.37 ± 0.04	0.02 ± 0.00
$\Delta R_{[\text{L}]}$ as in vdH2014	390	1684	1373	87.7	< 0.001	**	67	-0.49 ± 0.08	1.70 ± 0.06	0.16 ± 0.01	0
ΔT_g as in vdH2014	390	742	658	49.4	< 0.001	**	66	0.13 ± 0.12	1.13 ± 0.08	0.08 ± 0.01	0
ΔT_g , CO_2 , $\Delta R_{[\text{L}]}$ as in vdH2014	390	788	744	22.9	< 0.001	**	62	0.25 ± 0.14	1.12 ± 0.10	0.07 ± 0.01	0
data binned in $\Delta R_{[\text{CO}_2, \text{L}]}$ to bins of 0.2 W m^2											
this study	31	56	37	14.4	< 0.001	**	81	-0.66 ± 0.37	1.61 ± 0.26	0.14 ± 0.04	0
CO_2 as in vdH2014	31	60	42	12.0	0.002	*	80	-0.68 ± 0.36	1.56 ± 0.25	0.14 ± 0.04	0
$\Delta R_{[\text{L}]}$ as in vdH2014	27	43	32	8.3	0.008	*	79	-0.41 ± 0.43	1.75 ± 0.34	0.16 ± 0.06	0
ΔT_g as in vdH2014	31	42	35	5.6	0.025	/	73	-0.34 ± 0.23	0.63 ± 0.08	0	0
ΔT_g , CO_2 , $\Delta R_{[\text{L}]}$ as in vdH2014	28	35	32	2.3	0.138	/	74	-0.07 ± 0.26	0.72 ± 0.09	0	0
data binned in ΔT_g to bins of 0.2 K											
this study	32	203	148	10.8	0.003	*	87	-0.20 ± 0.18	1.70 ± 0.20	0.14 ± 0.04	0
CO_2 as in vdH2014	32	213	160	9.6	0.004	*	85	-0.20 ± 0.19	1.67 ± 0.21	0.13 ± 0.04	0
$\Delta R_{[\text{L}]}$ as in vdH2014	32	193	164	5.1	0.031	/	82	-0.39 ± 0.16	1.08 ± 0.08	0	0
ΔT_g as in vdH2014	24	40	34	3.7	0.068	/	77	-0.05 ± 0.25	0.70 ± 0.09	0	0
ΔT_g , CO_2 , $\Delta R_{[\text{L}]}$ as in vdH2014	24	42	39	1.6	0.218	/	76	0.23 ± 0.30	0.80 ± 0.11	0	0

n : number of data points in data set.

χ^2 : weighted sum of squares following either a linear fit (1st order) or a non-linear fit (2nd order polynomial), for some data sets (labelled: ^a) also of 2nd or 3rd order polynomials.

F : F ratio for F test to determine, if the higher order fit describes the data better than the lower order fit (1st vs. 2nd order polynomial or 2nd vs. 3rd order polynomial).

p : p value of the F test.

L : significance level of F test (/: not significant ($p > 0.01$); *: significant at 1% level ($0.001 < p \leq 0.01$); **: significant at 0.1% level ($p \leq 0.001$)).

r^2 : correlation coefficient of the fit.

a, b, c, d : derived coefficients of fitted polynomial $y(x) = a + bx + cx^2 + dx^3$.

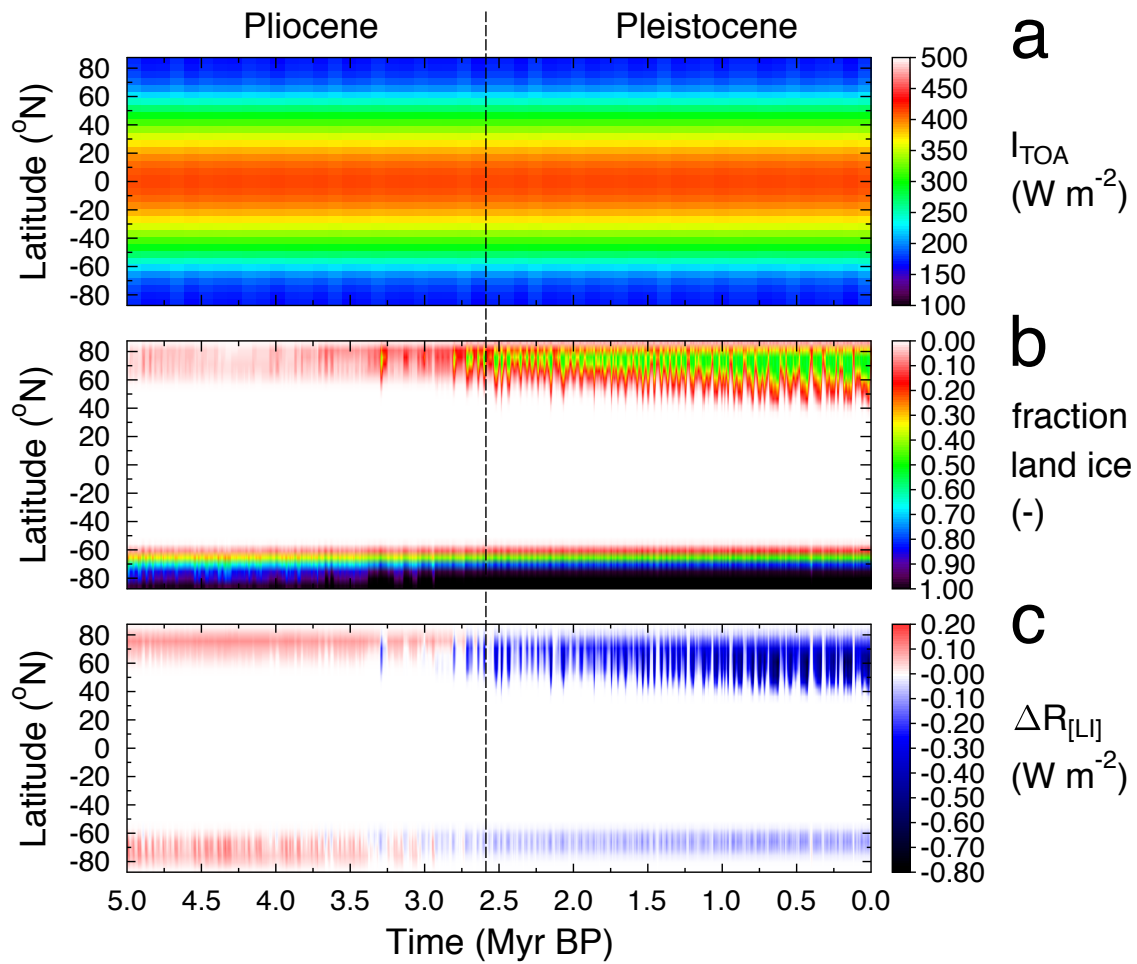


Figure 1. Radiative forcing of land ice sheets averaged for latitudinal bands of 5° . **(a)** Annual mean insolation at the top of the atmosphere I_{TOA} based on orbital variations (Laskar et al., 2004). **(b)** Fraction of each latitudinal bands of 5° covered by land ice as simulated by the 3-D ice-sheet model ANICE (de Boer et al., 2014). **(c)** Calculated radiative forcing of land ice sheets $\Delta R_{[\text{LI}]}$ normalised to global-scale impact.

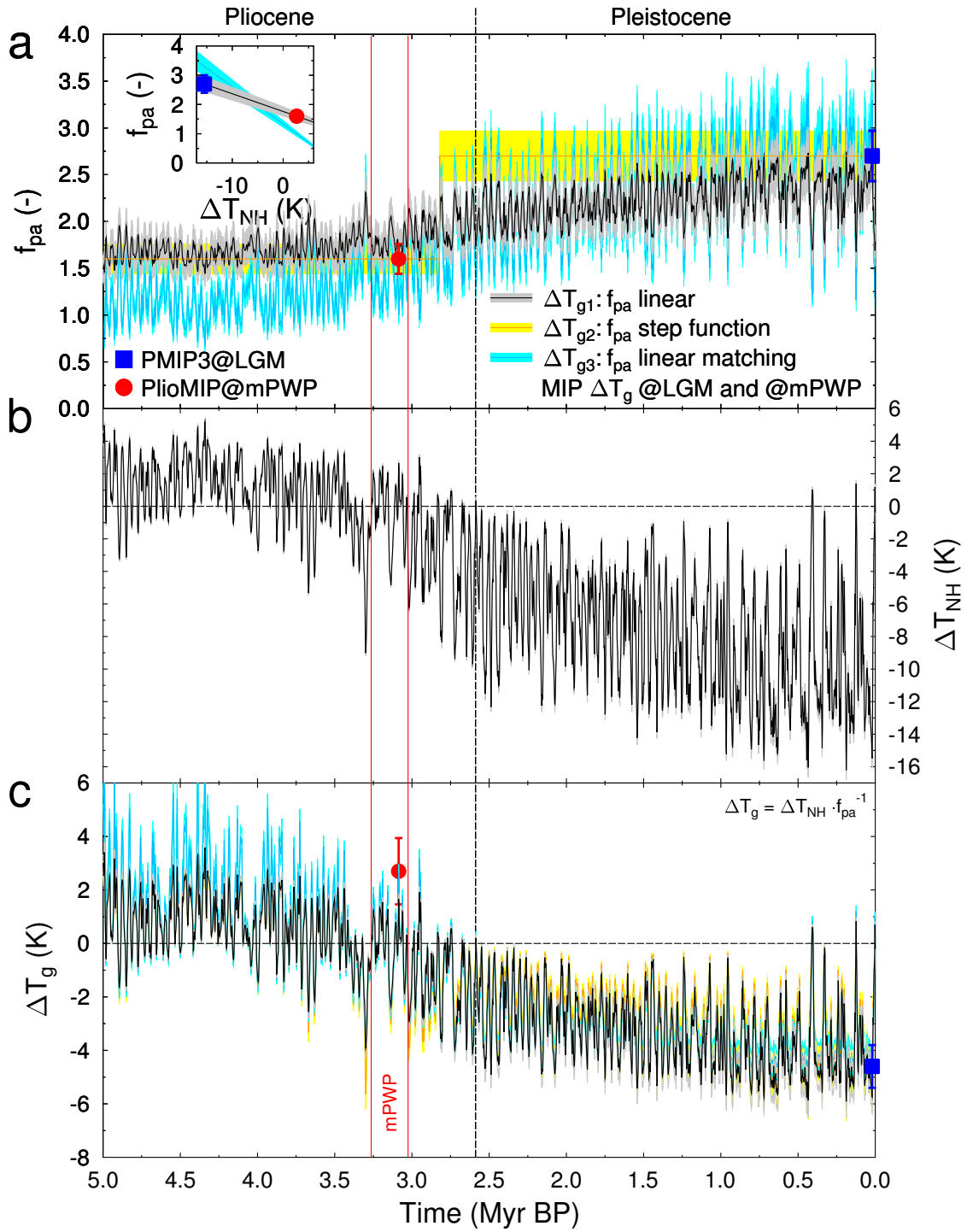


Figure 2. See next Page.

Caption Figure 2: Calculating global surface temperature change ΔT_g . **(a)** Polar amplification factor f_{pa} , the ratio between Northern Hemisphere (NH) land temperature change ΔT_{NH} and global temperature change ΔT_g , as function of time based on values for LGM (blue square) and mid-Pliocene Warm Period (mPWP) (red circle) derived from the Model Intercomparison Projects (MIP) PMIP3/CMIP5 and PlioMIP (Haywood et al., 2013), respectively. In our standard application ΔT_{g1} (black line) f_{pa} is calculated as a linear function depending on northern hemispheric temperature change ΔT_{NH} (insert), inter- and extrapolated between these two PMIP3 and PlioMIP-based values. Alternatively (ΔT_{g2} , orange line), f_{pa} varies as a step function with high values for the Pleistocene (periods with Northern Hemisphere land ice sheets) and low values for the Pliocene (periods mainly without NH land ice sheets) with the step between both values occurring at 2.82 Myr BP, when our results indicate large changes in NH land ice. In ΔT_{g3} (blue line) f_{pa} varied freely to meet ΔT_g reconstructed for LGM by PMIP3 (-4.6K) and for the mPWP by PlioMIP ($+2.7\text{K}$). See methods for further details. **(b)** NH temperature change ΔT_{NH} as deconvolved from the benthic $\delta^{18}\text{O}$ stack LR04 (Lisiecki and Raymo, 2005) by applying a 3-D ice-sheet model in an inverse mode (de Boer et al., 2014). Uncertainty in ΔT_{NH} (grey) is the 1σ error calculated from 8 different model realisations (de Boer et al., 2014). **(c)** Global surface temperature change ΔT_g as used here based on $\Delta T_g = \Delta T_{NH} \cdot f_{pa}^{-1}$. Results for ΔT_g based on all three approaches for f_{pa} are given (same colour code as in sub-figure **(a)**). Symbols show $\Delta T_g \pm 1\sigma$ as derived within PlioMIP (mPWP, red circle) and PMIP3/CMIP5 (LGM, blue square). Red vertical lines mark the time period of the mPWP.

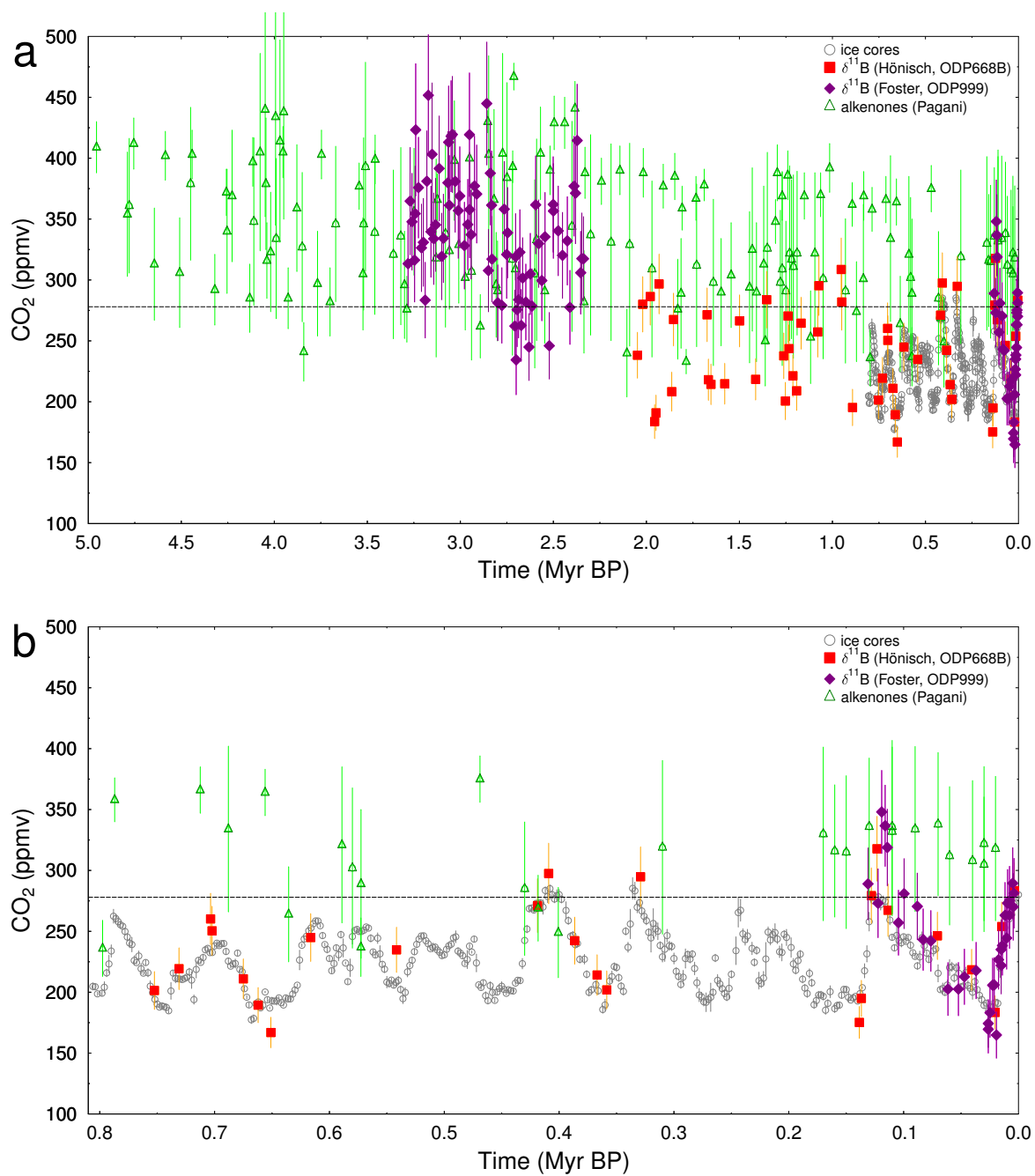


Figure 3. CO₂ data. **(a)** CO₂ data from ice cores (Rubino et al., 2013; MacFarling-Meure et al., 2006; Monnin et al., 2001, 2004; Schneider et al., 2013; Siegenthaler et al., 2005; Bereiter et al., 2015, 2012; Marcott et al., 2014; Ahn and Brook, 2014; Petit et al., 1999) at Law Dome, EPICA Dome C, West Antarctic Ice Sheet Divide, Siple Dome, Talos Dome, EPICA Dronning Maud Land and Vostok (resampled to time steps of 2 kyr), and based on either $\delta^{11}\text{B}$ (Hönisch et al., 2009; Foster, 2008; Martínez-Botí et al., 2015) or alkenones (Pagani et al., 2010; Zhang et al., 2013) from the three labs Hönisch, Foster and Pagani. **(b)** Zoom-in on ice core window of the last 0.8 Myr.

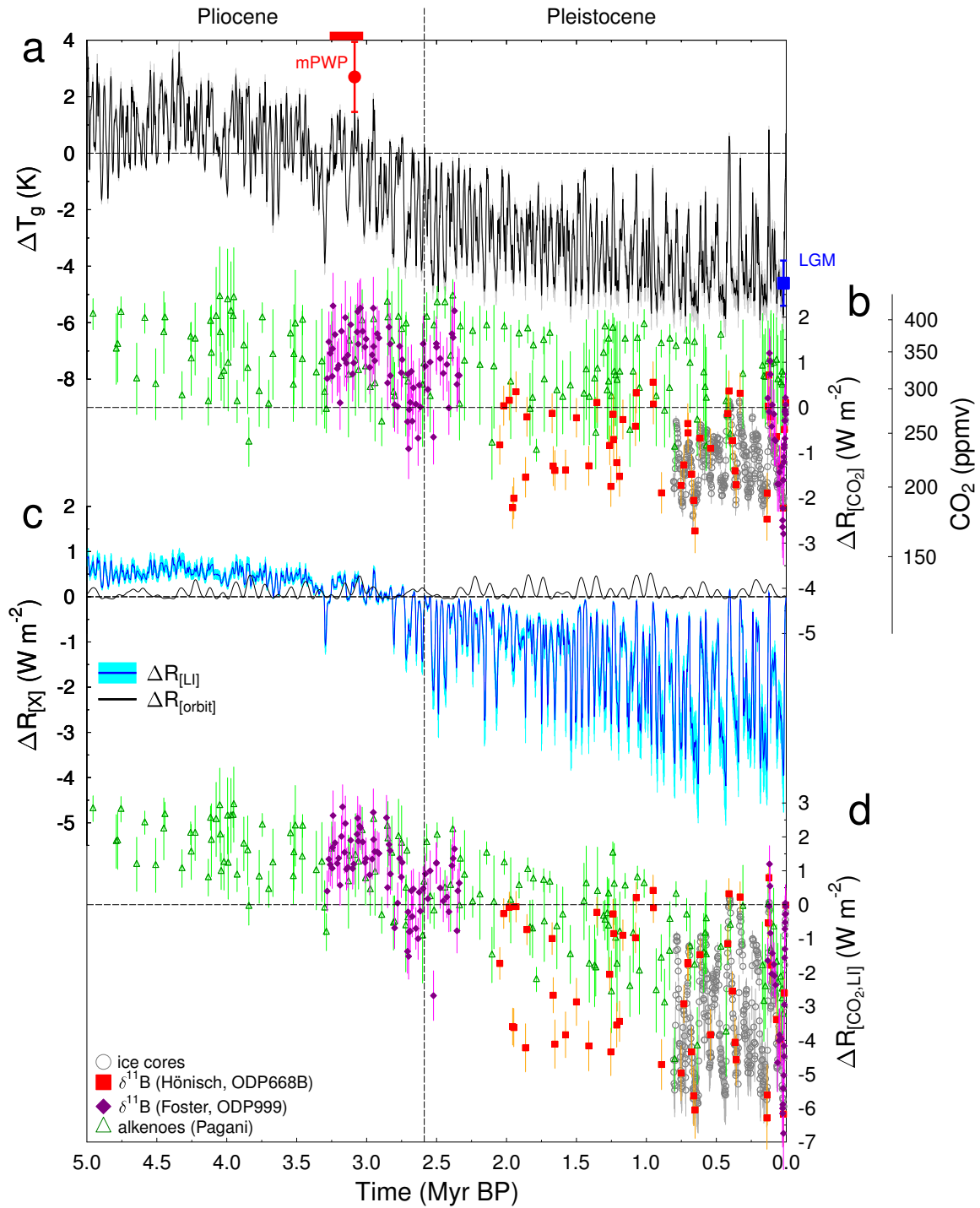


Figure 4. See next page.

Caption Figure 4: Changes in temperature and radiative forcing over the last 5 Myr. **(a)** Global mean surface temperature change ΔT_g calculated with the polar amplification factor f_{pa} being a linear function of the Northern Hemisphere land temperature change ΔT_{NH} . Marked are the mid-Pliocene Warm Period (mPWP) (red horizontal bar), global warming calculated within PlioMIP (red circle), and global cooling during the LGM derived from PMIP3/CMIP5 (blue square). **(b)** Changes in radiative forcing based on atmospheric CO_2 ($\Delta R_{[CO_2]}$). CO_2 data from ice cores (Bereiter et al., 2015) and based on $\delta^{11}B$ (Hönisch-lab (Hönisch et al., 2009), Foster-lab (Foster, 2008; Martínez-Botí et al., 2015)) and on alkenones (Pagani-lab (Pagani et al., 2010; Zhang et al., 2013)), **(c)** radiative forcing of land ice $\Delta R_{[LI]}$ and for comparison global annual mean insolation changes due to orbital variation $\Delta R_{[orbit]}$. **(d)** The sum of the radiative forcing changes due to CO_2 and land ice sheets ($\Delta R_{[CO_2,LI]}$) whenever CO_2 data allow its calculation. Uncertainties show 1σ .

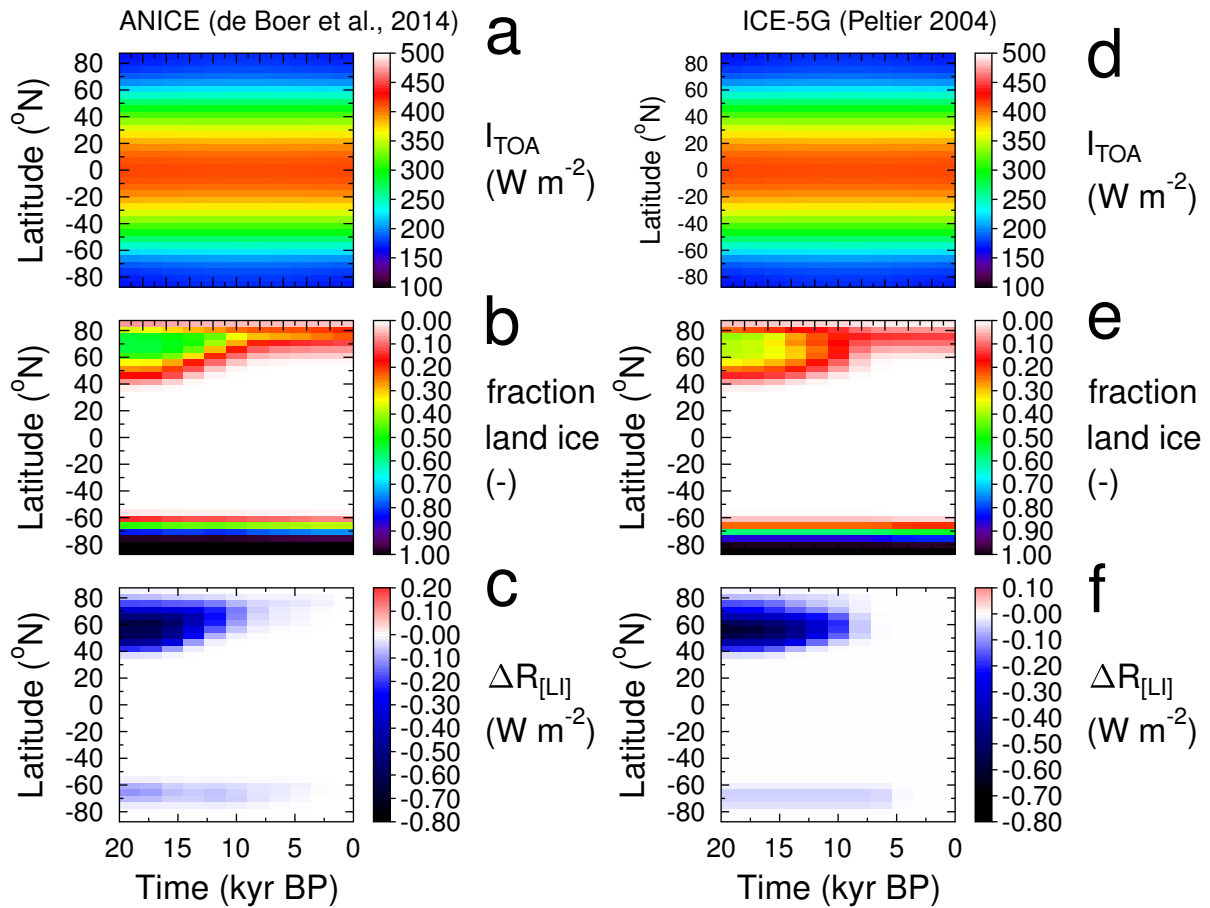


Figure 5. Comparing the calculation of radiative forcing of land ice sheets for the last 20 kyr for two different ice sheet setups. Left: the 3-D ice sheet model ANICE used in this study (de Boer et al., 2014); right: based on $1^\circ \times 1^\circ$ model output from ICE-5G (Peltier, 2004), results for radiative forcing of land ice sheets $\Delta R_{[LI]}$ is then based on similar aggregation to latitudinal bands of 5° as for ANICE. **(a, d)** Annual mean insolation at the top of the atmosphere I_{TOA} based on orbital variations (Laskar et al., 2004). **(b, e)** Fraction of each latitudinal bands of 5° covered by land ice as simulated by the 3-D ice-sheet models. **(c, f)** Calculated radiative forcing of land ice sheets $\Delta R_{[LI]}$ normalised to global-scale impact.

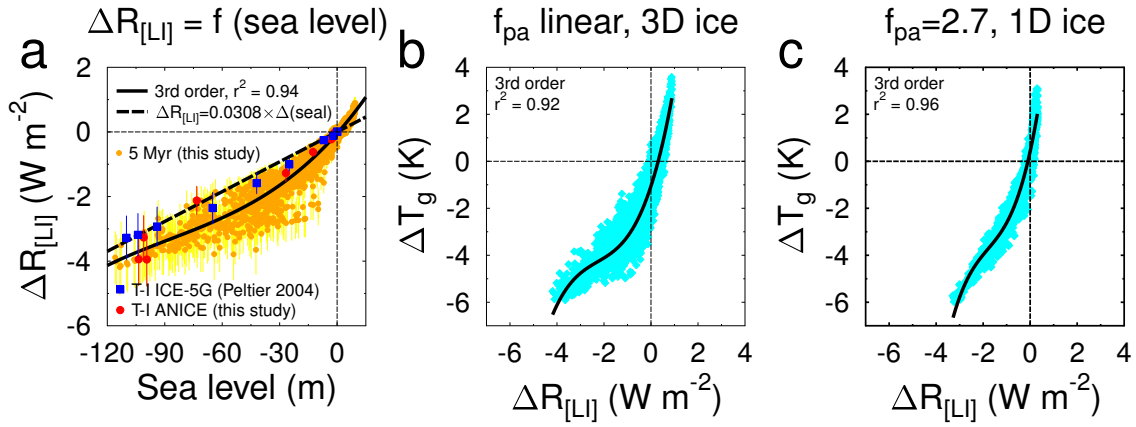


Figure 6. Details on land ice-albedo forcing ($\Delta R_{[LI]}$). **(a)** Scatter plot of sea level change (de Boer et al., 2014) against land ice albedo forcing $\Delta R_{[LI]}$ (this study) based on the 3-D ice-sheet model ANICE. Data are approximated with a third order non-linear fit. For comparison a fit based on sea level change as applied in other applications (Hansen et al., 2008; Martínez-Botí et al., 2015) is shown as dashed line. Furthermore, for Termination I (T-I) results based on ANICE and on ICE-5G (Peltier, 2004) are compared. **(b, c)** Relationship between global surface temperature change ΔT_g and land ice-albedo forcing $\Delta R_{[LI]}$ for different setups. Results plotted over the whole last 5 Myr (one data points every 2 kyr). **(b)** Standard setup with $\Delta T_g = \Delta T_{g1} = \Delta T_{NH} \cdot f_{pa}^{-1}$ using a polar amplification f_{pa} that varies linear-linearly as a function of ΔT_{NH} . $\Delta R_{[LI]}$ as based on 3-D ice-sheet models as calculated in this study (see Fig. 1c). **(c)** Setup with a constant $f_{pa} = 2.7$ as applied previously in van de Wal et al. (2011). $\Delta R_{[LI]}$ is based on 1-D ice-sheet model results and is calculated from sea level change with 0.0308 W m^{-2} per m sea level change. Underlying 1-D ice-sheet model results of ΔT_{NH} and sea level were published before in de Boer et al. (2010) and used elsewhere (Martínez-Botí et al., 2015).

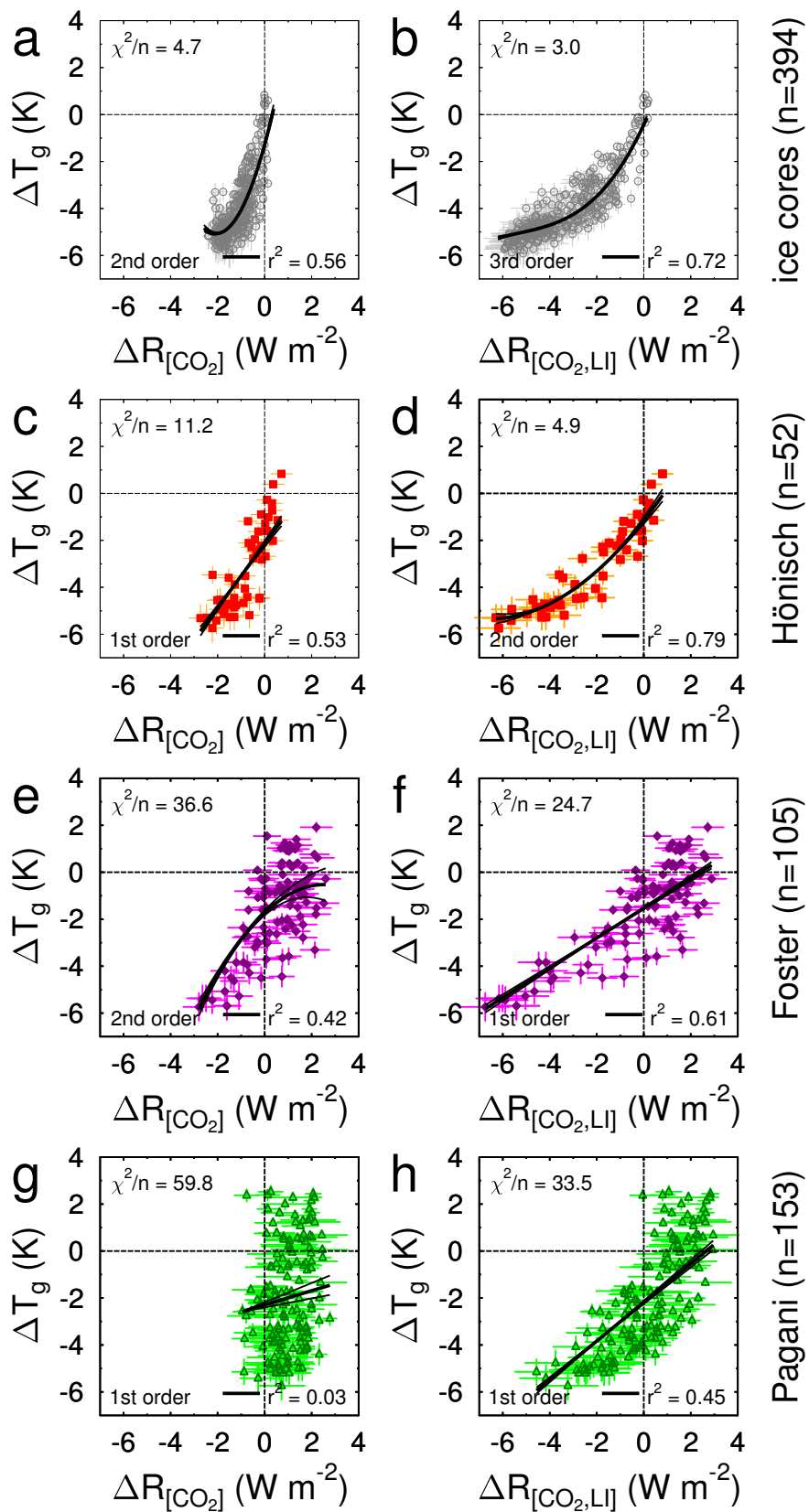


Figure 7. See next page.

Caption Figure 7: Scatter-plots of data of global temperature change ΔT_g against radiative forcing $\Delta R_{[X]}$. ΔT_g is calculated with the polar amplification factor f_{pa} being a linear function of ΔT_{NH} . Left column **(a, c, e, g)**: radiative forcing of CO_2 ($\Delta R_{[CO_2]}$). Right column **(b, d, f, h)**: radiative forcing of CO_2 and land-ice albedo ($\Delta R_{[CO_2,LI]}$). Lines show average best fits (1st, 2nd, or 3rd order polynomials) to 5000 Monte-Carlo realisations of the data (details in Table 1). Sub-figures differ by the CO_2 data they are based on: **(a, b)** ice cores (Bereiter et al., 2015); **(c, d)** $\delta^{11}B$ from Hönisch-lab (Hönisch et al., 2009); **(e, f)** $\delta^{11}B$ from Foster-lab (Foster, 2008; Martínez-Botí et al., 2015); **(g, h)** alkenones from Pagani-lab (Pagani et al., 2010; Zhang et al., 2013); each row contains information on the number of data points n , each sub-figure the mean uncertainty of the fit by dividing χ^2 (the weighted sum of squares from the regression analysis) by n and the correlation coefficient r^2 . Uncertainties show 1σ .

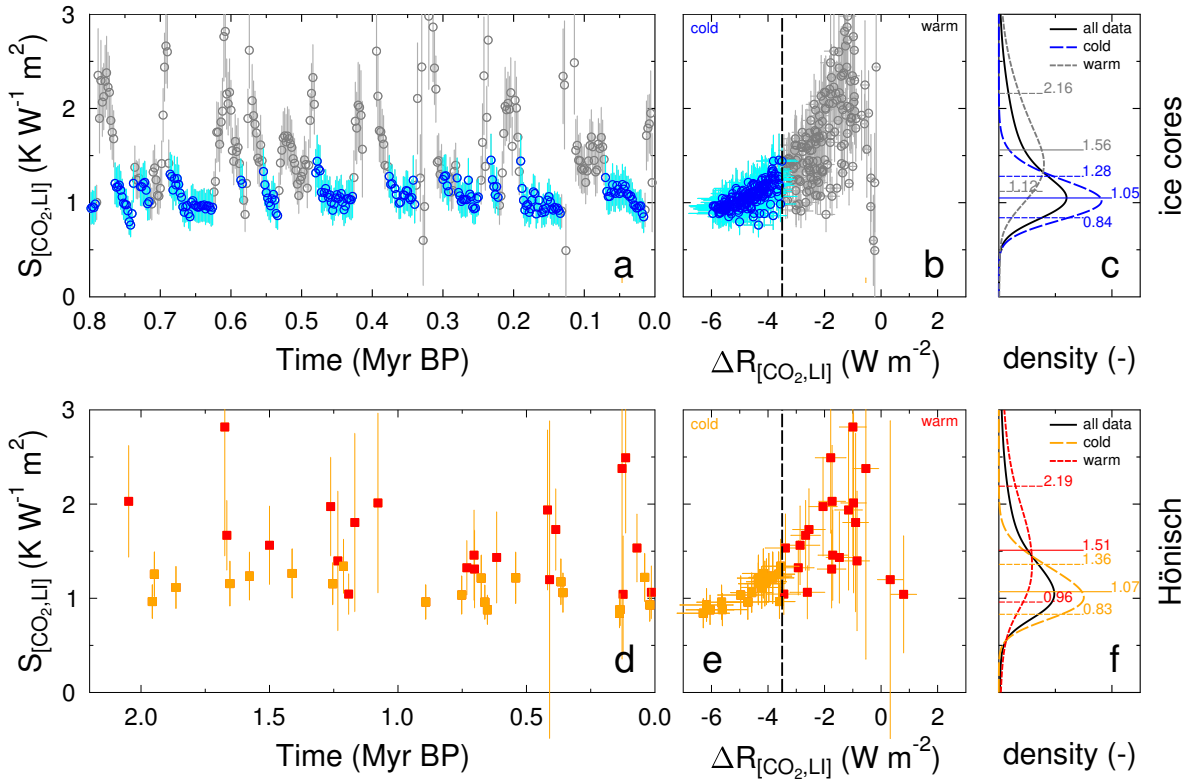


Figure 8. Calculating specific equilibrium climate sensitivity $S_{[\text{CO}_2, \text{LI}]}$. Only data with their mean in $S_{[\text{CO}_2, \text{LI}]}$ in the range $[0, 3] \text{ K W}^{-1} \text{ m}^2$ are analysed and plotted. **(a)** Ice core-based time series of point-wise calculations of $S_{[\text{CO}_2, \text{LI}]}$ for the last 0.8 Myr. **(b)** Same data as in **(a)** in a scatter plot of $S_{[\text{CO}_2, \text{LI}]}$ against radiative forcing $\Delta R_{[\text{CO}_2, \text{LI}]}$. **(c)** Probability density distribution of ice core-based $S_{[\text{CO}_2, \text{LI}]}$. Data from “cold” periods ($\Delta R_{[\text{CO}_2, \text{LI}]} < -3.5 \text{ W m}^{-2}$) and “warm” periods ($\Delta R_{[\text{CO}_2, \text{LI}]} > -3.5 \text{ W m}^{-2}$) are analysed separately. Labels in **(c)** denote 16th, 50th and 84th percentile. **(d, e, f)** Same as **(a, b, c)**, but for Hönlisch data over the last 2.1 Myr.

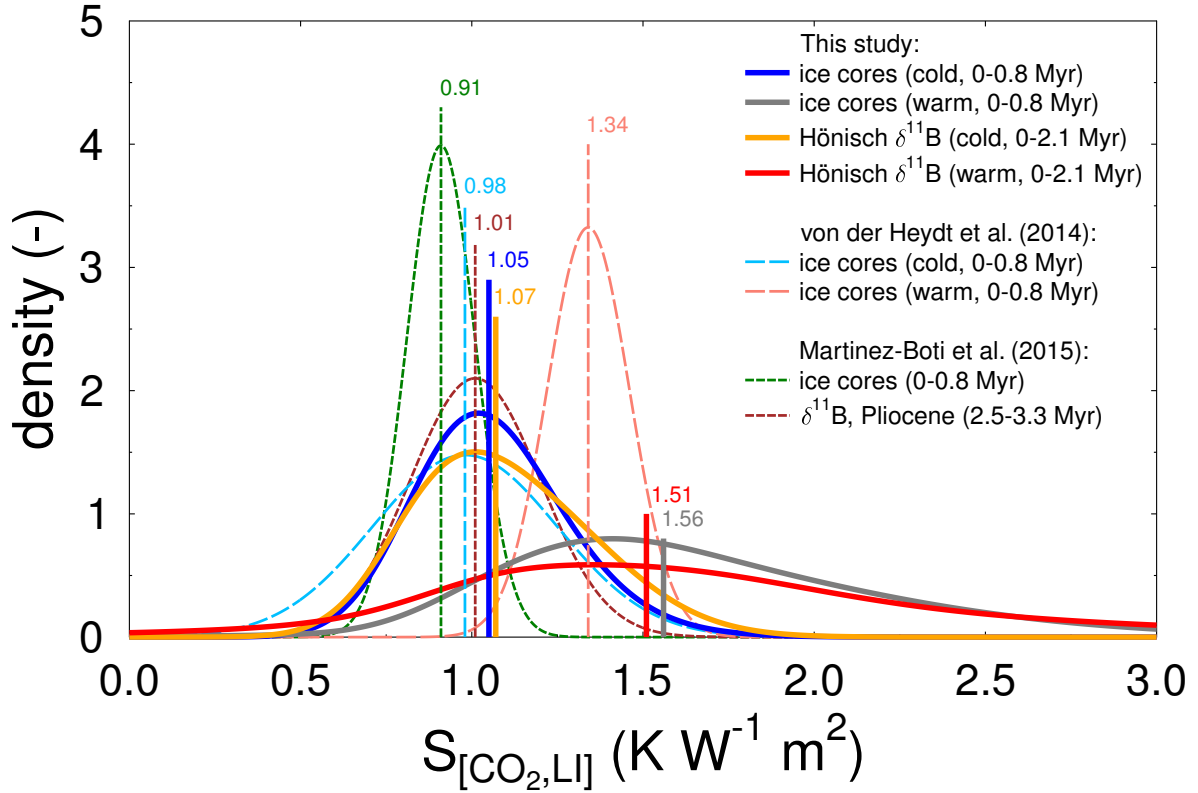


Figure 9. Probability density function of different approaches to calculate specific equilibrium climate sensitivity $S_{[\text{CO}_2, \text{LI}]}$. Results of this study are based on point-wise analysis of the ice core (last 0.8 Myr) and Hönisch (last 2.1 Myr) data for “cold” periods ($\Delta R_{[\text{CO}_2, \text{LI}]} < -3.5 \text{ W m}^{-2}$) and “warm” periods ($\Delta R_{[\text{CO}_2, \text{LI}]} > -3.5 \text{ W m}^{-2}$). von der Heydt et al. (2014) calculated $S_{[\text{CO}_2, \text{LI}]}$ based on ice core data for similar split of the data. We show their results based on similar ΔT_g than obtained here published in the SI in von der Heydt et al. (2014). Martínez-Botí et al. (2015) calculated $S_{[\text{CO}_2, \text{LI}]}$ for either ice core data of the whole last 0.8 Myr or based on $\delta^{11}\text{B}$ for 0.8 Myr of the Pliocene between 2.5–3.3 Myr BP. Vertical lines and labels give the mean of the different results.

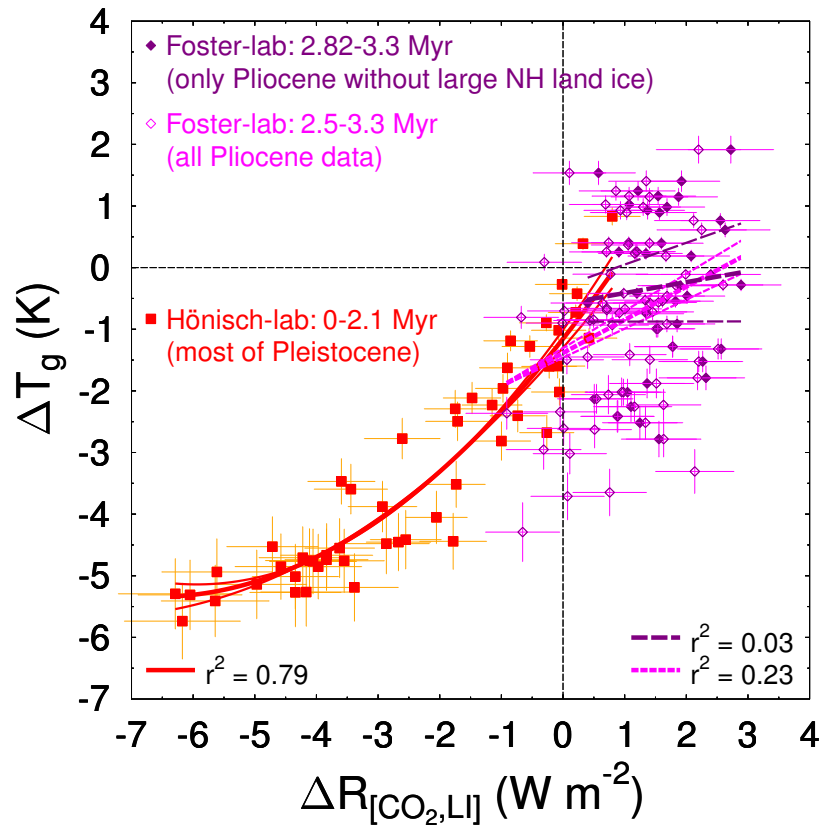


Figure 10. Best-guess 3.3Myr scatter-plot of global temperature change ΔT_g against the radiative forcing of CO_2 and land-ice albedo ($\Delta R_{[\text{CO}_2, \text{LI}]}$). The Hönlisch-lab (Hönlisch et al., 2009) data for the last 2.1Myr (most of the Pleistocene) and the Pliocene part of the Foster-lab data (Martínez-Botí et al., 2015), complete (2.5–3.3 Myr BP) and only for the almost land-ice free Northern Hemisphere times (2.82–3.3 Myr BP) are compiled to illustrate how the functional dependency between ΔT_g and $\Delta R_{[\text{CO}_2, \text{LI}]}$ changed as function of background climate state.